ANTIMICROBIAL ACTIVITY AND CONSTITUENTS OF THE ROOT BARK OF *LONCOCARPUS ERIOCALYX*

By

MUBIU JEDIEL KIRIA

B. Pharm. (Nairobi)

U59/74606/2014

A thesis submitted in partial fulfillment of the requirements for the degree of Master of Pharmacy in Pharmaceutical Analysis of the University of Nairobi

Department of Pharmaceutical Chemistry

School of Pharmacy

UNIVERSITY OF NAIROBI

October, 2018

DECLARATION

This thesis research proposal is my original work and has not been presented elsewhere for examination.

.....Date 07/11/2018.....

MUBIU JEDIEL KIRIA

U59/74606/2014

This thesis research proposal has been submitted for examination with our approval as University supervisors.

Sign.....**Date** 7.11.2018.....

FOR

DR. S.N. NDWIGAH, PhD.

Senior Lecturer,

Department of Pharmaceutical Chemistry,

Sign.....**Date** 07-11-2018.....

DR. K.O. ABUGA, PhD.

Senior Lecturer,

Department of Pharmaceutical Chemistry,

Sign.....**Date** 7/11/2018.....

DR. D.S.B. ONGARORA, PhD.

Lecturer,

Department of Pharmaceutical Chemistry,

DECLARATION OF ORIGINALITY

Name of the student:	Mubiu Jediel Kiria
Registration number:	U59/74606/2014
College:	Health sciences
School:	Pharmacy
Department:	Pharmaceutical Chemistry
Course name:	Master of Pharmacy in Pharmaceutical Analysis
Title of the work:	Antimicrobial activity and constituents of the root bark extracts of *Lonchocarpus eriocalyx*

DECLARATION

1. I understand what plagiarism is and I am aware of the university's policy in this regard.

2. I declare that this thesis is my original work and has not been submitted elsewhere for examination, award of a degree or publication. Where other people's work or my own work has been used, this has properly been acknowledged and referenced in accordance with the University of Nairobi's requirements.

3. I have not sought or used the services of any professional agencies to produce this work

4. I have not allowed, and shall not allow anyone to copy my work with the intention of passing it off as his/her own.

5. I understand that any false claim in respect to this work shall result in disciplinary action, in accordance with the University plagiarism policy.

Signature _____ Date 07/11/2018

TABLE OF CONTENTS

.

LIST OF SYMBOLS AND ABBREVIATIONS

ACN	Acetonitrile
AIDs	Acquired immunodeficiency syndrome
AD	*Anno Domini*
dd	Doublets of doublets
APT	Attached proton test
$CDCl_3$	Deuterated chloroform
CCl_4	Carbon tetrachloride
^{13}C	Carbon-13
DARU	Drug research and analysis laboratory
DCM	Dichloromethane
DMSO	Dimethyl sulfoxide
EA	Ethyl acetate
eV	Electron volts
^{1}H	Proton
HIV	Human immunodeficiency virus
HRMS	High Resolution Mass spectrometry
IC_{50}	Concentration that causes 50% inhibition
IR	Infra-red
J	Coupling constant
KBr	Potassium bromide
kPa	KiloPascal

m	Multiplet
MeOD	Deuterated methanol
MeOH	Methanol
mg	Milligrams
MHz	MegaHertz
MIC	Mean inhibitory concentration
ml	Milliliters
mm	Millimeters
m/z	Mass to charge ratio
NMR	Nuclear magnetic resonance
ppm	Parts per million
R_f	Retention factor
s	Singlet
SDA	Sabourauds dextrose agar
Spp.	Species
t	Triplet
TB	Tuberculosis
TLC	Thin layer chromatography
TMS	Tetramethylsilane
UV	Ultraviolet
λ	Wavelength
WHO	World Health Organization
w/v	Weight by volume

LIST OF FIGURES

LIST OF TABLES

LIST OF APPENDICES

ACKNOWLEDGEMENTS

I am forever grateful to the LORD JESUS for His gift of life and bodily strength during this rigorous exercise.

I wish to sincerely thank my supervisors Dr. S.N. Ndwigah, Dr. K.O. Abuga and Dr. D.S.B. Ongarora for their guidance, support and encouragement during the research.

My appreciation also goes to the technical staff of the Drug Analysis and Research Unit (D.A.R.U.) especially Mr. Hannington Mugo and Mr Obed King'ondu for their technical assistance as I carried out the analytical work. I also acknowledge technical staff from the Department of Pharmacognosy, especially, Mr. Josphat Mwalukumbi for his assistance during the phytochemical analysis.

I appreciate Dr. Ferdinand Ndubi and Prof. Kelly Chibale of the University of Cape Town, South Africa, for their key role in carrying out high resolution mass spectrometry and NMR analysis of the isolated compounds.

DEDICATION

Dedicated to

My wife, *Eunice Jediel*, my daughters *Claudia* and *Blessed Jediel*, and my son *Prince Jediel* for their unwavering support.

ABSTRACT

Conventional anti- infectives are expensive and in most cases unavailable to the target population. This has led to greater reliance on alternative medicine such as decoctions from plants. *Lonchocarpus eriocalyx* root bark, for example, has been used traditionally by many African communities for treatment of various ailments including microbial infections.

This plant has previously been investigated for antibacterial and antiprotozooal activities. Lupeol, a triterpenoid, has been isolated from *L. eriocalyx* root bark in connection to the plant's antiplasmodial activity. This study sought to investigate the antifungal and antibacterial activity of the root back extracts of *L. eriocalyx* and to isolate more compounds responsible for activity, with a view to giving scientific credence to the forklore use of the plant.

Lonchocarpus eriocalyx root bark was collected from Makanyanga sub-location, Igamba-Ng'ombe division, Tharaka-Nithi County. The collected root bark was chopped into small pieces and dried at room temperature for 2 weeks. The dried plant material was ground to powder and stored at room temperature before use.

Sequential extraction was carried out using methanol, chloroform and water. All the four extracts were screened for antibacterial activity against *Staphylococcus aureus, Escherichia coli* and *Pseudomonas aeruginosa*, and for antifungal activity against *Saccharomyces cerevisiae* using agar diffusion method. Gentamicin and nystatin were used as positive controls for antibacterial and antifungal tests respectively.

Four compounds were isolated by column chromatography in a gradient mode using silica gel 60-120 mesh, monitored by TLC. They were identified as β- sitosterol/stigmasterol mixture, lupenone, and lupeol using UV, IR, MS and NMR analysis. This is the first time that β-sitosterol, stigmasterol and lupenone have been isolated from *L. eriocalyx.*

The four compounds exhibited antibacterial activity against *S. aureus, E. coli* and *P. aeruginosa*, and antifungal activity against *S. cerevisiae.* The greatest activity was against *S. cerevisiae,* with zones on inhibition of 1.1 cm, 1.2 cm and 1.3 cm for β-sitosterol/stigmasterol mixture, lupenone and lupeol respectively. This gives scientific credence to the forklore use of the root bark of *Lonchocarpus eriocalyx* in the treatment of bacterial and fungal infections.

CHAPTER ONE: INTRODUCTION AND LITERATURE REVIEW

1.1 Introduction

Natural products have been in use for therapeutic purposes since the beginning of human civilization. Decoctions from plants, animal products and minerals were, for centuries, the primary sources of drugs in curative medicine [1]. Even with the current surge in drug discovery, available statistics show increased preference to alternative medicine. In Kenya, for example, over 70 percent of the population use traditional medicine, in addition to conventional medicine, for essential health care [2]. Over 90% of Kenyans have also been reported to have, once or more, used medicinal plants [2].

Reasons that precipitate this shift range from limited accessibility of contemporary medicine especially in the rural areas since pharmacies and hospitals are located in towns, to limited health staff. The doctor- patient ratios in Kenya are as low as 1: 5250, against the lowest World Health Organization (WHO) recommended ratio of 1:1000 [3]. The ratio of traditional medical practitioners to patients stands at 1:987, making it more convenient to visit a traditional practitioner as opposed to visiting a conventional doctor. Contemporary drugs are also perceived to possess serious adverse drug reactions [4].

Phytotherapy is part of the strategic health care programs of the world health organization [1]. The organization also recommends that individual countries develop standard procedures to validate medicinal products for incorporation into the contemporary health care. Many countries such as China, India, Germany and France have already embraced this change [1].

1.2 Plants as sources of drugs

Plants are major sources of drugs [5]. A large number of current medicines in the market are obtained from plants, either directly or semi-synthetically. These compounds are products of secondary metabolism whose key role in plants is self-defense against herbivores, microbes and parasitic plants [5]. Many life-saving drugs of plant origin have entered into the drug markets, for example the anticancer taxanes and camptothecins [6]. Tables 1.1 and 1.2 below shows drugs obtained from plants directly and by semi-synthesis, respectively.

Table 1.1 Examples of drugs obtained directly from plants

Drug	Plant source	Part of the plant	Medicinal use	References
Digoxin	*Digitalis purpurea*	Leaves	Cardiotonic	[7]
Quinine	*Cinchona pubescens*	Stem bark	Antimalarial	[8]
Vincristine/vinblastine	*Catharanthus roseus*	Leaves	Anticancer	[9]
Reserpine	*Rauwolfia serpentina*	Roots	Antihypertensive	[7]
Atropine	*Atropa belladonna*	Leaves	Anti-muscarinic agent	[10]
Morphine/ codeine	*Papaver somniferum*	Leaves	Analgesic	[10]
Podophyllotoxin	*Podophyllum peltatum*	Roots and rhizomes	Antiviral in genital warts	[7]
Paclitaxel	*Taxus brevifolia*	Stem bark	Anticancer	[10]
Caffeine	*Coffea arabica*	Berries	Anti-migraine	[10]

Table 1.2 Examples of drugs obtained by semi-synthesis from plant precursors

Chemical class	Examples	Plant source	Medicinal use	References
Artemisinin derivatives	Dihydroartemisinin, artesunate	*Artemisia annua*	Antimalarial	[10]
Taxanes	Decotaxel	*Taxus brevifolia*	Anticancer	[10]
Camptothecins	Topotecan, irinotecan	*Camptothecum acuminata*	Anticancer	[9]
Opioids	Oxycodone, hydrocodone	*Papaver somniferum*	Analgesic	[8]

1.3 Infectious diseases

Infectious diseases are caused by pathogens like viruses, fungi, bacteria or parasites and can be transmitted from one person to the next, either directly or indirectly [11]. Infectious diseases have an ancient history. As early as 1500s *anno Domini* (AD), diseases such as leprosy, smallpox, cholera, plague and typhoid were a norm. Egyptian papyrus paintings show evidence of poliomyelitis and small pox outbreaks over 3000 years ago [12]. Small pox is said to have

killed more people than all the wars of history [13]. Plague is estimated to have killed 1.5m people in England in 1348, about 1.6m in China 1894 and more than 12.5m in India between 1897 and 1957 [14].

The industrial revolution in 1600s AD led to the invention of the microscope hence the culturing and identification of microbes. This enabled the development of vaccines as well as infection prevention methods such as pasteurization. The discovery of antibiotics in 20th century helped to contain epidemics [12].

However, emerging infectious diseases remain a health concern in different parts of the world today. These are infections that have increased in incidence during the last couple of decades (since late 1980s to date) or whose occurrence is predicted to rise in the coming days. Ebola, bubonic plague, and multi-drug resistant tuberculosis are some of the emerging infections [15] with huge economic and health impact [16].

Infectious diseases are of clinical and public importance because they are common and cause severe diseases, disability and death. Some cause widespread outbreaks of disease epidemics that are particularly more serious in infants and children [15].

1.3.1 Bacterial infections

Bacteria are the commonest cause of pathology, both in humans and animals [17]. Only 1% of bacterial species on earth are pathogenic although some of the normal flora become pathogenic secondary to immune-suppression [18]. Risks of infections are therefore increased tremendously in conditions such as human immunodeficiency virus/acquired immunodeficiency syndrome (HIV/AIDs), liver cirrhosis and other conditions that lower immune function [19]. For example, skin and mucosal opportunistic infections are reported in over 90 percent of people living with HIV/AIDS [20].

1.3.2 Fungal infections

Fungi are non-photosynthetic, either saprophytic or parasitic organisms. They possess relatively rigid cell wall and take in soluble nutrients by diffusion by their cell surfaces. Fungi cause a variety of superficial, subcutaneous and systemic infections called mycoses [21].

Superficial mycoses affect the skin, hair, nails and the mucous membranes including dermatophytosis and candidiasis. They are the most common of all fungal infections, with a worldwide distribution [22].

Subcutaneous mycosis mainly affect the dermis and commonly occur following inoculation of saprobic fungi from the soil into the subcutaneous tissue during trauma. They include sporotrichosis, chromoblastomycosis and mycetoma [23].

Systemic mycoses result from inhalation of air-borne fungal spores. Initially, there is pulmonary infection but the organism may be later disseminated to other organs. Fungi that cause systemic mycoses can either be true pathogens or opportunistic [22]. True pathogens cause diseases such as blastomycosis, coccidioidomycosis, histoplasmosis, and paracoccidioidomycosis [22]. Opportunistic pathogens become pathological following immune-suppression either by disease or drug treatment, for example aspergillosis and cryptococcosis [21].

1.3.3 Viral infections

Viruses are microscopic in nature and consist of a genetic material surrounded by a glycoprotein, protein or lipid coat. They do not reproduce outside the host cell [24]. The most common viral disease in the world is common cold, an upper respiratory tract infection caused by rhinovirus. Chicken pox, influenza, herpes, HIV/AIDS, human papillomavirus, hepatitis and viral hepatitis are some of the other common viral infections [23].

Spread of viral diseases is via physical or sexual contact, inhalation, ingestion or by vectors. Symptoms vary in character and severity depending on the type of virus involved [25]. Most viral diseases are self limiting [26] like viral influenza and viral rhinitis. Others are severe and potentially fatal such as polio and hepatitis B [25].

1.4 The role of plants in treatment of infectious diseases

Medicinal plants constitute an important part of medical care throughout the world [25]. In South Africa, herbalists in Maputland province alone use over 20 plant species in management of diarrhoeal infections. The commonest of these species are *Acacia burkei*, *Brachylaena transvaalensis, Cissampelos hirta* and *Sarcostemma viminale* [28].

In Kenya, typhoid has been managed in different communities using *Cassia singueana, Commiphora Africana, Grewia tembensis, Launaea cornuta* and *Solanum renschii* [29]. All the five plants or those related to them have been tested elsewhere and found to contain antibacterial activity. *Launaea cornuta* for example was found to have activity against *Salmonella typhi* and *S. typhimurium* with minimum inhibitory concentration (MIC) comparable to that of ciprofloxacin [30]. *Cassia singueana* [31], *Commiphora Africana* [32], *Grewia tembensis* [33], and *Solanum renschii* [34] have been reported as to having activity against *E.coli* and *S.aureus* and *P.aeruginosa.*

The Maasai, Teso, Kikuyu, Luyha, Luo, Taita, Digo, Kamba, Meru and kikuyu communities of Kenya use decoctions of the roots of *Solanum incanum* to manage abdominal infections. An infusion of the leaves of the *S. incanum* is applied to the ear as a remedy for earache. The fruit exudate is applied on the skin to cure ringworms [35].

1.5 Epidemiology of infectious diseases

Out of the ten leading global causes of death each year, 3 (lower respiratory infections, HIV/AIDs, diarrheal diseases) are from infectious diseases. The list of the 10 leading causes of death, in order of their decreasing mortality rate, is as follows: ischaemic heart disease, stroke, chronic obstructive pulmonary disease, tracheal/bronchial/lung cancers, lower respiratory infections, lung disease, HIV/AIDs, diarrheal diseases, diabetes, road accidents and hypertension [36].

Of over 6.3 million under-five child deaths that occur globally every year, about 44% occur in the neonatal period [37]. Majority of these cases occur in third countries and are attributed to manageable conditions such as lower respiratory infections, diarrhea, HIV/AIDS, TB, and malaria [36]. Although great efforts have been made at containing infectious diseases, those interventions in many cases do not adequately reach the target population, especially in developing countries [2].

Tuberculosis (TB), for example, remains among the communicable diseases with the greatest global health burden, being present in all the regions of the world [38]. Tuberculosis is latent in approximately 1/3 of the world's population [39]. There were about 1.5 million TB-related fatalities in 2013 [38].

Even in developed countries such as USA, infectious diseases are a major health burden [40]. Systemic fungal infections, for example, are amongst the most common health conditions in the United States. The burden of candideamia particularly among neonates is high, with an incidence as high as 160 cases per 100,000 population among black infants in Baltimore [41]. Coccidioidomycosis cases have increased exponentially in the United States [42], where it is the third most commonly reported infection in Arizona (after community acquired pneumonia and flu) with an overall prevalence of 150 per 100,000 population [41].

Viral epidemics have also increased in the recent past. Twenty six hemorrhagic fever pandemics due to ebola and marbug viruses.have been reported globally in less than two decades [43]. The outbreak of Ebola virus in West Africa in 2014, for example, was the largest and most complex in history [44], affecting over 5 countries (Sierra Leone, Guinea, Liberia, Senegal and Mali. By December 2014, over 17000 cases of Ebola and over 6000 Ebola-related fatalities had been reported [45].

1.6 Challenges in management of infectious diseases

Life processes such as population increase and patterns, urbanization, agricultural and industrial patterns, sanitation, and poor health systems enable microbial proliferation resulting in spread of infectious diseases [46]. Great efforts have been made at containing infectious diseases, those interventions in many cases do not adequately reach the target population, especially in developing countries [2, 47].

Globally, infection control remains a major health care challenge, especially in the wake of increased resistance to available antimicrobials [48] and poor laboratory technology [49].

1.7 *Lonchocarpus* genus

1.7.1 Botanical description

Lochocarpus is one of the genera in Fabaceae/*Leguminosae* family, order *fabales.* It is a pea family of flowering plants (angiosperms) [50]. *Fabaceae* is the third largest family among the angiosperms after *Orchidaceae* and *Asteraceae.* About 700 genera and 20,000 species of plants are found in this family [51].

Lonchocarpus species are called lancepods due to their fruit resembling an ornatelance tip or a few beads on a string [52]. They are trees, climbing shrubs, or woody lianas. The leaves are

alternate and odd-pinnate, and the flowers are violet, purple or white, growing in racemes or panicles [53]. A total of 323 plant species belong to this genus [50].

1.7.2 Distribution and ecology

Plants of the genus *Lonchocarpus* have a worldwide distribution although they grow best below 1680m of altitude [54]. *Lonchocarpus eriocalyx, L. utilis, L. urucu L.bussei, L. capassa, L. laxiflorus, L. xuul a*nd *L. yacatanensis a*re some of the species of medicinal value in the genus and are found throughout the world [54].

1.7.3 Compounds isolated from *Lonchocarpus* genus

Several compounds have been isolated from this genus as shown in table 1.3 below. Figure 1.1 gives the chemical structures of some of these compounds.

Table 1.3 Common compounds from the genus *Lonchocarpus* [55].

Compound	Species	Part of the plant
Rotenoids		
Deguelin	*L. utilis*	Root trunk
Rotenone	*L. utilis*	Root trunk
Lonchocarpic acid	*L. utilis*	Root bark
Tephrosin	*L. utilis*	Root trunk
isoflavones		
lonchocarpusone	*L. utilis, L. urucu*	Root trunk
Chalconoids		
2′,4-dimethoxy-6′-hydroxylonchocarpin	*L. xuul*	Root bark, seed pods
2′4′-Dihydroxy-3′-prenylchalcone	*L. xuul*	Root trunk
Flavones		
5,4′- Dimethoxy- (6:7) - 2,2-dimethylpyranoflavone	*L. yacatanensis*	Root trunk
Carpacromene	*L. yacatanensis*	Root trunk
Pterocarpanoids		
Flamichapparin	*L. urucu*	Root trunk
Medicarpin	*L. latiffolius*	Root trunk
Flavanones		
spinoflavanone	*L. xuul*	Root bark

Xuulanin	*L. xuul*	Root bark
Terpenes		
β-amyrin	*L. nesii*	Root trunk
Lupeol	*L. neuroscapha, L. eriocalyx*	Root bark

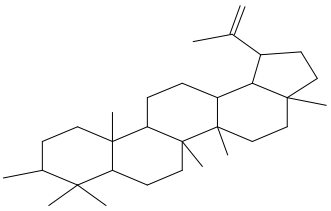

Lupeol

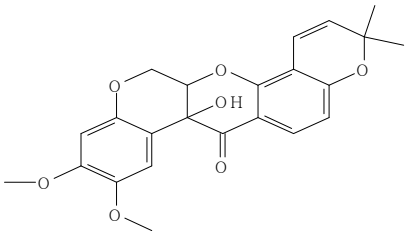

Trephosin

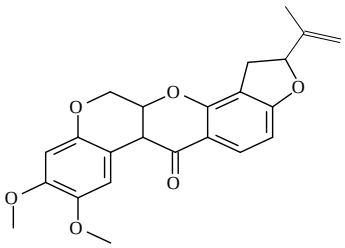

Rotenone

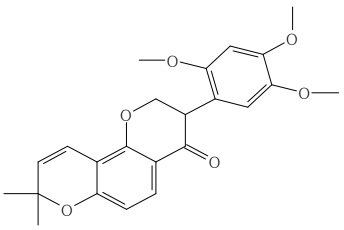

Lonchocarpusone

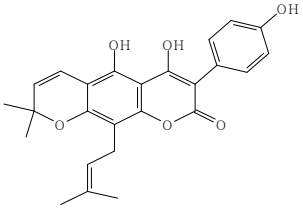

Lonchocarpic acid

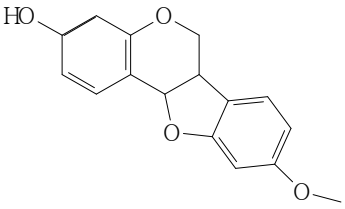

Medicarpin

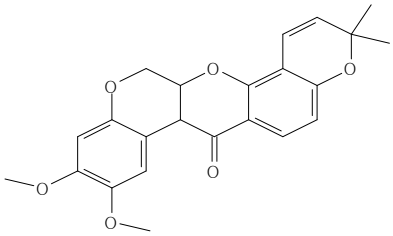

Capachromene

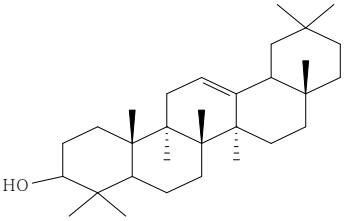

β-Amyrin

Figure 1.1 Chemical structures of common compounds in the *Lonchocarpus* genus [55].

1.7.4 *Lonchocarpus eriocalyx*

1.7.4.1 Botanical description of *Lonchocarpus eriocalyx*

Lochocarpus eriocalyx is a slender, deciduous tree or shrub, up to 15 m in height. The bark ranges from gray to pink, and smooth to reticulately fissured. The bark, when cut, produces a resinous exudate. Leaves are 10-26cm long, stipules linear, 2-10mm long. The lateral leaflet is in 3-5 pairs, elliptic or obovate. Usually, the terminal leaflet is the broadest. Primary lateral nerves are 5-8 on either side. Venation is similarly prominent [54]. The Photograph of *Lonchocarpus eriocalyx* plant is shown in figure 1.2.

1.7.4.2 Ecology and distribution of *Lonchocarpus eriocalyx*

Lonchocarpus eriocalyx is a native of South America, but grows naturally throughout the world between altitudes 500m and 1680m [54]. It is commonly found in Benin, Niger, Kenya, Tanzania and Zambia. In South America, especially the tropical regions of Brazil and Peru, *L. eriocalyx* together with others in the genus, such as, *L. utilis and L. urucu* no longer grow in the wild but are hand-cultivated for medicinal use [56]. In Kenya, *L. eriocalyx* is found in, among other areas, Elgoiyo Marakwet county, Kerio valley, Marsabit, Machakos, Kibwezi, Tharaka and Mbeere [51]. Local names of *L. eriocalyx* in East Africa are presented in table 1.4.

Table 1.4 Local names of *Lonchocarpus eriocalyx* in East Africa

Community	Country/Region	Local name	Reference
Tharaka	Eastern Kenya	*"Muthigiri"*	[57]
Mbeere	Eastern Kenya	*"Muthigiriri"*	[58]
Haya	North western Tanzania	*"Mware "*	[35]
Marakwet	North lift, Kenya	*"Sigirio"*	[59]
Pokot	Northern Kenya	*"Kipchurut"*	[59]
Usandawe	Central Tanzania	*"Kimani "*	[60]

.

Figure 1.2 Photograph of *Lonchocarpus eriocalyx* plant (taken in Makanyanga location, Igamba Ng'ombe Sub-county, Tharaka - Nithi County on 30/10/2016) and a local resident standing under it.

1.7.4.3 Ethnomedicinal use of *Lonchocarpus eriocalyx*

Lonchocarpus eriocalyx has been used by different communities in Africa to manage a variety of medical conditions. A decoction from boiled roots of the plant is used to treat high blood pressure amongst inhabitants of Eastern province, Kenya. In Mbeere, the decoction of boiled root bark of *L. eriocalyx* is used in the treatment for diabetes [58]. Natives of Tharaka in Tharaka-Nithi County apply the pulp from crushed leaves to wounds to hasten healing. Steam from boiling leaves is also believed to cure eye infections [57]. Powdered roots are used in water among the Haya community of Northwestern Tanzania to manage pimples [35].

1.7.4.4 Previous studies on *Lonchocarpus*

Most species already analyzed in the genus *Lonchocarpus* have been found to contain flavanoids (aurones, chalcones, flavones, flavans, flavanones, and stilbenes) [56]. Different rotenoids have been isolated from this genus, among them rotenone, lonchocarpic acid and deguelin which are potent natural insecticides and piscides [61]. Rotenone is still in the market today as an insecticide [62]. Also common in the genus are terpenoids and pterocarpanoids [63].

In a study by Kareru *et al.*, *L. eriocalyx* was found to inhibit bacterial growth. The zones of inhibition were 6.2, 10.3 and 11.0 mm on *E. coli, S. aureus* and *B. subtilis* respectively [58]. Sheila *et al.* reported weak antiviral activity on the stem bark of *L. eriocalyx* but having neither antibacterial nor antifungal activity [64]. In another study by Kiplagat (2006), the root bark of *L. eriocalyx* was found to possess *in vitro* activity against strains of *Plasmodium falciparum* that are resistant to chloroquine. A dichloromethane root extract gave an IC_{50} of 12.2 µg/ml against quinine's 0.08 µg/ml. Lupeol was isolated in connection to this activity [55]. There is no data in the available literature on antifungal activity of either crude extracts or isolates of the root bark of *L. eriocalyx.*

1.8 Study justification

Infectious diseases are a key cause of pathology in Africa [65]. Conventional anti- infectives are expensive and in most cases unavailable to the target population, leading to greater reliance on alternative medicine [4]. Complementary medicine is a good alternative to contemporary medicine among the African communities [65].

Lonchocarpus eriocalyx is a good example of alternative medicine, having been used by herbalists in Tharaka and Mbeere in eastern province for management of many health conditions such as hypertension, diabetes, eye infections, pimples and abdominal infections. There is therefore a need to provide scientific proof for this traditional claim.

According to the available literature only lupeol has been isolated from the stem of this plant in connection to its antibacterial activity. [55]. Evidence of phytochemical evaluation of the antibacterial activity of the roots of *L. eriocalyx* is missing in the literature. There is also no literature showing any attempts at evaluating its antifungal activity.

Lonchocarpus eriocalyx was selected because little work has been done on it, as shown in the literature, despite its vast forklore use. Screening for antimicrobial activity may reveal activity not previously reported. Phytochemical work on this plant could also provide a template for development of new drugs, or even a decoction that can be used as an anti-infective. Scientific credence to forklore use of *L. eriocalyx* will be helpful in the WHO's goal of incorporating alternative medicine in conventional treatment systems, especially in countries like China that have already put this into effect [1].

1.9 Objectives

1.9.1 General Objective

The main objective of this study is to investigate the antimicrobial activity of the root bark extracts of *L. eriocalyx* and isolate compounds which may be responsible for the activity.

1.9.2 Specific objectives

The specific objectives of the study are:

a. To investigate root bark extracts of *L. eriocalyx* for antifungal and antibacterial activity.
b. To isolate compounds from root bark extracts of *L. eriocalyx.*
c. To elucidate the chemical structures of the isolated compounds

CHAPTER TWO: EXPERIMENTAL

2.1 Collection and preparation of the plant material

Lonchocarpus eriocalyx root bark was collected from Makanyanga sub-location, Igamba-Ng'ombe division, Tharaka-Nithi County on September 10th, 2015. Taxonomic specimen authentication was done at the University of Nairobi after which the sample was given a voucher number (MJK/1/2015) and deposited with the University Herbarium for future reference. The collected root bark was chopped into small pieces, air dried at room temperature for 2 weeks, ground to powder and stored at room temperature in closed containers before use.

2.2 Solvents, reagents and materials

The reagents for extraction and fractionation of the plant material were general purpose grade and were glass-distilled once before use. Chloroform and methanol were from Alpha chemicals Ltd (Nairobi, Kenya) while hexane and ethyl acetate were from Synerchemie Chemicals (Nairobi, Kenya). Water used in extraction, phytochemical testing and preparation of culture media was freshly distilled in the Drug Analysis and Research Unit (DARU) before use.

For filtration purposes, Whatman filter paper No. 1 from Whatman International Ltd. (Maidstone, UK) and sintered glass filter funnel No. 4 from Schott Duran GmbH, Co. (Wertheim, Germany) were used. The TLC was performed on silica F_{254} aluminium pre-coated plates from EMD Millipore Corporation (Darmstadt, Germany). The TLC spots were visualized using a UV lamp and spray reagents. Meyer's and Dragendorf's reagent for detection of alkaloids and vanillin reagent for the detection of triterpenes were prepared in the laboratory as described in subsection 2.5.

For the preparation of Dragendorf's reagent, bismuth nitrate and tartaric acid were from May and Baker Limited (London, England) while glacial acetic acid and potassium iodide were from Howse & McGeorge laborex Limited (Nairobi, Kenya) and BDH Chemicals Limited (Yorkshire, England), respectively. Mercuric iodide from May and Baker Limited (London, England) was used to prepare Meyer's reagent.

Vanillin and sulfuric acid from BDH Chemicals Limited (Yorkshire, England) and Fisher Scientific Limited (Pittsburgh, USA) respectively were used for preparing vanillin reagent.

Ammonia solution and carbon tetrachloride used in the Borntrager's test for anthraquinones and ferric chloride for detection of tannins were from Loba Chemie PVT. (Mumbai, India). Iodine from Unilab Limited (Nairobi, Kenya) was used to visualize the spots. Fresh human blood (blood group B^+), sodium chloride from Howse & McGeorge laborex Limited (Nairobi, Kenya) and sodium citrate from Unilab Limited (Nairobi, Kenya) were used for hemolytic test for saponins.

Antimicrobial activity was evaluated against *Sacharomyces cereviceae* (local strain), *Staphylococcus aureus* (ATCC 29213), *Escherichia coli* (ATCC 25922) and *Pseudomonas aeruginosa* (ATCC 27853). Nutrient agar and Sabourauds Dextrose agar from HiMedia Laboratories PVT. Ltd (Mumbai, India) served as antibacterial and antifungal media, respectively. Nystatin reference standard (potency: 5480 IU/mg) and gentamicin working standard (potency: 671 IU/mg) from Yantaijusta Ware Pharmaceuticals (Mumbai, India) were used as positive antifungal and antibacterial controls, respectively. Dimethyl sulfoxide obtained from Loba Chemie PVT. (Mumbai, India) was used as a negative control.

2.3 Equipment

A Sartorius top loading balance (Sartorius, Goettingen, germany) was used to weigh samples above 100 g and a Sartorius analytical balance for samples below 100 g. A two- litre Soxhlet extractor equipped with a Graham condenser and a thermostatic heating mantle (Quickfit, Birmingham, U.K.) were used for solvent extractions. Glass columns of dimensions 100 × 2 cm and 150 × 3.5 cm fitted with a 250 ml reservoir were used for column chromatography. Fractions were collected with the aid of a SuperFrac fraction collector (Pharmacia LKB Biotechnology, Uppsala, Sweden), operating in the time mode. Evaporation of the extracts was done using a rotary evaporator (Heidolph VV200, Heidelberg, Germany) accompanied with a 9106 Polyscience refrigerating circulator (Polyscience Inc., Warrington PA, USA) and a rotary vacuum. A Mini UV/Vis box (Desaga GMBH, Heidelberg, Germany) was used for visualizing TLC spots.

A VG Platform II GC/LC mass spectrometer (Fison Instruments, Manchester, England) was used for mass spectrometric analysis. The melting points of purified compounds were determined using a SMP 10 Stuart melting point apparatus (Barloworld Scientific, Staffordshire, UK). Infrared spectroscopy was performed using a Perkin- Elmer IR apparatus FT 1000 (Beaconsfield,

England) as KBr discs. Proton NMR spectra were recorded on a Varian Mercury (300 MHz), a Bruker Ultrashield-Plus (400 MHz) spectrometer or a Bruker (600 MHz) with Me_4Si as internal standard. Carbon- 13 NMR spectra were recorded on the same instruments at 101 MHz or 151 MHz with TMS as internal standard. Samples for NMR spectroscopy were dissolved in deuterated dimethylsulfoxide (DMSO-d_6), chloroform ($CDCl_3$) or Methanol (MeOD). Chemical shifts (δ) were reported in parts per million (ppm) to 2 decimal places downfield from TMS as the internal standard. Coupling constants (*J*) were reported in Hertz (Hz) to two decimal places.

2.4 Preparation of the plant extracts

2.4.1 Chloroform extract

About 1 kg of the pulverized root bark was packed into a cotton muslin bag and subjected to Soxhlet extraction with chloroform for 48 hours. The resulting extract was filtered through a filter paper, followed by evaporation of the solvent using a rotary vacuum evaporator to yield a residue which was stored in glass containers at 2-8°C.

2.4.2 Methanol Extract

The plant material pre-extracted with chloroform was further extracted with methanol for 48 hours using a Soxhlet extractor. Filtration followed by rotary evaporation of the solvent was done and the resulting dry residue stored in glass containers in a refrigerator, at 2-8°C.

2.4.3 Macerate

Fresh root powder 500 g was subjected to maceration in 1L of distilled water at 25°C for 8 hours, with regular stirring. The liquid was strained out and filtered. The resultant extract was reduced *in vacuo* to about 100 ml, freeze-dried and the residue stored in glass containers in a refrigerator, at 2-8°C.

2.4.3 Decoction

Fresh root powder (300 g) was boiled in 1L of water for 5 minutes with continuous stirring. Upon cooling, the liquid was strained out and consequently filtered. The filtrate was reduced *in vacuo* to about 100 ml, freeze-dried, and the residue stored in glass containers in a refrigerator, at 2-8°C.

2.5 Preparation of reagents

2.5.1 Reagents used for general phytochemical tests

2.5.1.1 Dragendorf's reagent

Bismuth nitrate (1.7 g), tartaric acid (20 g) and glacial acetic acid (20 ml) were added to H_2O (80 ml) and stirred to form solution A. sixteen grams of KI was dissolved in H_2O (40 ml) to form solution B. A stock solution was obtained by mixing 10 ml of solution A and 10 ml of B. Five ml of the stock solution was added to tartaric acid solution (10 ml) and made to 50 ml with water to yield Dragendorf's reagent [66].

2.5.1.2 Meyer's reagent.

Mercuric iodide (1.4 g) was dissolved in H_2O (60 ml). Separately, KI (5 g) was dissolved in H_2O (20 ml). The 2 solutions were mixed and topped with H_2O to 100 ml. The resultant potassium mercuric iodide was the Meyer's reagent [66].

2.5.2 Reagents for visualizing TLC plates

2.5.2.1 Vanillin reagent

Vanillin (0.5 g) was weighed into a 100 ml flat bottomed flask and mixed with 50 ml conc. Sulfuric acid to make a 1% solution of vanillin in conc. sulfuric acid. This solution was sprayed on chromatographic plates. The plates were heated at 110 °C for 5 minutes before being observed for color change [67].

2.5.2.2 Iodine

About 2 g of iodine crystals was placed in a glass tank, the lid fitted and the iodine allowed to sublime and saturate the tank with iodine vapor for 1 hour. Developed TLC plates were incubated in the tank for 5 minutes to visualize [68].

2.6 General phytochemical tests

2.6.1 Tannins

The root bark powder (0.2 g) was mixed with water and heated on a water bath for 5 minutes. The mixture was filtered and ferric chloride added to the filtrate. A resultant dark green solution indicated the presence of tannins [67].

2.6.2 Saponins

Froth test: About 0.2 g of root bark powder in 5 ml of water was boiled for 5 minutes and filtered. Three ml of water was added to the filtrate, vigorously shaken for 5 minutes and observed for persistent frothing [68].

Hemolysis test: Plant powder (0.2 g) was extracted with 10 ml water and filtered, retaining the filtrate. Two 2 ml volumes of 1.8% NaCl solution were measured separately and poured into two test tubes. To one of the tubes (control), 2 ml water was added and to the other (test) 2 ml of the extract was added so that the concentration of NaCl in each tube was isotonic to the blood serum. A drop of fresh citrated blood was added to each tube and the tubes inverted gently to mix the contents. Hemolysis in the test experiment was indicative of saponins [67].

2.6.3 Alkaloids

Acid alcohol was made by mixing 1 ml of 1% acetic acid with 99 ml of 75% ethanol. About 1 g of the root bark powder was then boiled with 10 ml of the acid alcohol in a boiling tube for 1 minute and cooled before filtration. To 1 ml of the filtrate, three drops of Dragendorf's reagent were added shaken and observed for precipitation, which is indicative of alkaloids [68].

2.6.4 Anthraquinones

About 0.2 g of the root bark powder was shaken with 10 ml of hot water for five minutes and filtered while hot. The filtrate was cooled and extracted with 10 ml of CCl_4. The CCl_4 layer was washed with 5 ml distilled water before 5 ml of 10% solution of ammonia was added and shaken. The ammoniacal (lower) phase was observed for pink, red or violet color, which is indicative of free anthraquinones [66].

2.7 Column chromatography and isolation of compounds

2.7.1. Choice of mobile phase

The right solvent systems for column chromatography was determined by spotting samples of the chloroform extract on TLC plates and running them using various mobile phases/ mobile phase combinations to identify the one that gave the best separation,as follows: chloroform,

chloroform-MeOH, DCM; DCM-MeOH, ethyl acetate, ethyl acetate-MeOH, hexane, and hexane-ethyl acetate.

Hexane-ethyl acetate showed the best separation hence was used in column chromatography, 95.0:5.0, 90.0:10.0 and 85.0:15.0, in a gradient mode. The spots in the developed chromatograms were observed under both short UV (254 nm), long UV (366 nm), iodine and vanillin reagent.

2.7.2 Sample preparation

The chloroform extract was not readily soluble in the proposed mobile phase and therefore was adsorbed onto silica gel in the ratio of 1:1. To achieve adsorption, 12.5 g of dry extract was re-dissolved in 25 ml of chloroform. About 12.5 mg of silica was added, stirred vigorously to ensure proper mixing. The mixture was dried *in vacuo* using rotary evaporator and ground to fine powder using mortar and pestle. This adsorbed sample was introduced to the chromatographic column.

2.7.3 Column packing

A 1 cm layer of acid washed sand was added to the column already layered with glass wool, followed by slurry of 320 g silica gel in 1.5 L hexane/ethyl acetate 95:5. The column was compacted using a hand held pump to produce a uniform silica packing.

2.7.4 Sample loading

The sample-silica powder (25 g) was steadily poured into the column, with continuous tapping on the column. The mobile phase was allowed to flow through the sample, a piece of cotton wool introduced and mobile phase reservoir connected. The mobile phase flow rate was set at 15- 20 drops/min (equivalent to 0.5 ml/min) and fractions collected every 15 minutes.

2.7.5 Thin layer chromatography profiles of different fractions

Fractions were monitored on pre-coated silica gel F_{254} TLC plates using hexane 95%/ethyl acetate 5% as the mobile phase and their profiles visualized using $UV_{254\ nm}$, $UV_{366\ nm}$, iodine and vanillin reagent. Fractions from different columns that gave similar TLC profiles were pooled

together to form five major fractions, designated fractions A-E, and allowed to dry at room temperature. Table 2.1 below gives the TLC profiles of the fractions A-E.

Table 2.1: The TLC profiles of the fractions from chroloform extract

(a) FRACTION A

Spot R_f value	UV $\lambda_{254\ nm}$	UV $\lambda_{366\ nm}$	Iodine reagent	Vanillin reagent
0.62	+	+	+	+
0.61	+	+	+	+
0.61	+	+	+	+

(b) FRACTION B

Spot R_f value	UV $\lambda_{254\ nm}$	UV $\lambda_{366\ nm}$	Iodine reagent	Vanillin reagent
0.42	+	-	+	+
0.42	+	+	+	+
0.41	-	+	+	+
0.40	+	+	+	+
0.40	+	+	+	+

(c) FRACTION C

Spot R_f value	UV $\lambda_{254\ nm}$	UV $\lambda_{366\ nm}$	Iodine reagent	Vanillin reagent
0.28	-	-	+	-
0.26	-	-	+	-
0.26	-	-	+	-

FRACTION D

Spot R_f value	UV $\lambda_{254\ nm}$	UV $_{\lambda 366\ nm}$	Iodine reagent	Vanillin reagent
0.17	+	+	+	+
0.17	+	+	+	+
0.15	+	+	+	+
0.15	+	+	+	+

FRACTION E

Spot R_f value	UV $\lambda_{254\ nm}$	UV $_{\lambda 366\ nm}$	Iodine reagent	Vanillin reagent
0.09	-	-	+	+
0.08	-	-	+	+
0.08	-	-	+	+
0.07	-	-	+	+
0.07	-	-	+	+

Key: + = The TLC spot visualized; - = spot not visualized.

2.7.6 Isolation and purification of compounds

Fraction A, upon evaporation of the mobile phase, was scooped into a test tube. Hexane (10 ml) was added with shaking to aid dissolution. A non crystalline fatty solid formed in the tube upon evaporation of hexane at room temperature, designated as amorphous fraction I.

Fraction B was dissolved in DCM (10 ml) with gentle warming over a water bath and sonication. The solution was left to stand overnight during which crystals were formed. The crystals were cleaned using EA in which they were found to be poorly soluble and designated compound 1. Further attempts to recrystallize the mother liquor using DCM as above did not yield crystals.

Fraction C formed crystals upon evaporation of the mobile phase. The crystals were cleaned with EA and gave a single spot on TLC. Due to the poor yields and limited research time, enough

amounts could not be isolated for purification and identification. The crystals were therefore designated crystalline fraction I.

Acetone (30 ml) was added to fraction D in a test tube and shaken to form a concentrated solution. Two drops of water were added (to aid crystallization) and the solution left to stand at room temperature. White flabby crystals formed as acetone evaporated. The crystals were cleaned with chloroform and designated D_1. Chloroform was evaporated and recrystallization done using acetone to yield another batch of crystals designated D_2. The D_1 and D_2 gave the same R_f on TLC and were, therefore, combined and designated compound 2.

Fraction E purification followed the same procedure as fraction B. Filtration and recrystallization with DCM monitored with TLC was repeated until there was no physical evidence of crystals in the filtrate upon overnight evaporation of the DCM at room temperature. The resultant shiny needle-like crystals were designated mixture 1.

The isolated compounds were weighed and their yields determined as a percentage of the initial powdered plant material that produced the loaded extract. Photos of the TLC spectra of the isolated compounds developed together and visualized with vanillin and iodine were taken.

2.7.2 Antimicrobial testing

The extracts, namely methanol, chloroform, decoction and the macerate were independently evaluated for antimicrobial activity by agar diffusion. Nutrient agar (NA) and Sabourauds Dextrose agar (SDA) served as antibacterial and antifungal media respectively. Antifungal activity was tested against *Sacharomyces cerevisiae* whereas antibacterial activity evaluation involved three bacterial strains: *Staphyllococcus aureus*, *Escherichia coli* and *Pseudomonas aeruginosa*. Analytical grade dimethyl sulfoxide 99.9 % (DMSO) was used as the negative control for the chloroform extract and distilled water for methanol and water extracts. Gentamicin (0.3 mg/ml) and nystatin (0.3 mg/ml) were the antibacterial and antifungal positive controls, respectively.

Freshly prepared NA and SDA were separately heated at 80 °C for about 5 minutes and allowed to cool to about 45°C. To 100 ml of this media, 1 ml of the suspension of the appropriate micro-organism was evenly inoculated to give a micro-organism: media concentration of 1ml/100 ml.

The media was then poured into Petri-dishes to a depth of 3 mm and allowed to cool and set. Wells were dug on the surface using a sterile metal borer, 4 for the extracts and 2 for the controls. Solutions of the test samples, 100 mg/ml were prepared using dimethyl sulfoxide (for the chloroform extract) and distilled water (for methanol and water extracts).A micro-titer pipette was used to introduce about 50 µL of the sample solution into the wells. The Petri-dishes were incubated at suitable conditions, 30 °C for 24 hours for fungi and 35 °C for 18 hours for bacteria. Diameters of the zones of inhibition were determined using vernier calipers [69]. The overall process of extraction and isolation of compounds is summarized in Figure 2.1.

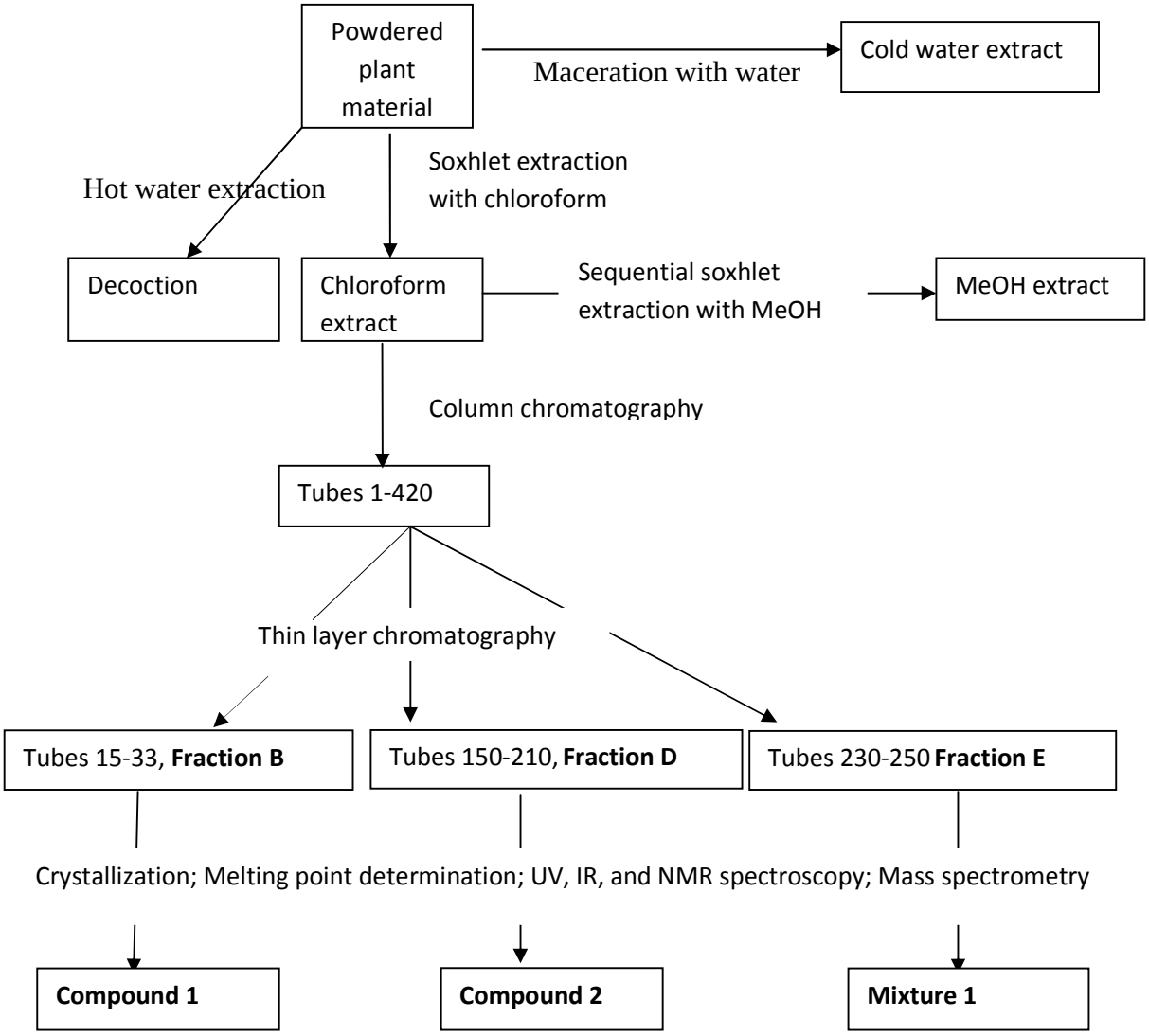

Figure 2.1: Scheme for extraction and isolation of compounds from the root bark of *L. eriocalyx*.

2.8 Analysis of the isolated compounds

Structural elucidation for the isolates involved melting point determination, high resolution mass spectrometry (HRMS) and ultra-violet (UV), infra-red (IR) and nuclear magnetic resonance (NMR) spectroscopy.

2.8.1 Melting point determination

Capillary tube method was used. Oven- dried powder of the isolate was tightly packed into a capillary tube to form a column of 4 to 6 mm in height. The capillary tube was mounted onto the melting point apparatus. The temperature of the metal block was raised rapidly to 50 °C after which the heating rate was readjusted to 1 °C/min. The temperature range within which the solid particles of the isolate passed into the liquid phase was noted as the melting point [70].

2.8.2 Infra-red spectroscopy

About 2 mg of the purified compound was triturated with 150 mg of potassium bromide using a motar and pestel, transferred to a die block and compressed into a disc by subjecting it to a pressure of 800 kPa. The disc was mounted onto the IR spectrophotometer and irradiated with a pulsed infra-red radiation between 4000 cm^{-1} and 400 $cm^{-1}$and the resulting spectrum recorded [71].

2.8.3 Ultra-violet spectroscopy

Two mg of the isolated compound was weighed into a test tube. Hexane (5 ml) was added and the tube shaken and gently heated over a water bath to aid dissolution. The solution was diluted serially to make 5 solutions of decreasing concentrations. Each solution was put in a cuvette 1 cm width and put in an appropriate sample holder alongside a blank hexane control. A pulsed UV radiation (400 nm-190 nm) was then applied to scan the sample [72].

2.8.4 High resolution mass spectrometry

The high resolution mass spectrometry (HRMS) and nuclear magnetic resonance spectrometry (NMR) analysis of the isolated compounds 1 and 2 and mixture 1 were performed at the University of Cape Town, South Africa. In HRMS, about 1 ml of sample-octacosane solution was introduced to the mass spectrometer by direct probe, with temperature and pressure at the

inlet system maintained at 200 °C and 0.005 Torr, respectively. Ionization was by electron impact at 4 eV and mass spectrum recorded.

2.8.5 Nuclear magnetic resonance spectroscopy

Samples were dissolved in deuterated DMSO, $CDCl_3$ or MeOD. Proton and ^{13}C-NMR spectra were recorded at 300 MHz and 600 MHz, respectively with TMS as internal standard. The δ were reported in ppm to 2 decimal places downfield from TMS. The *J* values were recorded in hertz (Hz) to one decimal place.

CHAPTER THREE: RESULTS AND DISCUSSION

3.1 Phytochemical tests

Table 3.1.below gives the phytochemical test results of the chloroform extract of the root bark of *L. eriocalx.*

Table 3.1: Phytochemical screening results

Test	Result	Inference
Test for tannins	Blue precipitate with ferric chloride	Tannins present
Dragendorff's Test	Precipitation observed	Alkaloids present
Meyer's test	A white buffy precipitate observed	Alkaloids present
Test for saponins	Persistent frothing observed	Saponins present
	Haemolysis observed in the test experiment	Saponins present
Borntrager's test	No observable color change in the ammoniacal (lower) layer	Anthraquinones absent

3.2 Yields of extracts and isolated compounds.

Table 3.2 below gives the yields of different extracts as a percentage of powdered plant material.

Table 3.2: Percentage yields of extracts.

Extract	Weight of powdered plant material (g)	Weight of the extract (g)	%Yield (as a percentage of the dry powdered plant material)
Chloroform extract	970.85	29.73	3.06
Decoction	300.05	4.97	1.66
MeOH extract	970.85	62.83	6.47
Macerate	700.28	19.30	2.76

Key: Chloroform and methanol extracts were obtained after 48 hours of soxhlet extraction hence had more yields compared to the macerate and the decoction which were extracted for only 8 hours and 5 minutes respectively.

Approximately 970.85 g of plant material gave 19.731 g of chloroform extract from which 12.5 g was loaded into the column. The weights of compounds isolated from the chloroform extract and their yields as % of loaded extract and the powdered plant material are given in table 3.3.

Table 3.3: Percentage yields of isolated compounds.

Compound/ Isolate	Weight (mg)	% Yield (relative to the loaded extract)	% Yield (relative to the powdered plant material)
Amorphous fraction I	68.20	0.54	0.01109
Compound 1	96.40	0.77	0.01567
Compound 2	1278.2	10.22	0.20781
Mixture 1	82.70	0.66	0.01344
Crystalline fraction I	2.00	0.016	0.00033

3.3 Antibacterial and antifungal activity

In both antibacterial and antifungal tests, the decoction showed the greatest activity compared to chloroform and methanol extracts, as indicated by the diameters of the zones of inhibition. The decoction exhibited activity against all the micro-organisms used. The isolated compounds 1 and 2 and mixture 1 isolated by column chromatography exhibited antibacterial and antifungal activity. The amorphous fraction I did not show activity against any of the microorganisms used.

3.3.1 Antibacterial activity

The decoction showed the broadest antibacterial spectrum, showing activity against the three micro-organisms used. Methanol and chloroform extracts lacked activity against *E. coli.* The three extracts show notable activity against *P. aeruginosa* compared to (gentamicin) with percentage diameters of the zones of inhibition ranging between 24-38%. The antibacterial potency of the decoction (100 mg/ml) was approximately 1/4 that of the gentamicin standard 0.3 mg/ml, with percentage diameters of their zones of inhibition ranging between 20-35%.

All the isolated compounds had more than 30% the activity of gentamicin. Compound 2 had the greatest activity (of the isolated compounds) with an average diameter of the zone of inhibition against the 3 micro-organisms of 1.3 cm.

3.3.2 Antifungal activity

The three extracts (decoction, methanol and chloroform extracts) showed activity against *S. cerevisiae,* the decoction showing the greatest activity with a zone of inhibition of 1.6 cm. All the extracts and isolated compounds had antifungal activity above 60% that of nystatin, as shown by their percentage diameter of the zones on inhibition. Of the isolated compounds, Compound 2 had the greatest antifungal activity, having a zone of inhibition of 1.3 cm. Compound 1 and mixture 1 had equal antifungal activity with zone of inhibition of 1.2 cm.

Table 3.4 below gives a summary of the zone of inhibition diameters of extracts and isolates (concentrations of the extracts and isolated compounds being 100 mg/ml, against 0.3 mg/ml of the standards).

Table 3.4 zones of inhibition of extracts and isolated compounds

Extracts/Isolated compounds	Zones of inhibition (cm)							
	S. aureus		*P. aeruginosa*		*E. coli*		*S. cerevisiae*	
	D	%D	D	%D	D	%D	D	%D
Decoction	1.1	34.8	1.1	32.0	1.1	20.4	1.6	86.8
Methanol extract	0.3	-	0.9	24.0	0.3	-	1.4	73.3
Chloroform extract	1.0	30.4	1.0	28.0	0.3	-	1.5	80.0
Non crystalline fraction I	0.3	-	0.3	-	0.3	-	0.3	-
Compound 1	1.0	30.4	1.2	36.0	1.1	33.3	1.2	60.0
Compound 2	1.2	39.1	1.5	48.0	1.3	47.6	1.3	66.7
Mixture 1	1.1	34.8	1.1	32.0	1.0	33.3	1.2	60.0
Gentamicin	2.6	100	2.8	100	2.4	100	-	-
Nystatin	-		-		-		1.8	100

Key: Where the zone of inhibition is 0.3 cm (which is equivalent to the diameter of the well), it means there was no activity; D=diameter of the zone of inhibition less the diameter of the well; %D= percentage diameter of the zone of inhibition; - = Test was not done [Appendices 6-7].

3.4 STRUCTURAL ELUCIDATION

Four compounds were isolated from the chloroform extract compounds 1 and 2 and mixture 1, which consisted of 2 compounds. The compounds were identified by different spectroscopic methods. Infra-red and UV data indicated the functional groups and chromophores in the compounds. The ^{13}C-NMR and ^{1}H-NMR integration indicated the number of hydrogens and carbons present in the compound. Attached proton test (APT) was used to distinguish methyl and methine carbon atoms from methylene and quaternary carbon atoms. The molecular weight was obtained from the base peak (molecular ion mass) in the high resolution mass spectral data. Comparison was made between the melting points of isolates and the documented literature values.

3.4.1 LUPENONE (compound 1)

It was isolated from fraction B as white shiny crystals in dichloromethane. This compound gave a brown TLC spot in iodine and a light purple colored spot with vanillin reagent. The crystals had a melting point of 165-167 °C (literature value: 166-170 °C) [73, 74].

The spectroscopic data of compound 1 was as follows:

IR (KBr) cm^{-1}: 2926 (CH_3, C-H str), 2856 (= C-H str), 1705 (ketone C=0 str), 1620 (C=C) and 1381 (C-Cstr) [Appendix 2a].

EI-MS (*m/z*): 424 (M^+, 100), 409 (M^+- CH_3, 76.4), 396 (40.8), 394 (20.9), 365 (12.5), 368 (34.5), 341 (2.7), 314 (56.0), 313 (59.8), 271 (12.6), 219 (44.8), 245 (44.0), 218 (65.4), 206 (54.6), 205 (76.6), 204 (52.4), 203 (52.0), 189 (46.8), 149 (38.2), 109 (40.2) [Appendices 2b-1, b-2, b-3].

^{1}H-NMR (300 MHz, $CDCl_3$) δ: 0.82 (3H, s, H-27), 0.96 (3H, s, H-25), 0.98 (3H, s, H-28), 1.05 (3H, s, H-23), 1.10 (3H, s, H-26), 1.28 (3H, s, H-24), 1.53 (2H, m, H-2), 1.71 (3H, s, H-30), 1.90-1.95 (1H, m, H-19), 2.40-2.51 (1H, m, H-19), 4.60 (1H, d, *J*=1.9 Hz, H-29b) and 4.71 (1H, d, *J*=1.9 Hz, H-29a) [Appendices 2c-1, c- 2, c-3].

^{13}C-NMR (600 MHz, $CDCl_3$) δ ppm: 39.63 (C-1), 34.15 (C-2), 218.10 (C-3), 47.33 (C-4), 54.96 (C-5), 19.70 (C-6), 33.60 (C-7), 40.81 (C-8), 49.82 (C-9), 36.90 (C-10), 21.50 (C-11), 25.19 (C-12), 38.21 (C-13), 42.91 (C-14), 27.45 (C-15), 35.54 (C-16), 43.00 (C-17), 48.28 (C-18), 47.97 (C-19), 150.87 (C-20), 29.86 (C-21), 39.99 (C-22), 26.67 (C-23), 21.04 (C-24), 15.96 (C-25),

15.80 (C-26), 14.49 (C-27), 18.02 (C-28), 109.39 (C-29) and 19.32 (C-30) [Appendices 2d-1, d-2].

The mass spectrum shows a molecular ion at *m/z* 424 as the base peak. The molecular weight of 424 corresponds to the molecular formula of $C_{30}H_{48}O$. Fragmentation of the molecular ion by removal of a methyl and a C_6H_{10} group produces fragment ions of *m/z* 409 and 341, respectively. The fragment ion at *m/z* 409 further fragments by losing $CH_2{=}CH_2$ group to yield a fragment ion at *m/z* 381. This fragmentation pattern is in agreement with the fragmentation pattern for steroidal systems in the literature [75, 76] [Appendices 2b-1, b-2, b-3].

The IR spectrum shows the presence of an aliphatic system, 2926 cm^{-1} and 2856 cm^{-1}, which are due to methyl and methylene C-H stretch vibrations, respectively. The broad peak at 1705 cm^{-1} is due to the ketone on C_3. Ketones in a 6-membered cyclic system vibrate between 1705- 1725 cm^{-1} [71]. The peak at 1460 and 1381 cm^{-1} are due to methyl and ethylene C-H bending vibrations, respectively [Appendix 2a].

In ^{1}H-NMR spectrum, the 7 singlets at δ 0.82, δ 0.96 and δ 0.98, δ 1.05, δ 1.10, δ 1.28 and δ 1.71 correspond to methyl protons on carbons 27, 25, 28, 23, 26, 24 and 30 respectively. Of the 7 methyl protons, C_{30} protons are the most downfield due to their proximity to the C_{20}-C_{29} double bond.

The conformation around C_4 makes the gem-dimethyl protons on carbons 23 and 24 to be magnetically non-equivalent giving separate peaks at δ 0.99 and 0.78, respectively [77]. Their downfield shift from the other methyl protons is due to the electronegativity of the C_3 carbonyl group. The C_3 keto group also gives the proximal C_2 methylene protons a dowfield shift giving the multiplet at δ 1.53 [78].

The 2 peaks at δ 4.60 and δ 4.71 represent the exocyclic double bond protons on C_{29} (H-29b and H-29a, respectively). A proton attached to an unsaturated system will have an approximate chemical shift between δ 4.5- 6.0. These protons couple with each other with a *J* value of 1.9 Hz which is characteristic of geminal vinylic protons [78]. The C_{20}-C_{29} double bond prohibits free rotation of the carbons hence making them magnetically non-equevalent and also makes them

highly deshielded [79]. The C_{20}-C_{29} double bond also deshields the C_{19} methine and C_{21} ethylene protons giving the multiplets at δ 2.40-2.51 and 1.90-1.95, respectively [Appendices 2c-1, c- 2, c-3].

The ^{13}C-NMR spectrum showed a total of 30 peaks corresponding to a total of 30 carbons. This is in agreement with the formula $C_{30}H_{48}O$. The chemical shift at δ 218.08 is due to C_3 keto-group. Carbonyl groups in a cyclic aliphatic system resonate between δ 205- 220 [79]. The peaks at δ 150.87 and 109.39 are due to two sp^2 hybridized carbons 20 and 29, respectively. Alkenyl carbons are deshielded and resonate at low field between δ110-150 [78]. The triplet at δ 77.00 is due to deuterated methanol which was used as the solvent [Appendices 2d-1, d-2]. Figure 3.1 shows the chemical structure of lupenone.

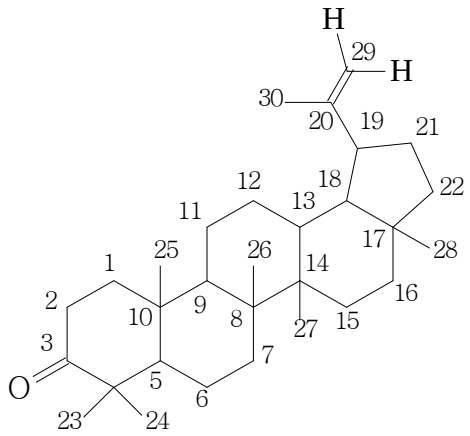

Figure 3.1 Chemical structure of Lupenone

Based on the above spectroscopic data which was in agreement with the literature values [73, 74, 80, 81], compound 1 was concluded to be lupenone. The other carbon atoms and protons were therefore assigned chemical shifts by comparison with figures for lupenone in the literature.

Tables 3.5 and 3.6 compares proton and carbon values, respectively, of compound 1 with literature values of lupenone.

Table 3.5: Comparison of ^{1}H-NMR δ values of compound 1 with literature values of lupenone.

Proton	Chemical shifts for compound 1	Lupenone literature values	
		[80]	[82]
1	0.92 (2H,m)	-	1.6 (m), 0.92 (m)
2	1.53 (2H,m)	-	1.55 (m)
5	-	-	0.6 (m)
6	1.49-1.53 (2H,m)	-	1.40 (m), 1.51 (m)
7	1.32-1.35 (2H,m)	-	1.34 (m)
9	1.24 (2H,m)	-	1.22 (dd, J= 2.7,12.9 Hz)
11	1.39-1.42 (2H,m)	-	1.40 (m), 1.12 (m)
12	1.08 (2H,m)	-	1.64 (m), 1.08 (dd, J=4.8,13.3 Hz)
13	1.67 (1H,m)	-	1.64 (m)
15	1.74 (2H,m)	-	1.71 (m), 1.01(ddd, J=2.5,4.2,13.8 Hz)
16	1.44-1.48 (2H,m)	-	1.47 (ddd,J=2.7,4.5,12.9 Hz)
18	1.36 (2H,m)	-	1.35 (m)
19	2.40-2.51 (1H, m)	2.24-2.52 (1H, m)	2.4 (ddd, J=5.8,11.1,11.1 Hz)
21	1.90-1.95 (1H, m)	1.84-1.97 (1H, m)	2.03(dddd, J=8.6, 10.5,10.5,13.5 Hz; 1.31(m)
22	1.39-1.42 (2H,m)	-	1.37 (m), 1.20 (m)
23	1.05 (3H, s)	1.04 (3H, s)	0.92
24	1.28 (3H, s)	1.00 (3H, s)	0.74
25	0.96 (3H, s)	0.90 (3H, s)	0.84
26	1.10 (3H, s)	1.22 3H, s)	1.04
27	0.82 (3H, s)	0.93 (3H, s)	0.97
28	0.98 (3H, s)	0.77 (3H, s)	0.79
29	4.71 (1H, d, *J*=1.9 Hz, H-29a);	4.66 (1H, s, H-29a)	
	4.60 (1H, d, *J*=1.9 Hz, H-29b)	4.55 (1H, s, H-29b)	4.74 (d,J=2.5); 4.60 (ddd, J=1.3,2.6,2.7 Hz)
30	1.71 (3H, s)	1.66 (3H, s)	1.68 (m)

Table 3.6: Comparison of ^{13}C-NMR δ values of compound 1 and literature values of lupenone [80].

Carbon	Compound 1	Lupenone	Carbon	Compound 1	Lupenone
1	39.63	39.6	16	35.54	35.5
2	34.15	34.1	17	43.00	42.9
3	218.10	218.2	18	48.28	48.2
4	47.33	47.3	19	47.97	47.9
5	54.96	54.9	20	150.86	150.8
6	19.70	19.2	21	29.86	29.6
7	33.60	33.5	22	39.99	39.6
8	40.82	40.7	23	29.70	26.6
9	49.82	49.7	24	21.04	21.0
10	36.90	36.8	25	15.96	15.9
11	21.50	21.4	26	15.80	15.7
12	25.19	25.1	27	14.49	14.4
13	38.21	38.1	28	18.02	17.9
14	42.91	42.8	29	109.39	109.3
15	27.45	27.4	30	19.32	19.6

The attached proton test (APT) - NMR distinguishes methylene and quaternary peaks from methyl and methine peaks. Methylene and quaternary peaks are due to carbons 1, 2, 3, 4, 6, 7, 8, 10, 11, 12, 14, 15, 16, 17, 20, 21, 22 and 29 while methyl and methine peaks are due to carbons 5, 9, 13, 18, 19, 23, 24, 25, 26, 27, 28 and 30 (Appendix 2e-1, e-2). This is in agreement with the chemical structure of lupenone. The proposed fragmentation for lupenone is shown in figure 3.2.

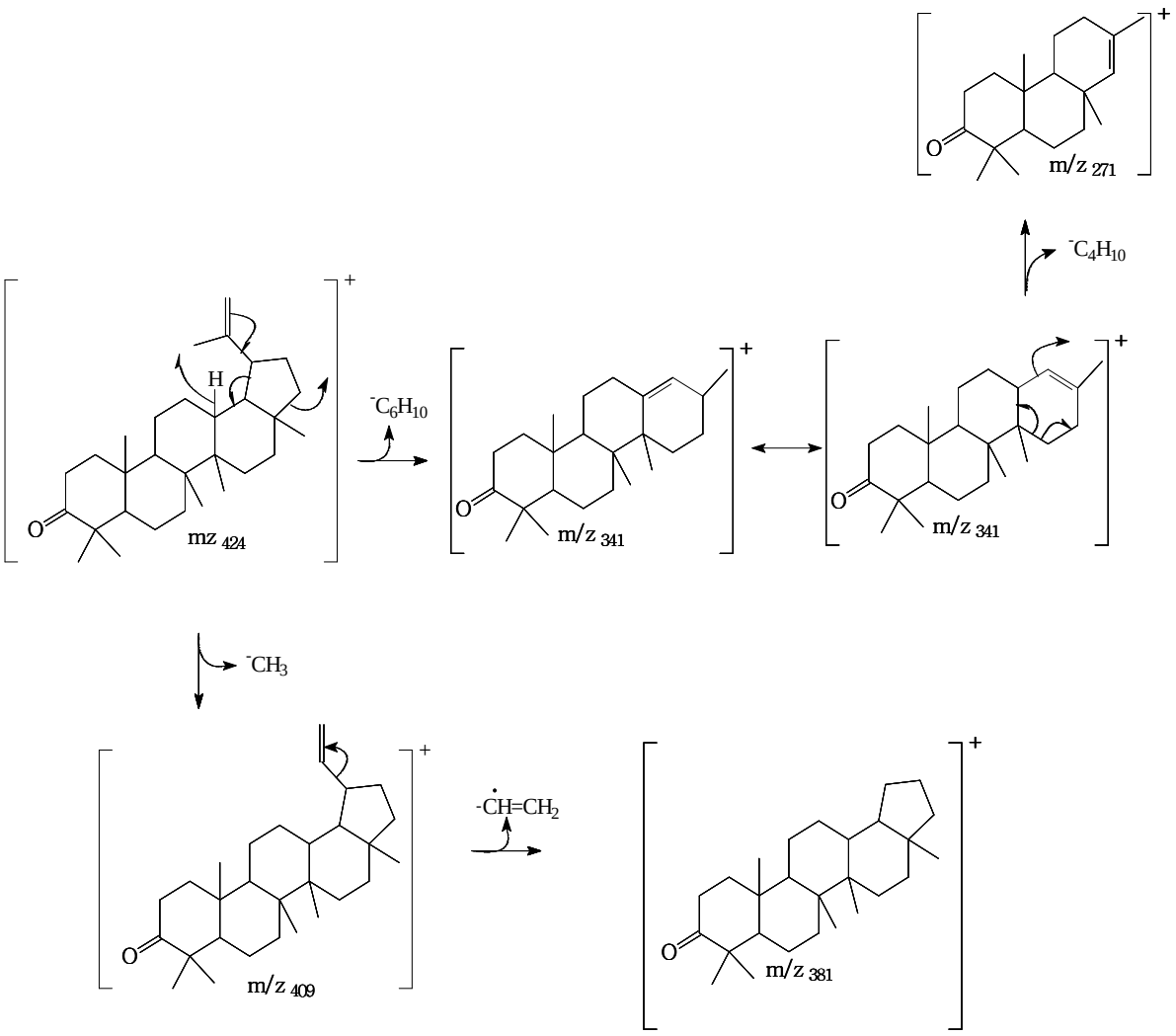

Figure 3.2: Proposed fragmentation pattern of lupenone [75].

3.4.2 LUPEOL (COMPOUND 2)

Compound 2 had white flabby crystals in chloroform. The crystals gave a brown TLC spot in iodine and a deep purple spot in vanillin reagent. The crystals had a melting point: 211-213 °C (literature value: 212-214 [83].

The spectroscopic data was as follows:

IR (KBr) cm^{-1}: 3356 (O-H str), 2939 (CH_3, C-H str), 2872 (CH_2, str), 1643 (C=C str), 1458 (CH_3, C-H bend), 1377 (CH_2, bend), 1055 (cycloalkane) and 879 (=C-H bend) [Appendix 3a].

EI-MS (*m/z*): 426 (M^+, 100), 411 (M^+-CH_3, 42.5), 409 (M^+-OH, 74), 397 (53.0), 396 (83.6), 394 (47.2), 365 (20.9) 344 (9.4), 207 (59.3), 205 (46.9), 204 (49.6), 203 (53.1), 218 (63.5), 191 (49.6), 190 (46.5), 189 (57.5), 135 (44.0), 121 (40.4) [Appendices 3b-1, b-2, b-3].

^{1}H-NMR (300 MHz, $CDCl_3$) δ: 0.69 (1H, m, H-5), 0.78 (3H, s, H-24), 0.81 (3H, s, H-28), 0.86 (3H, s, H-25), 0.97 (3H, s, H-27), 0.99 (3H, s, H-23), 1.06 (3H, s, H-26), 1.62 (1H, m, H-2), 1.71 (3H, s, H-30), 1.91-1.95 (2H, m, H-21), 2.36-2.43 (1H, m, H-19), 3.20 (1H, dd, *J*=3.4, 8.4 Hz, 8.4 Hz, H-3), 4.60 (1H, d, *J*=1.9 Hz, H-29b) , 4.71 (2H, d, *J*=1.9 Hz, H-29a) [Appendices 3c-1, 3c-2].

^{13}C-NMR (600 MHz, $CDCl_3$) δ ppm: 38.75 (C-1), 27.45 (C-2), 79.01 (C-3), 38.88 (C-4), 55.35 (C-5), 18.35 (C-6), 34.33 (C-7), 40.87 (C-8), 50.49 (C-9), 37.21 (C-10), 20.97 (C-11), 25.19 (C-12), 38.10 (C-13), 42.86 (C-14), 27.49 (C-15), 35.61 (C-16), 43.02 (C-17), 48.35 (C-18), 48.00 (C-19), 150.95 (C-20), 29.89 (C-21), 40.03 (C-22), 28.01 (C-23), 15.38 (C-24), 16.13 (C-25), 16.01 (C-26), 14.57 (C-27), 18.03 (C-28), 109.33 (C-29), 19.33 (C-30) [Appendices 3d-1, d-2].

The IR spectrum shows the presence of OH group (3340 cm^{-1}, O-H stretch) and an aliphatic system (2945 cm^{-1} and 2870 cm^{-1} which are due to methyl and methylene C-H stretch vibrations, respectively). The peak at 1641 cm^{-1} indicates a non-conjugated C=C in the side chain while =C-H bend vibrations give the peak at 879 cm^{-1}. Methyl and methylene bend vibrations are responsible for peaks at 1458 cm^{-1} and 1375 cm^{-1}, respectively, [71] [Appendix 3a].

The MS data shows a molecular ion at *m/z* 426 as the base peak. The molecular weight of 426 corresponds to the molecular formula of $C_{30}H_{50}O$. Fragmentation of the molecular ion by

removal of a methyl and a C_6H_{10} group produces fragment ions of *m/z* 411 and 344, respectively. The fragment ion at *m/z* 411 further fragments by losing CH_2=CH_2 group to yield a fragment ion at *m/z* 383 which further fragments by losing water molecule to produce a fragment ion at *m/z* 365. This fragmentation pattern corresponds to the fragmentation pattern for steroidal compounds in the literature [75, 76] [Appendices 3b-1, b-2, b-3].

In ^{1}H-NMR spectrum, the peak at δ 0.69 was attributed to C_5 proton. The 6 singlets at δ 0.99, 0.78, 0.86, 1.06, 0.97 and 0.81 are due to the 6 methyl protons attached to carbons 23, 24, 25, 26, 27 and 28, respectively. The methyl protons on C_{30} resonate downfield at δ 1.71 due to the effect of C_{20}-C_{29} double bond. There are 2 peaks at δ 4.59 and δ 4.71 which are due to the C_{29} axial and equatorial protons (H-29b, H-29a), respectively [84]. These protons couple with each other with a *J* value of 1.9 Hz which is characteristic of geminal vinylic protons [78]. They were highly deshielded by C_{20}-C_{29} double bond [84]. The C_{20}-C_{29} double bond deshields C_{19} and C_{21} protons giving multiplets at δ 2.36-2.43 and δ 1.91-1.95, respectively.

The C_2 and C_3 protons, due to electro-negativity of oxygen on C_3, resonate downfield at δ 1.62 and 3.20, respectively. The peak at δ 3.66 is due to the hydroxyl proton on C_3 [85] [Appendices 3c-1, 3c-2].

The ^{13}C-NMR spectrum showed a total of 30 peaks corresponding to a total of 30 carbon atoms. This is in agreement to the formula $C_{30}H_{50}O$. The chemical shifts at δ 150.95 and 109.33 are due to two sp^2 hybridized carbons 20 and 29, respectively. Alkenyl carbons (sp^2-hybridized carbons) have chemical shifts between δ 80- 180 [76]. The peak at δ 79.00 was assigned to C_3 [84]. The 3 peaks δ 77.01 are due isotopic impurity of $CDCl_3$ [81] [Appendices 3d-1, d-2].

Based on the above spectroscopic data which was in agreement with literature values [83, 84, 85], compound 2 was concluded to be lupeol. The other protons and carbon atoms were therefore assigned chemical shifts by comparison with figures of lupeol in the literature, as shown in table 3.7 and 3.8, respectively.

Table 3.7: Comparison of ^{1}H-NMR δ values of compound 2 with literature values of lupeol [86].

Proton	Chemical shifts	Literature values	Proton	Chemical shifts	Literature values
1	1.68 (1H, m)	1.64 (1H, m, H-1a); 0.91 (1H, m, H-1b)	18	-	1.39 (1H, m)
2	1.62 (1H, m)	1.61 (1H, m)	19	2..36-2.43 (1H, m,)	2.38 (1H, m)
3	3.20 (1H, dd, J= 3.4; 8.4 Hz)	3.18 (1H, dd, *J*=11.0, 5.3 Hz)	21	1.91-1.95 (2H, m)	1.27 (1H, m, H-21a) 1.93 (1H, m, H-21b)
5	0.69 (1H, m)	0.66 (1H, m)	22	1.20 (2H, m)	1.19 (1H, m)
6	-	1.52 (1H, m, H-6a); 1.39 (1H, m, H-6b)	23	0.99 (3H, s)	0.97 (1H, s)
7	1.39 (2H, m)	1.38 (1H, m)	24	0.78 (3H, s)	0.77(1H, s)
9	-	1.30 (1H, m)	25	0.86 (3H, s)	0.84 (1H, s)
11	1.43 (1H, m)	1.43 (1H, m, H-1a); 1.29 (1H, m, H-11b)	26	1.06 (3H, s)	1.04 (1H, s)
12	1.74 (1H, m, H-12a) 1.22 (1H, m, H-12b)	1.70 (1H, m, H-12a); 1.10 (1H, m, H-12b)	27	0.97 (3H, s)	0.96 (1H, s)
13	-	1.62 (1H, m)	28	0.81(3H, s)	0.80 (1H, s)
15	-	1.61 (1H, m, H-15a); 0.96 (1H, m, H-15b)	29	4.71(1H, d, *J*=1.9 Hz, H-29a); 4.60 (1H, d, *J*=1 .9 Hz, H-29b)	4.68 (1H, s, H-29a); 4.56 (1H, s, H-29b)
16	1.49 (2H, m)	1.48 (1H, m)	30	1.70 (3H, s)	1.70 (1H, s)

Table 3.8: Comparison of ^{13}C-NMR δ values of compound 2 with literature values of lupeol [84].

Carbon	Compound 2	Lupeol	Carbon	Compound 2	Lupeol
1	38.75	38.67	16	35.61	35.54
2	27.45	27.35	17	43.02	42.95
3	79.00	78.94	18	48.35	48.24
4	38.88	38.81	19	48.00	47.94
5	55.35	55.25	20	150.95	150.88
6	18.35	18.28	21	29.89	29.80
7	34.33	34.23	22	40.03	39.96
8	40.87	40.78	23	28.01	27.95
9	50.49	50.38	24	15.38	15.35
10	37.21	37.11	25	16.13	16.09
11	20.97	20.89	26	16.01	15.94
12	25.19	25.08	27	14.57	14.51
13	38.10	38.00	28	18.03	17.97
14	42.86	42.78	29	109.33	109.31
15	29.71	27.41	30	19.33	19.28

The APT-NMR supports the allocation of peaks as above. It gives negative methylene and quaternary carbon atom peaks and positive methyl and methine carbon peaks (appendix 3e-1, e-2). Methylene and quaternary peaks are due to carbons 1, 2, 3, 4, 6, 7, 8, 10, 11, 12, 14, 15, 16, 17, 20, 21, 22 and 29. Methyl and methine peaks are due to carbons 5, 9, 13, 18, 19, 23, 24, 25, 26, 27, 28 and 30. Figures 3.3 and 3.4 below give the chemical structure and the proposed fragmentation pattern for lupeol, respectively.

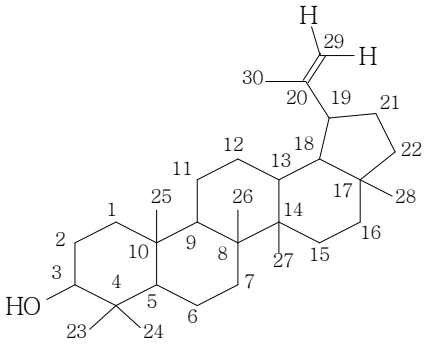

Figure 3.3: Molecular structure of lupeol

.

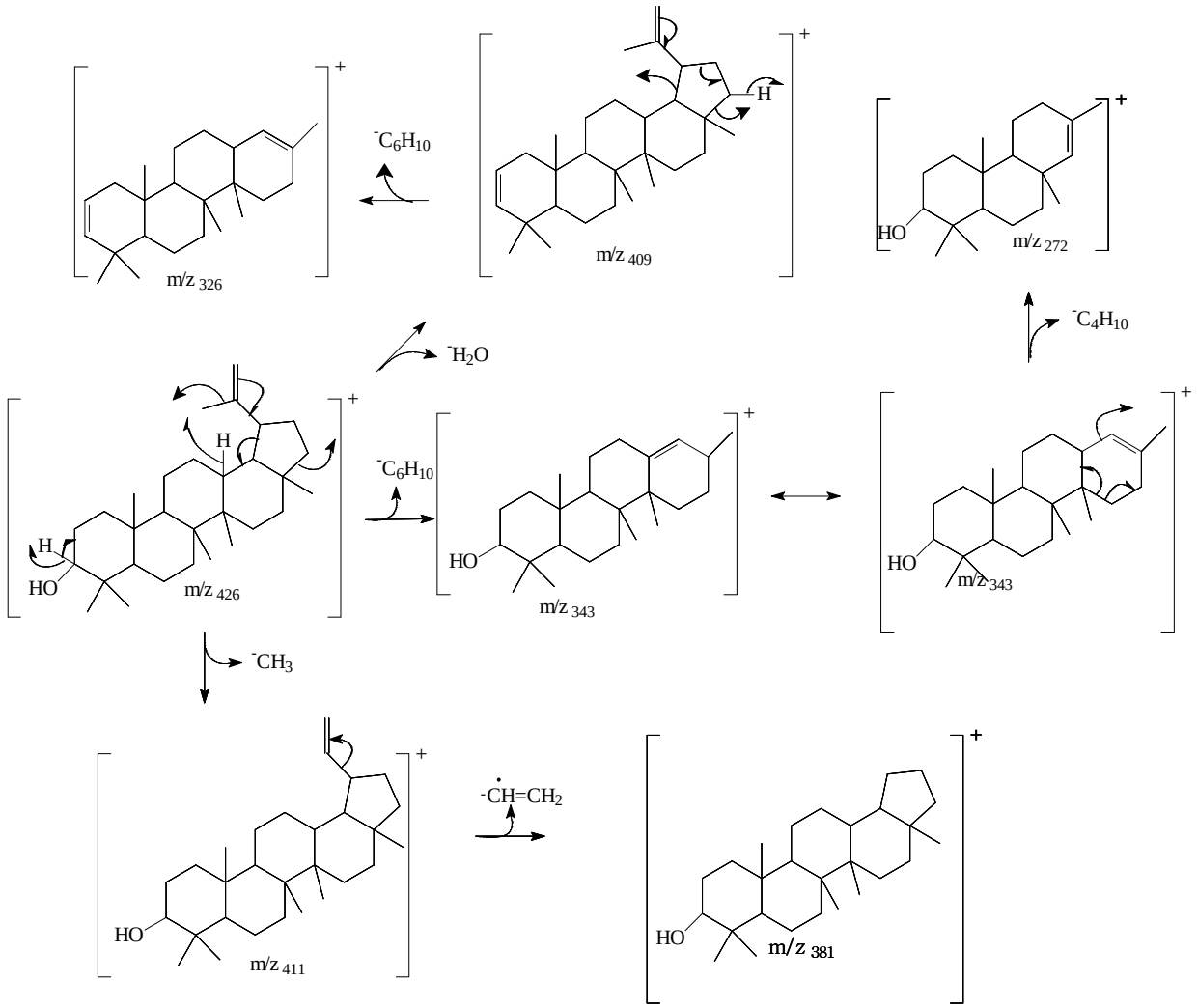

Figure 3.4: Proposed fragmentation pattern of lupeol.

3.4.3 β- SITOSTEROL AND STIGMASTEROL (MIXTURE 1)

Mixture 1 was isolated as colorless/shiny needle-like crystals in dichloromethane. The crystals gave a single TLC spot that was yellow in iodine and brown in vanillin reagent.

The spectroscopic data was as follows:

IR ν max (KBr) cm^{-1}: 3431.36 (O-H str), 2945.51 (C-H str), 2858.51 (=C-H stretch), 1651.07 (C=C str), 1462.04 (CH_3, bend), 1375.25 (CH_2, bend), 1055.06 and 962.48 (molecular vibrations) [appendix 4a].

EI-MS (*m/z)*: 414 ([M^+, 100), 412 (97) 409 (M^+-CH_3, 21.9), 400 (64.9), 396 (M^+-OH, 83.7), 394 (29.9), 382 (36.6), 381 (44.4), 369 (41.5), 329 (48.4), 303 (50.4), 300 (55.8), 273 (50.1), 272 (45.4), 271 (56.0), 255 (60.9), 231 (33.5), 213 (44.9), 163, (33.8), 147 (36.8), 145 (39.2), 123 (32.7), 121 (30.3), 107 (33.4), 105 (31.1), 97 (30.4), 95 (30.5), 81 (30.3) [Appendices 4b-1, b-2, b-3].

^{1}H-NMR ($CDCl_3$, 300 MHz): δ 0.71, 0.72 (3H, s, H-18), 0.85 (3H, d, *J*=1.1 Hz, H-26), 0.87 (3H, t, J= 1.1 Hz, H-29), 0.94 (3H, d, H-21), 1.04, 1.28 (3H, s, H-19), 2.25-2.31 (2H, m, H-4), 3.52-3.58 (1H, m, H-3), 5.07 (1H, dd *J*=6.3 Hz, H-23), 5.19 (1H, dd *J*=4.9, 11.4 Hz, H-22), 5.38 (1 H, t, *J*=1.9, 3.4 Hz, H-6), [Appendices 4c-1, c-2].

^{13}C-NMR (600 MHz, $CDCl_3$): δ 37.29 (C-1), 31.69 (C-2), 71.82 (C-3), 42.24, 42.33 (C-4), 140.78 (C-5), 121.71 (C-6), 29.70, 31.94 (C-7), 31.92 (C-8), 50.18, 50.20 (C-9), 36.53 (C-10), 21.11 (C-11), 39.71, 39.81 (C-12), 42.35 (C-13), 56.80, 56.90 (C-14), 24.32, 24.38 (C-15), 28.25, 28.90 (C-16), 56.01, 56.10 (C-17), 11.87,11.99 (C-18), 18.99, 19.06 (C-19), 36.16, 40.47 (C-20), 18.79, 21.22 (C-21), 33.98, 138.31 (C-22), 26.16, 129.32 (C-23), 45.89, 51.25 (C-24), 29.21, 31.89 (C-25), 19.40 (C-26), 19.06, 19.81 (C-27), 23.11, 25.40 (C-28), 12.06, 12.23 (C-29) [Appendices 4d-1, d-2].

Infrared spectroscopic data showed a broad peak at 3431cm^{-1} which could be attributed to a hydroxyl group (O-H). The broadening of the peak may be due to hydrogen bonding. Methyl and methylene C-H stretch is responsible for the peaks observed at 2946 cm^{-1} and 2850 cm^{-1},

respectively. The peak observed at 1651 cm^{-1}corresponds to C=C stretch which occurs between 1680-1620 cm^{-1}. Methyl and ethylene bending vibrations give the peaks at 1452 cm^{-1} and 1375 cm^{-1}, respectively. Molecular vibrations fall in the finger print region (1430-900 cm^{-1}) and are responsible for the peaks at 1055 cm^{-1} and 962 cm^{-1} [73] [appendix 4a].

In mass spectrometry, a molecular ion peak (M, 100%) was observed at m/z 414 which is in agreement with the molecular formulae $C_{29}H_{50}O$. A major peak (97%) was observed at m/z 412. This is consistent with the molecular formulae $C_{29}H_{48}O$. The observed fragmentation pattern giving fragments at m/z 414, 412, 400, 396, 394, 386, 381, 287, 271, 255, 213, 173 and 145 is characteristic of the fragmentation pattern of steroidal systems [76]. The fragment at m/z 400 corresponds to loss of a C_{18} angular methyl group from the molecular ion. Loss of a water molecule from the molecular ion formed the fragment ion with m/z 396 while that at m/z 386 corresponds to loss of an ethyl group at C_{24} from the molecular ion. Fragmentation of ion m/z 397 between C_{17} and C_{20} gave fragment ion with m/z 255 whose ring D further fragments to give fragment ion m/z 213 [87][88]. [Appendices 4b-1, b-2, b-3].

The ^{1}H- NMR, shows a triplet at δ 5.38 which is due to olefinic proton at C_6. The olefinic protons on C_{22} and C_{23} resonated downfield at δ 5.19 and 5.07, respectively. The multiplets at δ 3.52-3.58 and 2.25-2.31 were attributed to the OH proton attached to C_3 and the methylene protons on C_4, respectively. The methine proton on C_{20} gave the multiplet at δ 2.00-2.05. These protons (C_3 / C_4 and C_{20}) are expected to be deshielded due to the effect of the C_3-OH and the C_{22}= C_{23} double bonds, respectively. The two singlets at δ 0.71 and δ 1.04 accounting for 3 protons each are due to methyl protons at C_{18} and C_{19}, respectively. Methyl protons on C_{21} and C_{26} gave the doublets at δ 0.94 and 0.85, respectively [Appendices 4c-1, c-2].

The ^{13}C-NMR spectrum shows about 39 peaks. Several near-overlap peaks and enhanced peak heights show probability of a mixture. The peak at δ 140.78 was assigned to C_5 while that at δ 121.71 was assigned to C_6. Carbons C_{22} and C_{23} are responsible for the peaks at δ 138.31 and 129.32 respectively. The 4 carbons (C_5, C_6, C_{22} and C_{23}) are deshielded due to sp^2 hybridization. Alkenyl carbons are deshielded and resonate at low field between δ110-150 [77].

The peak at δ 71.82 was assigned to C_3, which was deshielded by the neighbouring OH group. Primary carbons are highly shielded. For this reason, the primary carbons C_{18}, C_{19}, C_{21}, C_{26}, C_{27} and C_{29} were the most upfield carbons at δ11.87, 18.99, 18.79, 19.40, 19.06 and 12.06 [77].]. Carbon 18 was assigned the peak at δ 11.99 as it experienced most shielding effect, being farthest from the C_5=C_6 and C_{22}=C_{23} double bond as compared to the other methyl carbons. [Appendices 4d-1, d-2].

Based on the above spectroscopic data which was in agreement with those reported in the literature [85, 89, 90, 91, 92], it was concluded that the mixture 1 contained β-sitosterol and stigmasterol.

According to the literature β-sitosterol and Stigmasterol exist, in most cases, as a mixture which may have a greater portion of stigmasterol as compared to β-sitosterol [90]. The two differ only by the bonding between C_{22} and C_{23} where stigmasterol has a double bond while β-sitosterol has a single bond. Stigmasterol and beta-sitosterol have the same R_f value and therefore difficult to separate. Furthermore, literature has shown that β-sitosterol is hard to isolate in a pure state [90]. There are many examples of these compounds having been isolated together in the literature [88, 89, 90]. Figure 3.5 shows the chemical structures of β-sitosterol.

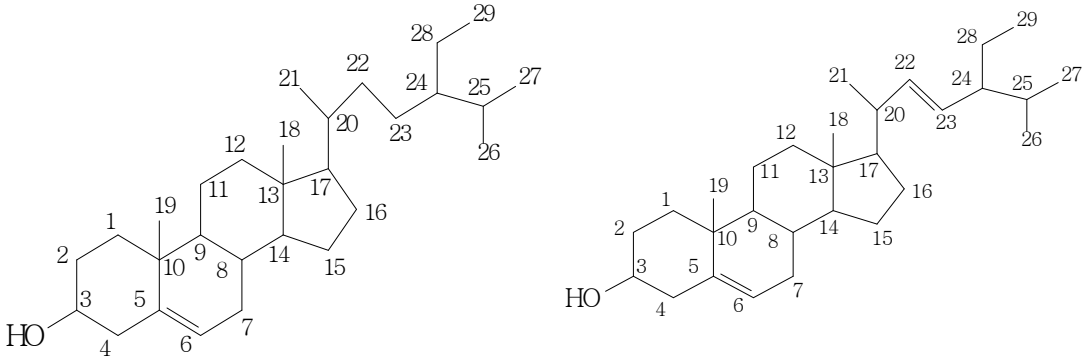

β-sitosterol Stigmasterol

Figure 3.5: Chemical structure of β-sitosterol and stigmasterol

The other carbon atoms and protons were assigned δ values by comparison with literature values for β-sitosterol and stigmasterol, as shown in table 3.9 and 3.10, respectively. Figure 3.6 shows the proposed fragmentation pattern for β-sitosterol in mixture 1.

Table 3.9: Comparison of ^{1}H-NMR δ values of mixture 1 with literature values of β-sitosterol and stigmasterol.

^{1}H	Chemical shift	B-sitosterol literature values		Stigmasterol literature values	B-sitosterol/ stigmasterol mixture literature values
		[91]	[93]	[94]	[95]
1	1.09-1.10 (2H,m)		1.46 (2H,m)	1.32, 1.56	1.08,183
2	1.50-1.56 (2H,m)		1.56 (2H,m)	0.80, 2.10	1.49,1.82
3	3.541-3.58 (1H, m)	3.53 (1H, m)	3.54(1H,m)	3.17 (1H, m)	3.53(1H, m)
4	2.25-2.31 (2H, m)	2.25 (2H, m)	2.32 (2H,m)	1.84, 2.76	2.24,2.28
6	5.38 (1H, t, *J*=3.4 Hz)	5.38 (1H, m)	5.37 (1H,t)	5.30 (1H,t)	5.35 (1H,d,J=4.7Hz)
7	2.00-2.04 (2H,m)	-	2.04 (2H,m)	1.62, 2.34	1.53,1.98
8	-	-	1.69 (1H,m)	1.34 (1H,m)	1.46 (1H,m)
9	-	-	1.55 (1H,m)	2.10	0.94
11	-	-	1.52 (2H,m)	0.84, 1.84	1.45,1.48
12	-	-	1.51 (2H,m)	0.95, 1.34	1.15,1.97
14	-	-	1.50 (1H,m)	1.07	1.00
15	-	-	1.58 (2H,m)	1.53, 2.18	1.06,1.55
16	1.86-1.89 (2H,m)	-	1.85 (2H,m)	1.53, 2.18	1.27,1.71
17	-	-	1.45 (1H,m)	1.56	1.13
18	0.71[a] (3H,s), 0.72[b] (3H,s)	0.68 (3H, s)	0.70 (3H,s)	1.36	1.70 (3H,s)
19	1.04[a], 1.28[b] (3H, s)	1.00 (3H, s)	1.03 (3H,s)	0.71 (t, J=7.5 Hz)	1.01 (3H,s)
20	-	-	1.60 (1H,m)	0.68 (s)	2.04
21	0.94 (3H, d, J= * Hz)	0.91 (3H, d, *)	0.94 (3H,d)	1.18 (s)	1.02 (3H,d,J=6.8Hz)

22	5.19 (1H, dd, *J*=4.9, 11.4 Hz)	5.19 (1H, dd, *J*= *, 11.4 Hz)	0.93 (2H,m)	5.24	5.15 (1H,dd, J=8.4,15.1 Hz)
23	5.07 (1H, dd, *J*=6.2, J= * Hz)	5.07 (1H, dd, *J*=6.3, * Hz)	1.15 (2H,m)	5.24	5.02 (1H,dd, J=8.4,15.1 Hz)
24	1.30 (1H,m)	-	1.38 (1H,m)	1.53 (d, J=7.5 Hz)	1.53
25	1.57 (1H,m)	-	1.57 (1H,m)	1.84	1.44
26	0.85 (3H, d, *J*=1.1 Hz)	-	0.84 (3H,d)	0.92 (d, J=6.5 Hz)	0.84 (3H,d,J=6.4Hz)
27	0.81 (3H,d, J= * Hz))	0.85 (3H, d, *)	0.86 (3H,d)	0.86 (d, J=6.5 Hz)	0.83 (3H,d,J=6.1Hz)
28	1.14 (2H,m)	-	1.10 (2H,m)	1.44	1.15
29	0.88 (3H, t, J=2.6 Hz)	0.81 (3H, m)	0.82 (3H,t)	1.00	0.80 (3H,t,J=6.0 Hz)

Key: The superscripts ‘a’ and ‘b’ represent δ values for β-sitosterol and stigmasterol, respectively, where there is no overlap. The asterisk (*) in the literature columns shows that the *J* value was not given in the literature. Only one J value is given for the doublet of doublet at δ 5.07 (H-23) because two of the daughter peaks on the spectra are not labeled. No *J* value is given for the doublet at 0.94 (corresponding to H-21, marked with an asterisk) for the same reason. It was not possible to identify all the proton peaks in this mixture due to low resolution of the equipment used.

Table 3.10: Comparison of ^{13}C-NMR δ values of mixture 1 with literature values of β-sitosterol/stigmasterol [88].

Carbon	Compound 3	Literature values	
		β-sitosterol	Stigmasterol
1	37.29	37.48	37.48
2	31.69	31.86	31.86
3	71.82	72.03	72.03
4	42.24[a], 42.33[b]	42.51	42.51
5	140.78	140.97	140.97
6	121.71	121.95	121.95
7	29.70[a], 31.94[b]	32.13	32.13
8	31.92	32.13	32.13
9	50.18[a], 50.20[b]	50.35	50.35
10	36.53	36.73	36.73
11	21.11	21.31	21.31
12	39.71[a], 39.81[b]	39.99	39.91
13	42.35	42.51	42.51
14	56.80[a], 56.90[b]	56.99	57.09
15	24.32[a], 24.38[b]	24.53	24.53
16	28.25[a], 28.80[b]	28.48	29.15
17	56.01[a], 56.17[b]	56.17	56.17
18	11.87[a], 11.99[b]	12.09	12.09
19	18.99[a], 19.06[b]	19.63	19.26
20	36.16[a], 40.47[b]	36.38	40.74
21	18.79[a], 21.22[b]	19.01	21.45
22	33.98[a], 138.31[b]	34.16	138.56
23	26.16[a], 129.32[b]	26.27	129.49
24	45.89[a], 51.25[b]	46.04	51.47
25	29.21[a], 31.89[b]	29.36	32.13
26	19.40	20.06	19.63
27	19.06[a], 19.81[b]	19.26	20.06
28	23.11[a], 25.40[b]	23.28	25.64
29	12.06[a], 12.23[b]	12.21	12.49

Key: The superscripts ‘a’ and ‘b’ represent values for β-sitosterol and stigmasterol, respectively, where there is no peak overlap. For carbons 1, 2, 3, 5, 6, 8, 10, 11, 13 and 26, there was peak overlap.

The APT-NMR spectrum (appendix 4e-1, e-2) gives a clear view of this picture, showing which carbon atoms give paired peaks. The position of methyl and methine carbon peaks against

methylene and quartenary carbon peaks in the APT-NMR spectra agrees with the data in the table above.

The proposed fragmentation pattern of β-sitosterol is shown in figure 3.6 below. Stigmasterol fragments in a similar manner giving either the same fragments or two mass units less than those of β-sitosterol when the side chain forms part of the daughter ion fragment structure.

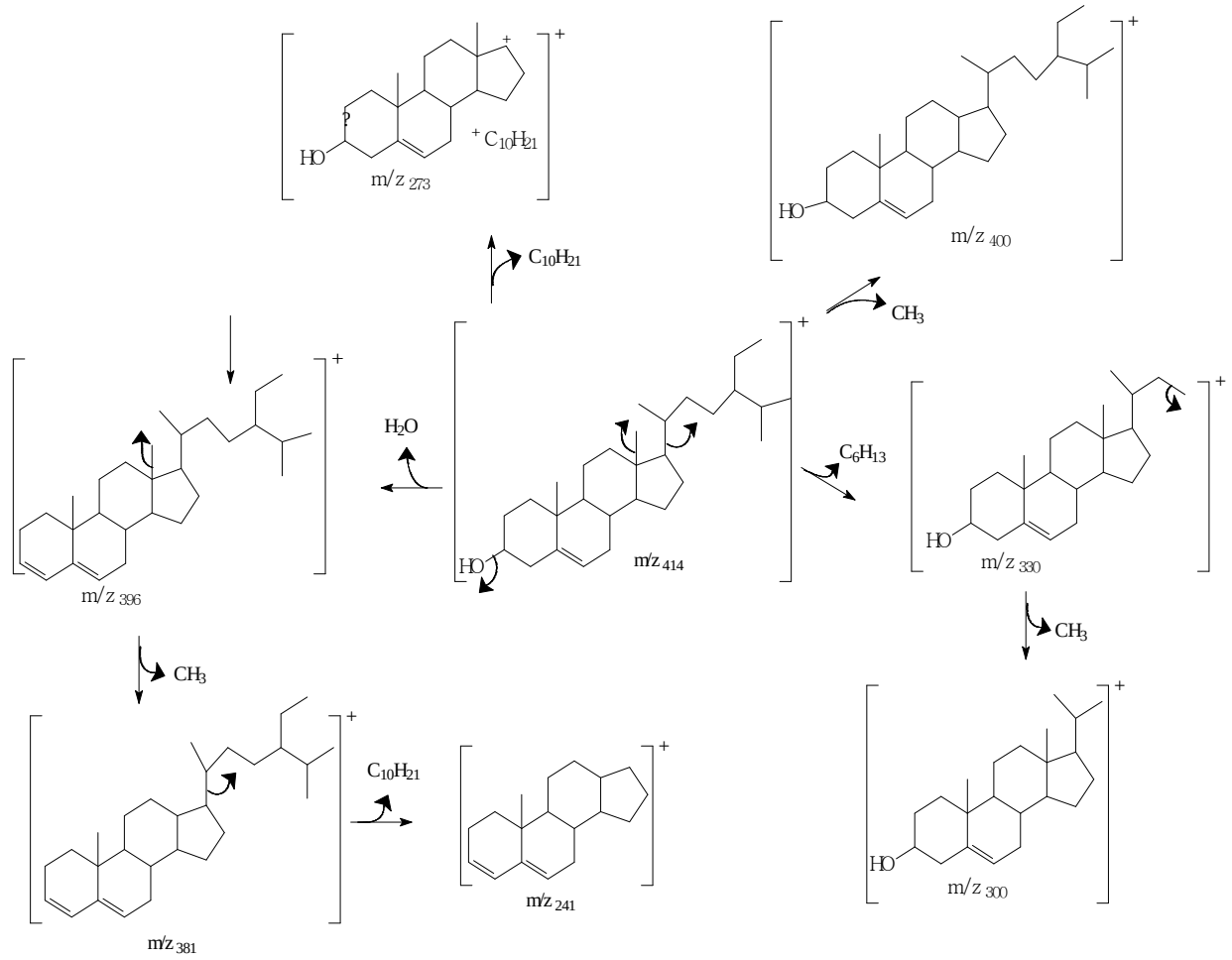

Figure 3.6 Proposed fragmentation pattern of β-sitosterol [88].

CHAPTER FOUR: CONCLUSION AND RECOMMENDATIONS

4.1 Conclusion

In this study, powdered root bark of *L. eriocalyx* was extracted with methanol, chloroform and water. The three extracts showed antibacterial and antifungal activity. Four compounds were isolated from the chloroform extract. They were identified as lupenone, lupeol and β- sitosterol/ stigmasterol mixture. Lupeol, a triterpene, has previously been isolated from this plant [55]. This is the first time that lupenone, β- sitosterol and stigmasterol have been reported from this plant.

The isolated compounds were tested for antimicrobial activity against *Staphyllococcus aureus, Pseudomonas aeruginosa, Escherichia coli* and *Saccharomyces cereiciae.* All the compounds showed antibacterial activity above 30% that of gentamicin and antifungal activity above 60% that of nystatin, as shown by their %D. Lupeol had the greatest antimicrobial activity. Available literature shows lupeol as a strong antibacterial and antifungal agent. Beta- sitosterol [96], lupenone [97] and stigmasterol [98] have also previously been reported to possess mild antimicrobial activity. The mechanism of action of these compounds has not been elucidated yet. Lupeol is thought to undergo *in vivo* biotransformation to yield different metabolites with antimicrobial activity [99].

The antimicrobial activity of the isolated compounds gives credence to the forklore use of the root bark of *Lonchocarpus eriocalyx* in the treatment of bacterial and fungal infections. This information will be helpful especially to countries like china and india that have taken up the WHO proposal of incorporating complementary medicine into the conventional health care systems. Once made available to the general population through publishing, the antimicrobial data will help boost patients' confidence in and adherence to the medical use of L. eriocalyx hence better prognosis. Photochemical tests on *L. eriocalyx* which revealed the presence of alkaloids, saponnins and tannins can act as a basis for drug discovery. The antifungal activity of the root bark of of *L. eriocalyx* had not been reported before together with its earlier reported antibacterial and antiprotozooal activity makes the plant a broad-spectrum antimicrobial agent.

Although the plant contained anthraquinones and the crude extract showed antimicrobial activity, it is highly unlikely that the anthraquinones were responsible for the activity since these compounds are known rather for their laxative effects.

4.2 Recommendations

Methanol and water extracts showed antimicrobial activity against the tested micro-organisms. Investigation of the compounds responsible for this activity needs to be done. Further investigation can be done to establish why decoction had more activity than chloroform and methanol extract. Whether it has other compounds besides lupenone, lupeol and β-sitosterol/stigmasterol mixture the make it more active or whether it has higher concentration of lupeol (that was shown to be the most active of the isolates) that make it more active than methanol and chloroform extract.

Further column chromatography should be done on the chloroform extract to yield more of compound C, whose physicochemical and biological properties can then be determined. Additional work need to be done to further purify fraction A using a smaller column for purification and characterization of the amorphous fatty content.

The saponins detected in this plant should be isolated for antimicrobial evaluation since some saponins are known to possess antimicrobial activity [100].

REFERENCES

1. Rates S. (2001). Plants as source of drugs. *Toxicon journal,* **39** (5), 603-613.
2. National museums of Kenya (2012). Conservation status and use of medicinal plants by traditional medical practitioners in Machakos district, Kenya. Http://citeseerx.ist.psu.edu/viewdoc/download?doi=10.1.1.164.7152&rep=rep1&type=pdf. Accessed on 09/10/2015.
3. Aruyaru S. (2012). From a dream to resounding reality: the inception of a Doctor's union in Kenya. *The Pan Afr. Med. J.* **11** (16), 18-21.
4. World Health Organization (2008). World Health Statistics 2008, **112**. Http://www.who.int/whosis/whostat/ENWHS08TOCintro.pdf. Accessed on 09/10/2015.
5. Saklani A. & Kutty S. (2008). Plant-derived compounds in clinical trials. *Drug Discovery Today*, **13** (3-4), 161–171.
6. De Smet S. (1997). The role of plant-derived drugs and herbal medicines in healthcare. *Drugs*, **54** (6), 801–840.
7. Bruneton J. (1999). Phytochemistry of medicinal plants. Lavoisier Publishing Inc. 11, Rue Lavoisier, Paris (France), 2nd edition, 1017-1018.
8. Katzung G., Masters B. & Trevor J. (2012). Basic and clinical pharmacology. Tata McGraw- Hill Education Limited, New Delhi (India), 12th edition, 556, 921.
9. Rang H., Dale M., Ritter J., Flower R. & Graeme H. (2007). Rang and Dale's pharmacology. Elsevier Churchill Livingstone, London (England), 17th edition, 682.
10. Trease C. (2009). Trease and Evans Pharmacognosy. Saunders Elsevier, London (England), 16th edition, 18-23, 46-47.
11. World Health Organization (2008). Infectious diseases. Http://www.who.int/topics/infectious_diseases/en/. Accessed on 10/10/2015.
12. Brachman S. (2003). Infectious diseases- past, present and future. *Int. J. Epidem.* **32** (5), 684-686).
13. Morse S. (2009). Emerging infections: condemned to repeat. Columbia University, National Academic Institute of Sciences. Http: www.ncbi.nlm.nih.go. Accessed on 17/10/2017.
14. Williams B. (1997). Infectious diseases in history: a guide to causes and effects. Http:www.urbanrim.org.uk/diseases.htm. Accessed on 18/10/2017.

15. Nii-Trebi N. (2017). Emerging and neglected infectious diseases: insights, advances and challenges. *Biomed. Res. J.* **2**, 15.
16. Kate J., Nikkita P., Levy M., Storeygard A., Balk D. & Daszak P. (2008). Global trends in emerging infectious diseases. *Nature*, **451** (7181), 990–993.
17. *Nat. Rev. Microbiol.* (editorial, September, 2011) **9**,628. http://www.nature.com/ microbiology. Accessed on 15/10/2015.
18. Bikard D. & Marraffini L. (2012). Innate and adaptive immunity in bacteria: mechanisms of programmed genetic variation to fight bacteriophages. *Curr. Opin. Immunol.* **24** (1), 15–20.
19. Cengiz C., Park J., Saraf, N. & Dieterich T. (2005). HIV and liver diseases. J. *Rec Clin. Advances* **9** (4), 647–666.
20. Afolayan A., Grierson D. & Mbeng W. (2014). Ethnobotanical survey of medicinal plants used in the management of skin disorders among the Xhosa communities of the Amathole District, Eastern Cape. *S. Afr. J. Ethnopharmacol.* **153** (1), 220–232.
21. David G., Mike B., Richard S. & Will I. (2009) Medical Microbiology. Churchill Livingstone Elsevier, London (U.K.), 18th edition, 176-210.
22. Michael J., Chan E. & Noel R. (2002). Microbiology. Tata McGraw- Hill Education Private Limited, 7 West Patel Nagar, New Delhi (India), 4th edition, 333.
23. Bryan S. (2002). Infectious diseases in primary care. Saunders W.B. Company, Elsevier Science, Sidney (Australia), 508-514.
24. Bailey R. (2010). Viruses. Http://biology.about.com/od/virology/ss/viruses.htm#step2. Accessed on 20/10/2015.
25. Piech R. (July 2009). Medical News Today. Http://www.medicalnewstoday.com. Accessed on 20/10/2015.
26. Kane M. & Golovkina T. (2010). Common treads in persistent viral infections. *J. Virol.* **84** (9), 4116–4123.
27. Alviano D. & Alviano C. (2009). Plant extracts: search for new alternatives to treat microbial diseases. *Curr. Pharmaceut. Biotech.* **10** (1), 106–121.

28. Wet H., Nkwanyana M. & Vuuren S. (2010). Medicinal plants used for the treatment of diarhoea in North Maputaland, KwaZulu-NATAL Province, South Africa. *J. Ethnopharmacol.* **130** (2), 284-289.
29. Kokwaro O. (2009). Medicinal plants of east Africa. University of Nairobi press, Nairobi, (Kenya), 3rd edition, 270.
30. Ogoti P., Magiri E., Magoma G., Kariuki D. & Bii C. (2015). In vitro anti-Salmonela activity of extracts from selected Kenyan medicinal plants. *J. Med. plants Res.* **9** (8), 254-261.
31. Olusola A., Olajide O., Afolayan M. & Khan I. (2011). Phytochemical and antimicrobial screening of the leaf extract of *Cassia singueana* Del. *Afr. J. pure Appl. Chem.* **5** (4), 65-68.
32. Banso A. & A Mann (2006). Antimicrobial alkaloid fraction from *Commiphora africana*. *J. Pharm. Bioresourc.* **3** (2), 98-102.
33. Shagal M. (2012). Phytochemical screening and antimicrobial activity of roots, stem-bark and leave extracts of *Grewia mollis. Afr. J. Biotech.* **11** (51), 11350–11353.
34. Chah K., Muko N., & Oboegbulem I. (2000). Antimicrobial activity of methanolic extract of *Solanum torvum* fruit. *Fitoterapia,* **71** (2), 187–189.
35. Kokwaro J. (2009). Medicinal plants of east Africa. University of Nairobi press, Nairobi (Kenya), 3rd edition, 180.
36. Haines C. (August 2013). Viral diseases, health grades operating company Inc. Https://www.healthgrades.com/conditions/viral-diseases. Accessed on 1/11/2015.
37. Sankar M., Natarajan K., Paul V., Das R., Agarwal & Chandrasekaran (2016). When do newborns die? A systematic review of timing of overall andcause-specificneonatal deaths indeveloping countries. *J. Perinatol.* **36**, 1-11.
38. WHO, Global tuberculosis report (2014). Http://apps.WHO.int_iris_9789241564809. Accessed on 21/10/2015
39. Sharma K., Mohanan S. & Sharma A. (2012). Relevance of latent TB infection in areas of high TB prevalence. *Chest*, **142** (3), 761–773.
40. Khabbaz R., Moseley R., Steiner R., Levitt A., & Bell P. (2014). Challenges of infectious diseases in the USA. *Lancet*, **384** (9937), 53–63.

41. Benjamin J., Tom M., Mary E. & Warnock D. (2011). Epidemiology of systemic fungal diseases: An overview. Http://link.springer.com/ chapter/10.1007%2F978-1-4419-6640-7_2. Accessed on 20/11/2015.
42. Park B., Sigel K., Vaz V., Komatsu K., McRill C., Phelan M. & Hajjeh R. (2005). An epidemic of coccidioidomycosis in Arizona associated with climatic changes, 1998-2001. *J. Inf. Dis.* **191** (11), 1981–1987.
43. Allaranga Y., Kone M., Formenty P., Libama F., Boumandouki P., Woodfill C. & Yada A. (2010). Lessons learned during active epidemiological surveillance of Ebola and Marburg viral hemorrhagic fever epidemics in Africa. *E. Afr. J. Public Health* **7** (1), 30–36..
44. Meyers L., Frawley T., Goss S. & Kang, C. (2014). Ebola Virus Outbreak 2014: Clinical Review for Emergency Physicians. *Annals Emerg. Med.* **65** (1), 101–108.
45. Centres for disease control and prevention (2014). Ebola virus disease epidemic - West Africa. Http://www.afro.who.int/en/clusters-a-programmes/dpc/epidemic-a-pandemic-alert-and-response/outbreak-news/4239-ebola-virus-disease-west-africa-4-august-2014.html. Accessed on 20/11/2015.
46. Coker R., Hunter B., Rudge J., Liverani M. & Hanvoravongchai P. (2011). Emerging infectious diseases in South East Asia: regional challenges to control. *Lancet*, **377** (9765), 599–609.
47. World Health Organizaton (2004). The global burden of disease. Http://www.who.int/health info/global_burden_disease/2004_report_update/en/. Accessed on 25/ 11/2015.
48. Khabbaz R., Moseley R., Steiner R., Levitt A. & Bell B. (2014). Challenges of infectious diseases in the USA. *Lancet*, **384** (9937), 53–63.
49. Birx D., de Souza M. & Nkengasong J. (2009). Laboratory challenges in the scaling up of HIV, TB, and malaria programs: The interaction of health and laboratory systems, clinical research, and service delivery. *Am. J. Clin. Pathol.* **131** (6), 849–851.
50. *Fabaceae* (2015). In Encyclopædia Britannica. Http://www.britannica.com/plant/Fabaceae. Accessed on 25/11/2015.
51. Gao, T., Song H., Liu C., Zhu Y., Ma X. & Chen S. (2010). Identification of medicinal plants in the family *Fabaceae* using a potential DNA barcode ITS2. *J. Ethnopharmacol.* **130** (1), 116–121.

52. Royal botanical gardens, Kew and Missouri Botanical Garden. The plant list (2010). Version 1. Published on the internet; http://www.theplantlist.org/. Accessed 01/12/20 15.
53. Encyclopedia **2** (1979). The genus *Loncocarpus; http://encyclopedia2.thefreedictionary.com/ Lonchocarpus. Accessed on 29/09/2016.*
54. Journal storage (JSTOR) Global plants (1971) *Lonchocarpus eriocalyx*. Https://plants.jstor.org/search?filter=name&so=ps_group_by_genus_species+asc&Query=*Lonchocarpus+eriocalyx*. Accessed 1/12/2015.
55. Kiplagat J. (2006) lavicidal and antiplasmodial compounds from *Derris trifoliate*, *Lonchocarpus eriocalyx* and *Erythrina sacleuxii*. A masters of Science (Chemistry) thesis, Department of Chemistry, University of Nairobi. Available at the Chiromo Campus Library, University of Nairobi.
56. Marrs T. (2012). Mammalian toxicology of insecticides, in the Issues of toxicology **12**, 258-259. Http: books.google.co.ke. Accessed on 1/12/2015.
57. Magrate M. & Fredrick M. (2015). Ethnobotanical study of medicinal plants used by Tharaka people. *Int'l. J. Ethnobiol. Ethnomed.* **1** (1), 1-8.
58. Kareru G., Kenji G., Gachanja N., Keriko M. & Mungai G. (2007). Traditional medicines among the Embu and Mbeere people. *Afr. J. Trad. Comp. Alt. Med.* **4** (1), 75-86.
59. Timberlake J. (1994). Vernacular names and uses of plants in Northern Kenya. *J. East Afr. Nat. Hist.* **83** (1), 31-69.
60. James L. (1971). Ecological basis for subsistence change among the Sandawe of Tanzania. National academy of sciences. The national academies copyright: 133-180. https://www.amazon.co.uk/Ecological-Subsistence-Change-Sandawe-Tanzania/dp/0309018 51X
61. Gosálvez M. (1983). Carcinogenesis with the insecticide rotenone. *J. Life Sci.* **32** (8), 809-816.
62. Maria G., Cavalcante B., Rochanne M., Paulo N., Helcio S., Otilia D., Raimundo B., Maria R. & Albuquerque R. (2012). Furanoflavones and other constituents of *Lonchocarpus obtusos*. *J. Brazilian Chem. Society* **23** (2), 1-9.

63. Mubo A., Shonibare S. & Esther T. (2012). Antipsychotic property of aqueous and ethanolic extracts of *Lonchocarpus cyanescens* (Schumach and Thonn.) Benth. (*Fabaceae*) in rodents. *J. Nat. Med.* **66** (1), 127-132.
64. Sheila M., Luc P., Olipa D., Sandra A., Rita V., Paul C., Dirk A. V. & Anold J. V. (2008). Screening of some Tanzanian medicinal plants from Bunda district for antibacterial, antifungal and antiviral activity. *J. Ethnopharmacol.* **119**, 58-66.
65. Njume, C. & Goduka N. (2012). Treatment of diarrhoea in rural African communities: an overview of measures to maximize the medicinal potentials of indigenous plants. *Int. J. Environ. Res. Public Health*, **9** (11), 3911–3933.
66. Brian K. & Turner D. (1975). The practical evaluation of pharmaceuticals. John Wright and Sons Ltd. The Dorset Press, Dorchester (U.K) 1st edition, 152-155.
67. Dhanlal D. (2000). Visualizing reagents for TLC and PC. Chemistry Department, St. Augustine Campus, UWI University, Republic of Trinidad and Tobago. Http://delloyd. 50megs.com®. Accessed on 19/01/2016.
68. Anees A. & Seemi S. (2008). Experimental Pharmaceutical Chemistry, CBS Publishers and Distributers, New Delhi (India) 2nd edition, 159-174.
69. Tankeshwar A. (2014). Stokes disk diffusion method: principle, procedure and interpretation of results in antibiotic resistance, bacteriology; Microbe online. Http// microbe online.com/stokes-disk-diffusion-method-principle-procedure-interprettation-results. Accessed on 10/10/2017.
70. Melting point determination in the assay of Eucalyptus oil (2008). British pharmacopoeia volume **I**, p. 877.
71. Watson D. (2005). Pharmaceutical analysis, a textbook for pharmacy students and pharmaceutical chemists. Elsevier limited, London (U.K.), 2nd edition, 118.
72. Faust, B. (1997). Ultraviolet/visible spectroscopy: In Modern Chemical Techniques **3**, 92–115. http://doi.org/10.1002/chin.200521298. Accessed on 20/01/2016.
73. Chaturvedula V. and Prakash I. (2012). Isolation and Structural Characterization of Lupane Triterpenes from *Polypodium Vulgare*. *Res. J. Pharmaceutical Sci.* **1** (1), 23-27.
74. Mohamed M., Khaled H., Ahlam, Ahmed H., & Maher. A. (2013). Lupane-type triterpenoid derivatives from resin of the socotra dragon tree, *Dracaena cinnabari (*Balf) *Agavaceae*. *World J. Pharm. Pharmaceutical Sci.* **4** (4), 182-194.

75. Martinez R. (2015). Mass spectrometry of labeled triterpenoids-Thermospray and electron impact analysis. Http://www.academia.edu/15694010/Mass_Spectrometry_of_Labelled_ Triterpenoids_Thermospray_and_Electron_ Impact_Ionization_Analysis Rubén Martínez. Accessed on 30th August, 2016.
76. Wulfson N., Zeretskii V., Zaikin V., Segel G., Tergev V. & Fradkina T. (1964). Mass spectrometric location of the double bond in steroidal systems. *Tetrahendron Letters*. **40**, 3015-3022.
77. Jennings W. (1975). Chemical shift non- equivalence in prochiral groups. *Chem. Rev. J.* **75** (3), 307-322.
78. Willard H., Merritt L., Dean J. & Seatle F. (1987). Instrumental methods of analysis, CBS Publishers and Distributors, New Delhi (India), 7th Edition, 839-842.
79. Braun R. (1987). Introduction to instrumental analysis Int. Ed. Mc-Graw Hill Book Company, New Delhi (India),1st edition, 839-842.
80. Supaluk P., Puttirat S., Rungrot C. & Virapong P. (2010). New bioactive triterpenoids and antimalarial activity of *Diospyros rubra* (Lec). *Exceli J.* (**9**), 1-10.
81. Shyamal K., Arindam G., Atasi S. & Dilip G. (2013). Phytochemical investigation of the hexane extract of stem bark of *Peltophorum pterocarpum* (DC). *Der Pharma Chemica*, **5** (5), 49-53.
82. Byamukama R., Ganza B., Namukobe J., Heydenreich M. & Kiremire T. (2015). Bioactive compounds in the stem bark of Albizia coriaria (Wwlw. Ex Oliver). Int. J. Biol. Chem. Sci. (9) 2, 1013-1024.
83. Basavaraja H., Nkita W., Pranay W., Rai K. & Kanwal R. (2010). Isolation and modification of pseudohybrid plant (Lupeol). *J. Pharm. Sci. & Res.* **2** (1), 13-25.
84. Reynolds F., Mc Lean S., Polplaski J., Enriquez G., Escopar I. & Leon I. (1986). Total Assignment of ^{13}C and ^{1}H Spectra of three isomeric triterpenoidol derivatives by 2D NMR: An investigation of the potential of ^{1}H chemical shift in structural investigation of complex natural products. *Tetrahedron* **42,** 3419.
85. Ndwigah S., Thoithi G., Mwangi J. & Kibwage I. (2005). Constituents of the Stem Bark of *Dombeya rotundifolia* (Hochst). *East Cent. Afr. J. Pharmaceutical. Sci*. **8**, 40-42.
86. Gonzalo R., Lothar H., Joachim S. & Bussmannb W. (2015). Constituents of *Corynaea crassa* (Peruvian Viagra). *Braz. J. Pharmacognosy* **25**, 95-97.

87. Luhata L. & Munkombwe N. (2015). Isolation and characterization of stigmasterol and β-sitosterol from *Odontonema Strictum* (Acanthaceae). *J. Innov. Pharmaceuticals Biol. Sci.* **2** (1), 88-95.

88. Ndwigah S. (2013). Phytochemical, antibacterial and antifungal study of *Dombeya torrida* (J. F. Gmel) and *Hydnora abyssinica* (A. Braun). A PhD thesis, School of Pharmacy, University of Nairobi. Available at the College of Health Sciences Library, University of Nairobi.
89. Enamul H., Nahidul I., Dipankar D.G., Mahbub H., Hossain U. & Biazid A. (2006). Triterpenoids from the Stem Bark of *Crataeva nurvala*. *Dhaka University J. Pharmaceutical Sci.* **7**, 12-13.
90. Anjoo A. & Ajay K. (2011). Isolation of stigmasterol and β-sitosterol from petroleum ether extract of aerial parts of *Ageratum conyzoides (asteraceae). Int. J. Pharm. Pharmaceutical sci.* **3** (1). 22-26.
91. Maima A., Thoithi G., Ndwigah S., Kamau F. & Kibwage I. (2008). Phytosterols from the stem bark of *Combretum fragrans* F. Foffm. *East & central Afr. J. Pharmaceutical sci*. **11**, 52-54.
92. Virgilio D., Chien-Chang S. & Consolacion Y. (2015). Terpenoids and Sterols from *Hoya multiflora* (Blume). *J. App. Pharmaceutical Sci*. **5** (4), 33-39.
93. Ododo M., Choudhury M. & Dekebo A. (2016). Structure elucidation of β-sitosterol with antibacterial activity from the root bark of *Malva parviflora*. Springerplus **5** (1), 1210.
94. Valasoa H., Rambeloson V., Rasoanaivo H., Wadouachi A. & Raharisololalao A. (2014). A new triterpenoid and stigmasterol from Anthostema madagascariense (Euphobiceae). Int. J. *Chem. Stud*. **1** (5), 42-48.
95. Jan-Michael C. and Consolacion Y. (2004).Structure elucidation of β-sitosterol and stigmasterol from *Sesbania grandiflora* [Linn] Pers and β-carotene from *Heliotropium indicum* [Linn] by NMR spectroscopy. *KIMIKA J*. **(20)** 1, 5-12.
96. Amit S., Poonam D., Kshitiz K.S., Sanjay S. & Tejovathi G. (2012). Analysis of IR, NMR and Antimicrobial Activity of β-Sitosterol Isolated from *Momordica charantia. Sci. Secure J. Biotech.* **1** (1**)**, 9-13.
97. Tsai P.W., De Castro K. & Consolacion R. (2012). Chemical constituents of *Broussonetia luzonicus*. *Pharmacognosy J.* **4** (31), 1-4.

98. Isah Y., Ndukwe I., Usman O. & Ayo R. (2014). Bioactivity of stigmasterol isolated from the aerial part of *Spillanthes acmella* (Murr) on selected microorganism. *Int. J. Curr. Microbiol. App. Sci.* **3** (2), 475-479.
99. Gallo M. & Sarachine M. (2009). Biological activities of lupeol. *Int. J. Biomed. Pharmaceutical Sci.* **3** (1), 46-66.
100. Avato P., Bucci R., Tava A., Jurzysta M., Bialy Z., Rosato A. & Vitali C. (2006). Antimicrobial activity of saponins from *Medicago sp.*: structure-activity relationship. *Phytother. Res. J.* **20** (6), 454-457.

APPENDICES

Appendix 1a: The TLC profile of compounds from chloroform extract visualized using vanillin reagent.

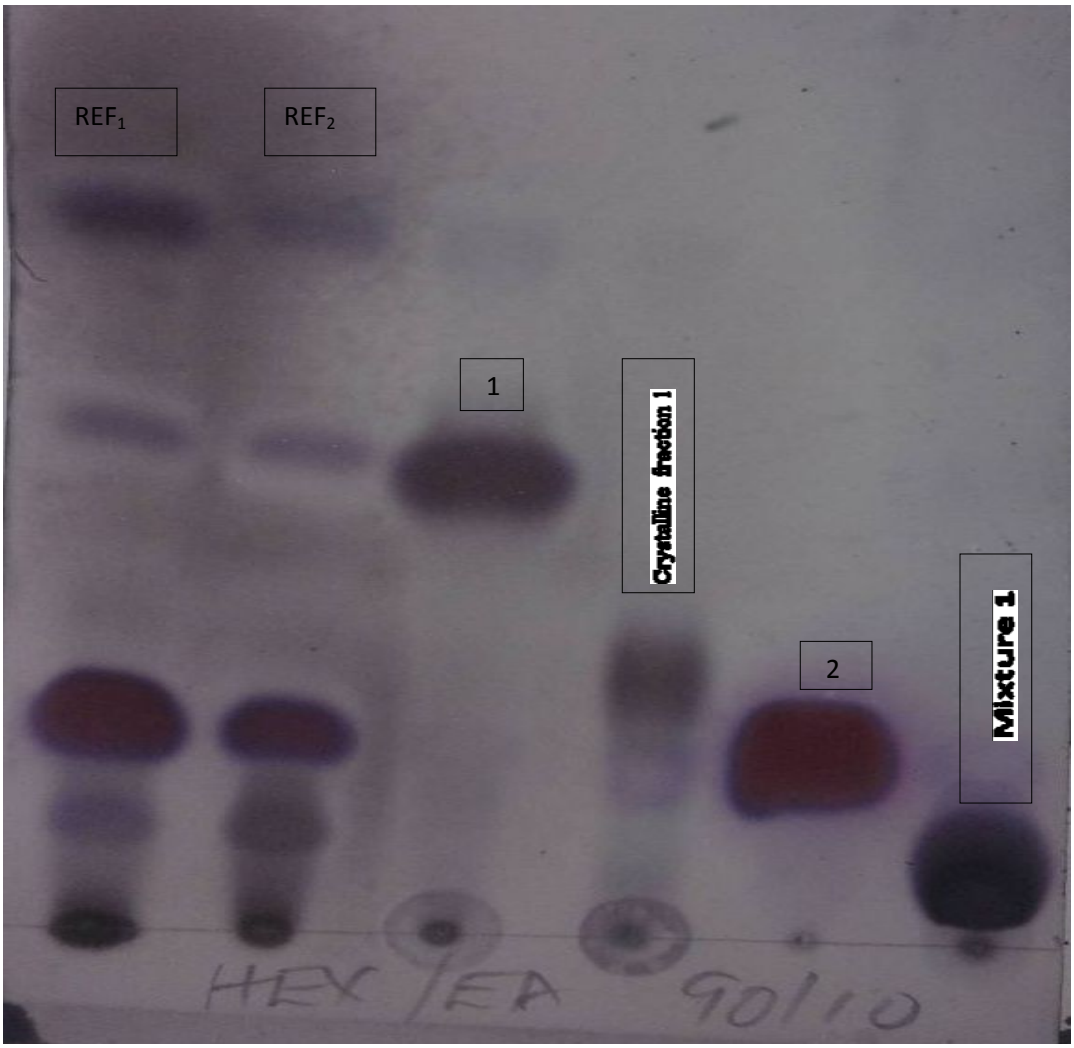

Key: REF_1 / REF_2 = crude chloroform extract as reference standard, spotted in duplicate; 1 = lupenone; 2 = lupeol; mixture 1= beta sitosterol and stigmasterol mixture; crystalline fraction 1 = the amorphous substance from fraction A.

Appendix 1b: The TLC profile of compounds from chloroform extract visualized using iodine.

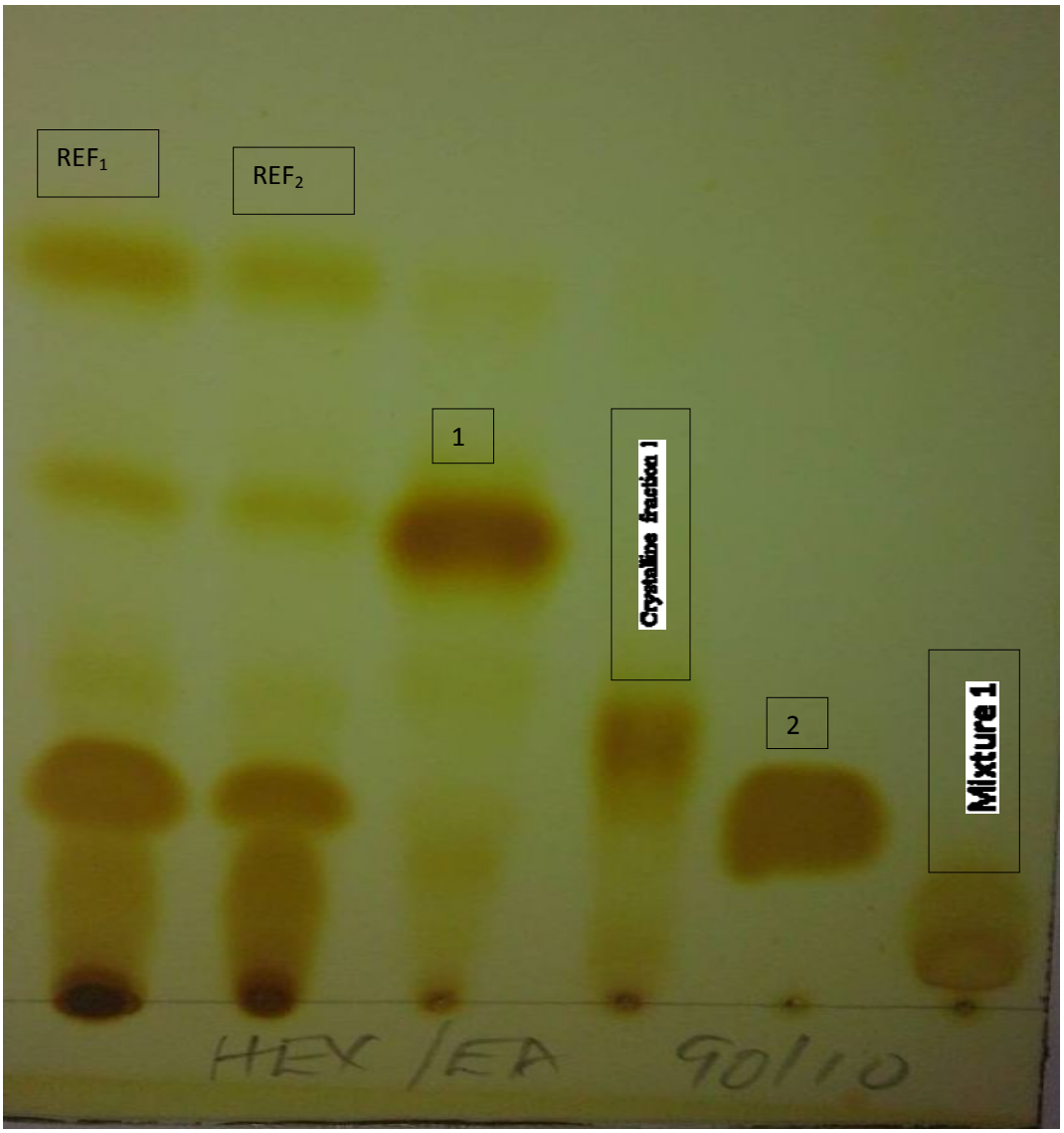

Key: REF_1 / REF_2 = crude chloroform extract as reference standard, spotted in duplicate; 1 = lupenone; 2 = lupeol; mixture 1= beta sitosterol and stigmasterol mixture; crystalline fraction 1 = the amorphous substance from fraction A.

Appendix 2a: Infra-red spectrum of lupenone in KBr

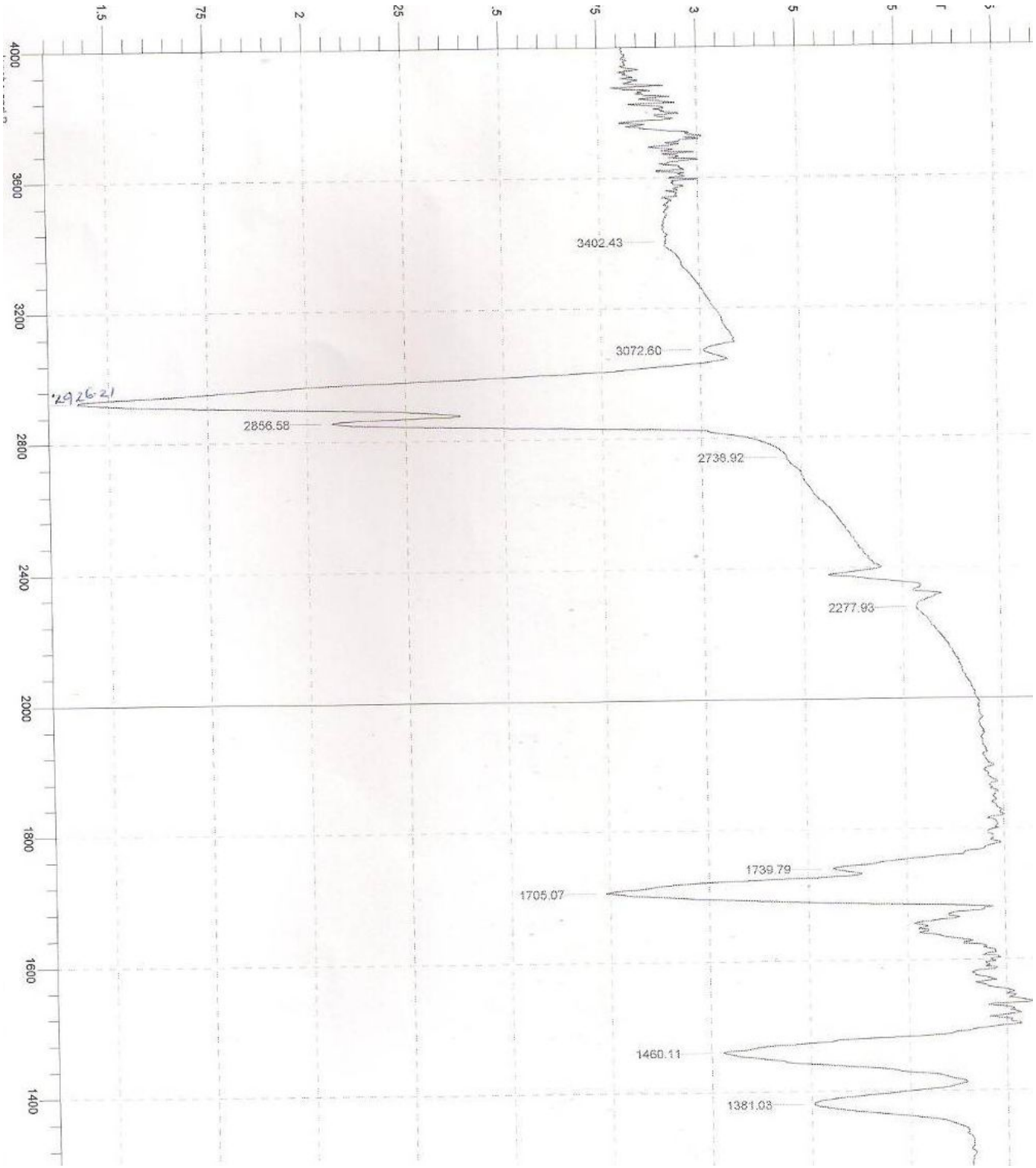

Appendix 2b-1: Mass spectrum of lupenone

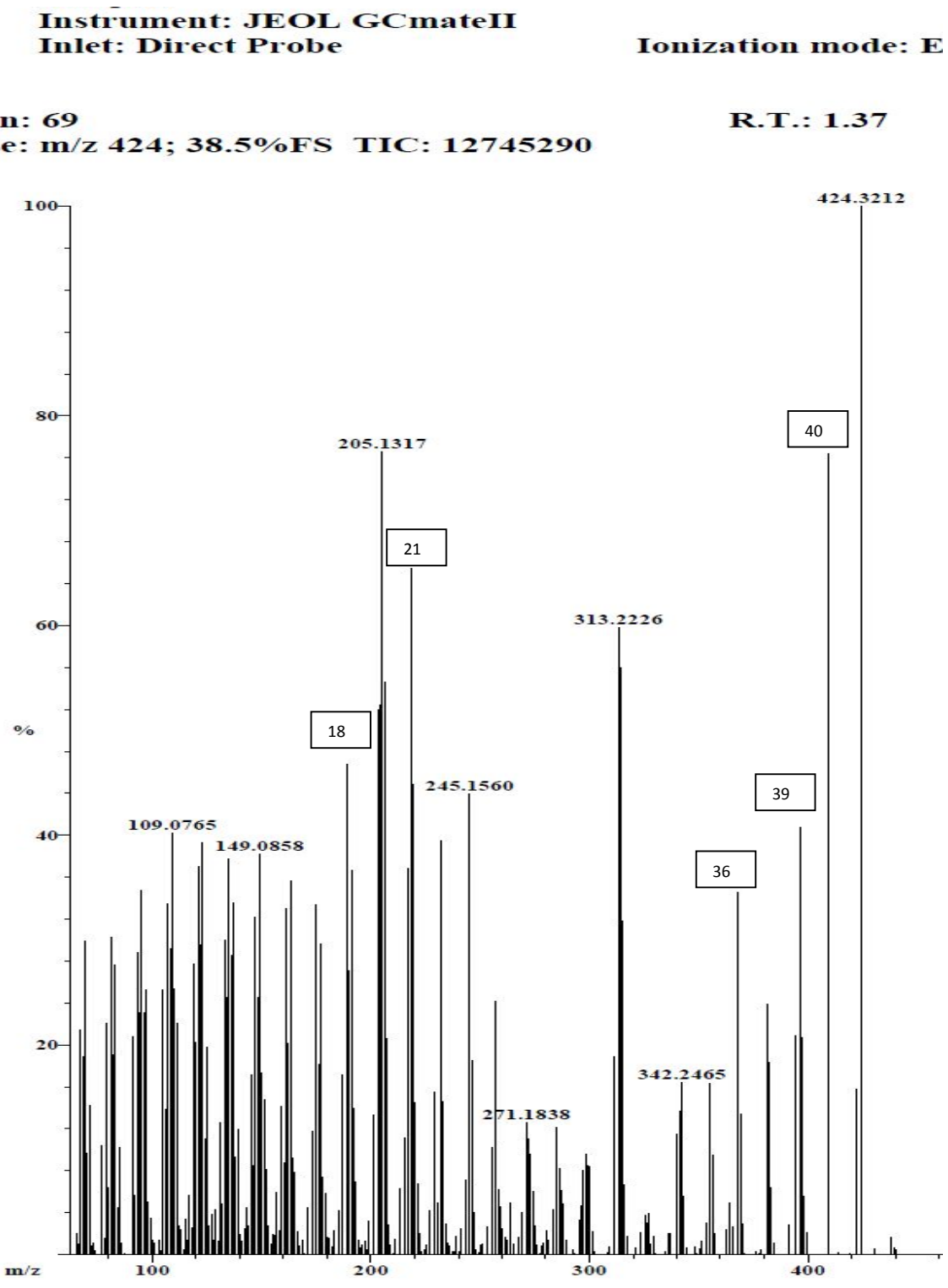

Appendix 2b-2: Mass spectral data 1 of lupenone

Instrument: JEOL GCmateII
Inlet: Direct Probe Ionization mode: EI+

Scan: 69 R.T.: 1.37
Base: m/z 424; 38.5%FS TIC: 12745290 #Ions: 311

Threshold: 1% of Base Displayed TIC: 1274529(

Mass	%Base	Mass	%Base	Mass	%Base	Mass	%Base	Mass	%Base
65.3399	2.0	115.0621	3.4	154.1136	1.0	207.1308	20.6	274.1856	6.1
66.2746	1.0	116.0663	1.3	155.0713	2.0	208.1208	2.9	275.2114	2.8
67.2041	21.4	117.0550	5.7	156.1104	1.8	211.1275	1.5	279.2377	1.1
68.1301	18.9	118.0876	2.6	157.0679	6.0	213.1244	6.3	280.2076	2.3
69.0616	29.9	119.0731	27.7	158.1236	2.3	215.1455	11.1	281.2051	1.4
70.0627	9.7	120.0827	20.3	159.0841	14.1	217.1715	36.8	283.2170	4.3
71.0689	14.2	121.0820	37.1	160.1137	8.8	218.1724	65.4	285.2037	12.2
73.0152	1.2	122.0911	29.5	161.1100	33.1	219.1638	44.8	286.2211	8.2
77.0299	10.4	123.0898	39.3	162.1162	20.2	220.1572	14.5	287.1962	6.2
78.0382	1.6	124.0925	11.1	163.1121	35.7	221.1604	6.7	288.2211	4.9
79.0437	22.0	125.0844	19.8	164.1177	9.2	222.1656	2.0	289.2081	1.3
80.0509	6.4	126.0979	2.8	165.1195	7.9	227.1612	4.2	295.2563	3.3
81.0550	30.3	127.0859	3.9	166.1446	2.2	229.1525	15.5	296.2424	4.6
82.0606	19.1	128.0925	1.4	169.1055	1.4	230.2026	4.9	297.2346	8.0
83.0509	27.6	129.0554	4.3	171.0924	4.5	232.1440	39.5	298.2018	9.6
84.0495	4.5	130.0755	1.3	173.1097	11.8	233.1495	14.6	299.2196	8.5
85.0541	10.3	131.0636	12.6	175.1202	33.3	234.1650	3.0	300.1899	8.4
86.0476	1.1	132.0795	4.8	176.1312	18.2	235.1509	1.1	301.2201	2.2
91.0365	20.8	133.0781	30.0	177.1276	29.7	239.1673	1.7	311.2094	18.9
92.0365	5.7	134.0925	24.6	178.1337	7.4	241.1660	2.5	313.2226	59.8
93.0471	28.8	135.0864	37.8	179.1286	5.8	243.1689	7.2	314.2155	56.0
94.0606	23.1	136.0930	28.6	180.1332	1.7	245.1560	44.0	315.2100	31.8
95.0643	34.8	137.1003	33.6	181.1232	1.6	246.1567	18.5	316.1921	6.7
96.0656	23.1	138.0867	9.3	183.1113	2.3	247.1676	4.0	317.2355	1.7
97.0721	25.2	139.0920	11.9	185.0926	4.2	253.1657	2.6	323.1855	2.1
98.0683	5.0	140.0886	1.9	187.1129	17.2	255.1771	10.2	325.2572	3.8
99.0775	3.4	141.0701	1.3	189.1228	46.8	257.1832	24.1	326.2486	3.0
100.0786	1.4	142.0612	2.5	190.1407	27.1	258.1974	6.2	327.1993	4.0
101.0453	1.1	143.0713	4.5	191.1325	36.7	259.1720	4.6	329.2396	1.7
103.0379	1.3	144.0537	2.7	192.1450	14.0	260.1984	2.5	336.3704	2.0
105.0497	25.3	145.0614	17.1	193.1347	6.9	261.2102	1.6	337.3060	2.0
106.0670	13.9	146.0979	8.5	194.1343	1.4	262.1610	1.4	340.2583	11.5
107.0673	33.5	147.0842	32.2	197.1229	1.3	264.1940	4.9	341.2755	13.7
108.0750	29.2	148.0992	24.5	199.1010	3.2	265.1881	1.1	342.2465	16.4
109.0765	40.2	149.0858	38.2	201.1332	13.3	267.1778	1.6	343.2141	5.6
110.0907	25.4	150.0885	17.3	203.1387	52.0	269.1834	4.0	351.2794	1.3
111.0901	22.0	151.0978	14.8	204.1600	52.4	271.1838	12.6	353.2848	3.0
112.0941	2.8	152.0944	8.1	205.1317	76.6	272.2082	11.1	355.2568	16.4
113.0913	2.4	153.0910	2.8	206.1431	54.6	273.1918	9.6	356.2373	9.5

Appendix 2b-3: Mass spectral data 2 of lupenone

Instrument: JEOL GCmateII
Inlet: Direct Probe **Ionization mode: EI+**

Scan: 69 **R.T.: 1.37**
Base: m/z 424; 38.5%FS TIC: 12745290 **#Ions: 311**

(Continued)

Threshold: 1% of Base **Displayed TIC: 12745290**

Mass	%Base	Mass	%Base	Mass	%Base	Mass	%Base	Mass	%Base
357.2431	2.1	381.2878	23.9	397.3117	20.7	606.5620	1.4	664.5311	4.3
362.2941	2.4	382.2955	18.3	398.3146	5.6	620.5670	7.8	676.5706	2.6
364.3413	4.9	383.2843	6.4	399.3289	2.1	634.5839	2.3	690.5788	2.2
365.2935	2.7	384.2643	1.1	409.2887	76.4	644.5551	1.5	692.5894	1.3
368.2570	34.5	391.2907	2.8	422.3080	15.8	646.4568	2.1	704.6308	2.6
369.2396	13.4	394.3107	20.9	424.3212	100.0	648.6885	5.3	732.7178	1.6
370.2682	3.0	396.3254	40.8	438.3610	1.7	662.5389	2.6		

Appendix 2c-1: ^{1}H- NMR spectrum 1 of lupenone

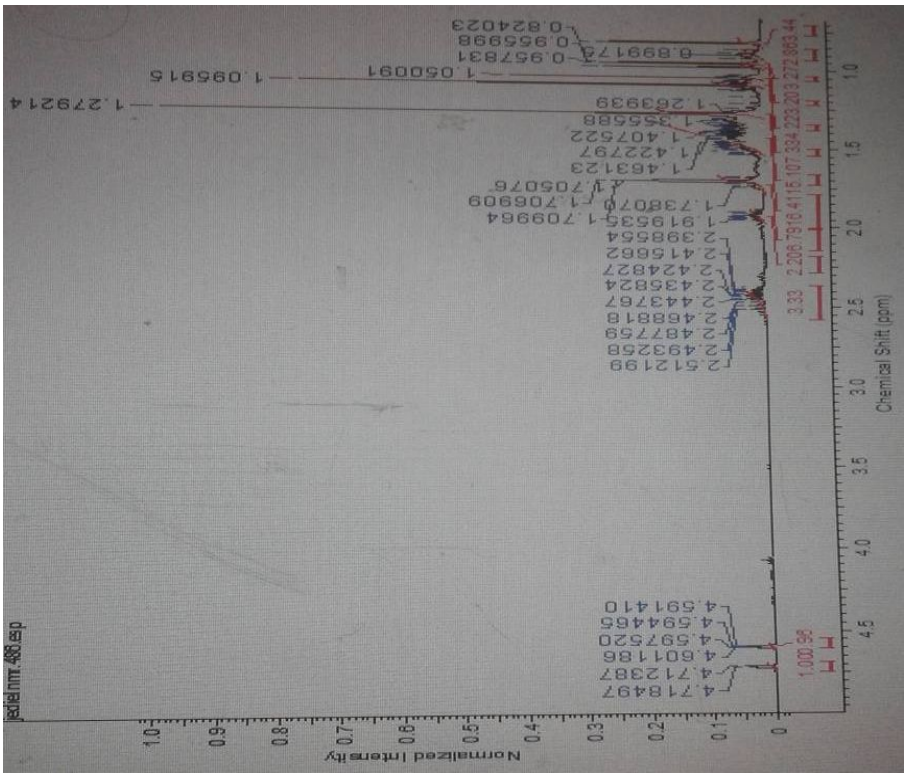

Appendix 2c-2: ^{1}H- NMR spectrum 2 of lupenone

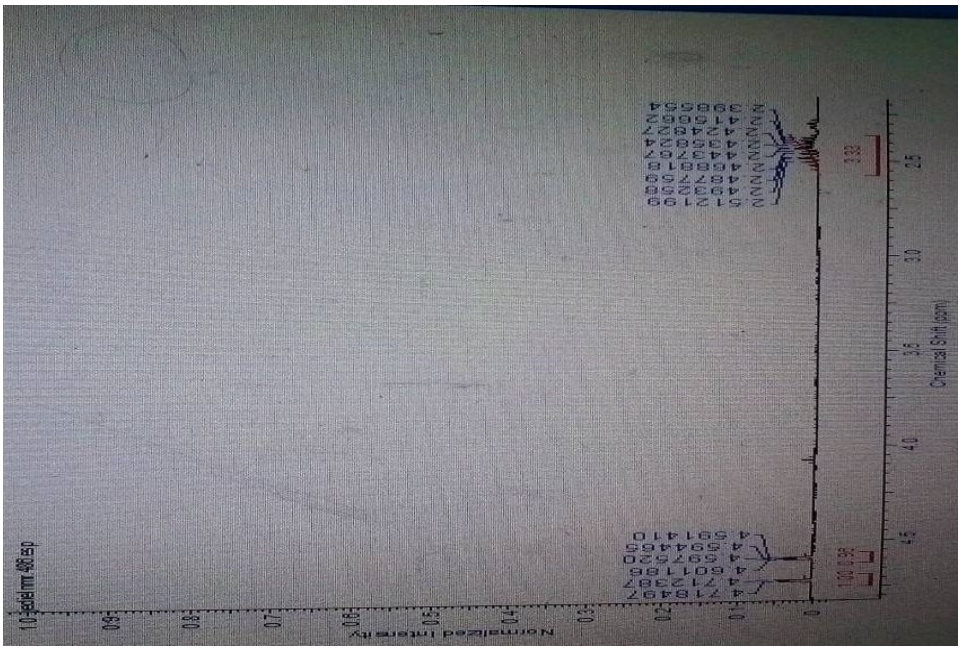

Appendix 2c-3: ^{1}H- NMR spectrum 3 of lupenone

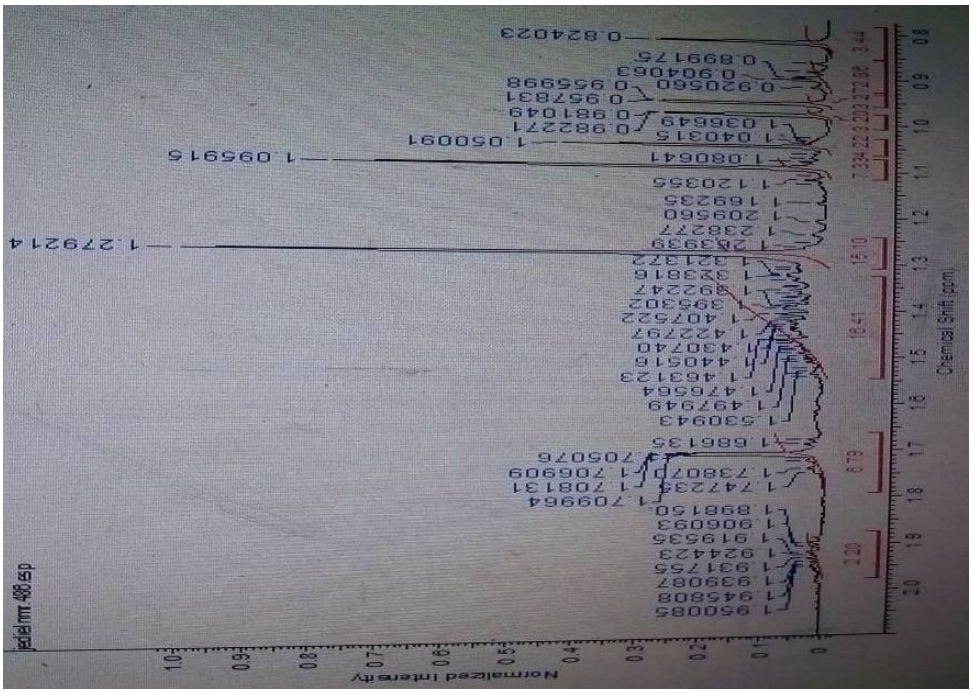

Appendix 2d-1: ^{13}C- NMR spectrum 1 of lupenone

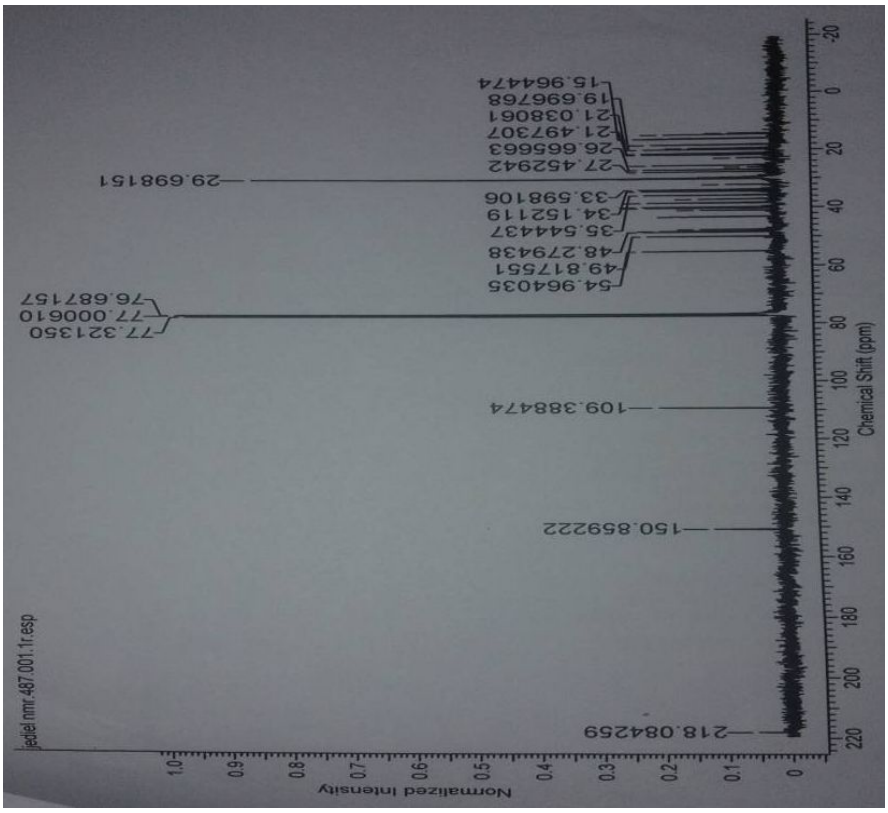

Appendix 2d-2: ^{13}C- NMR spectrum 2 of lupenone

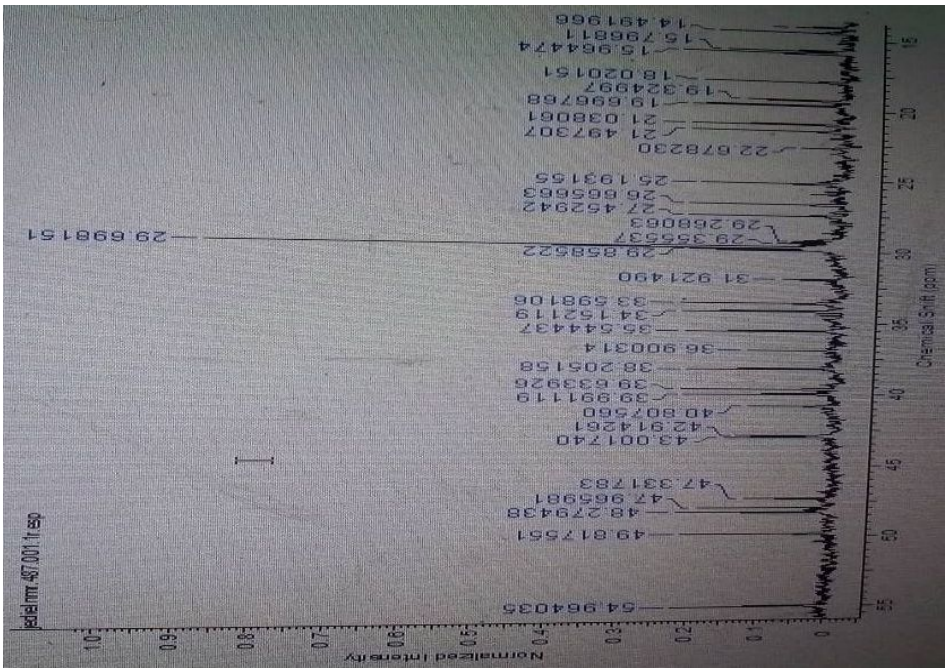

Appendix 2e-1: APT- NMR spectrum 1 of lupenone

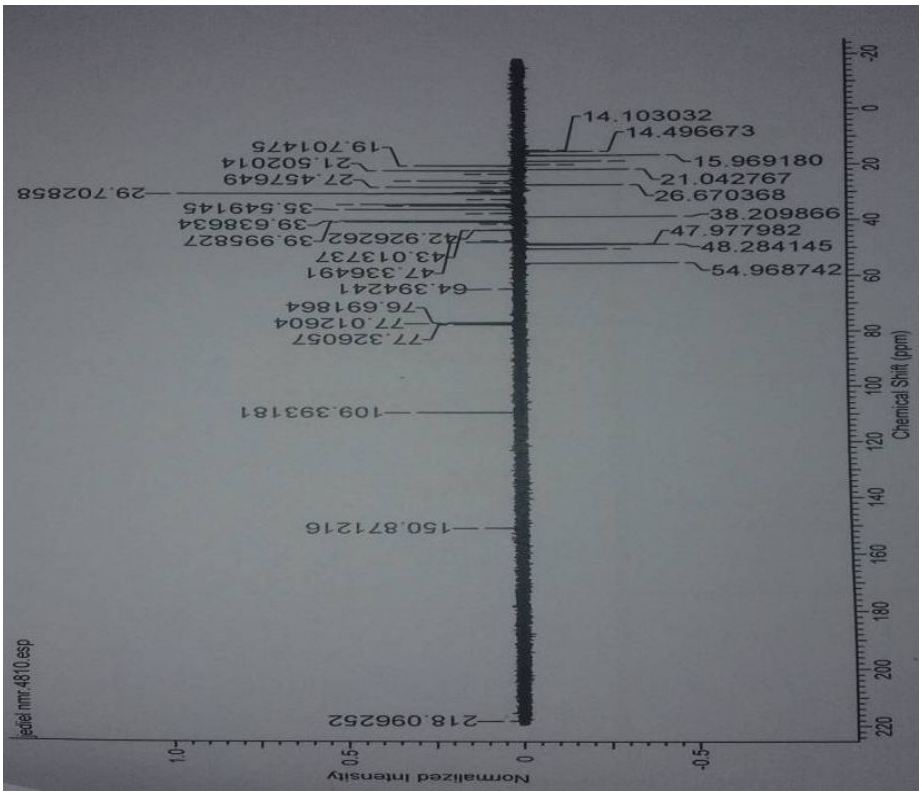

Appendix 2e-2: APT- NMR spectrum 2 of lupenone expanded

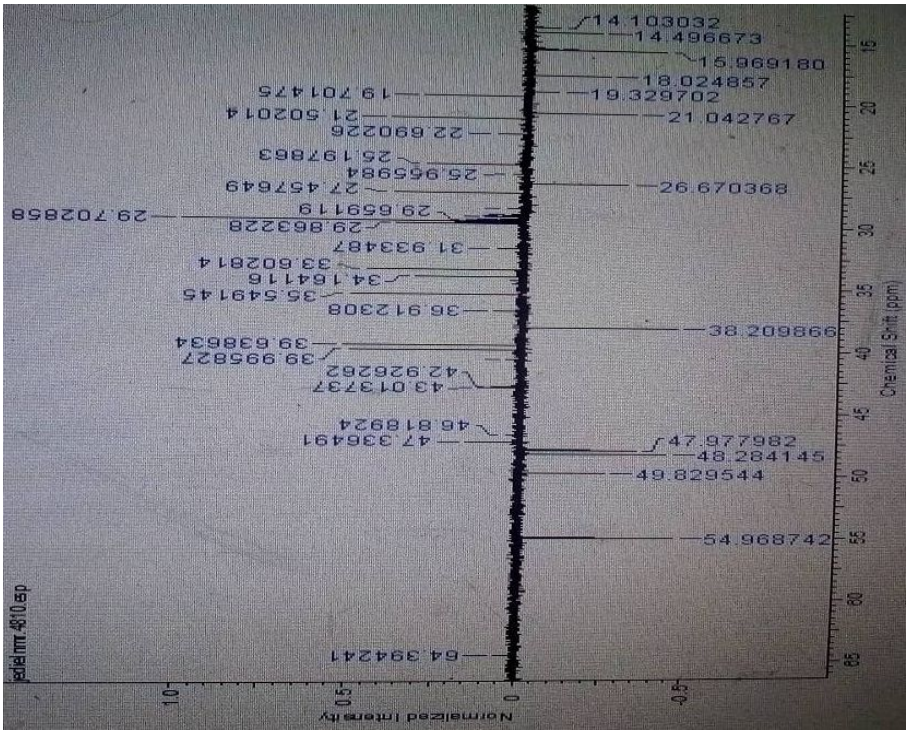

Appendix 3a: Infra-red spectrum of lupeol in KBr

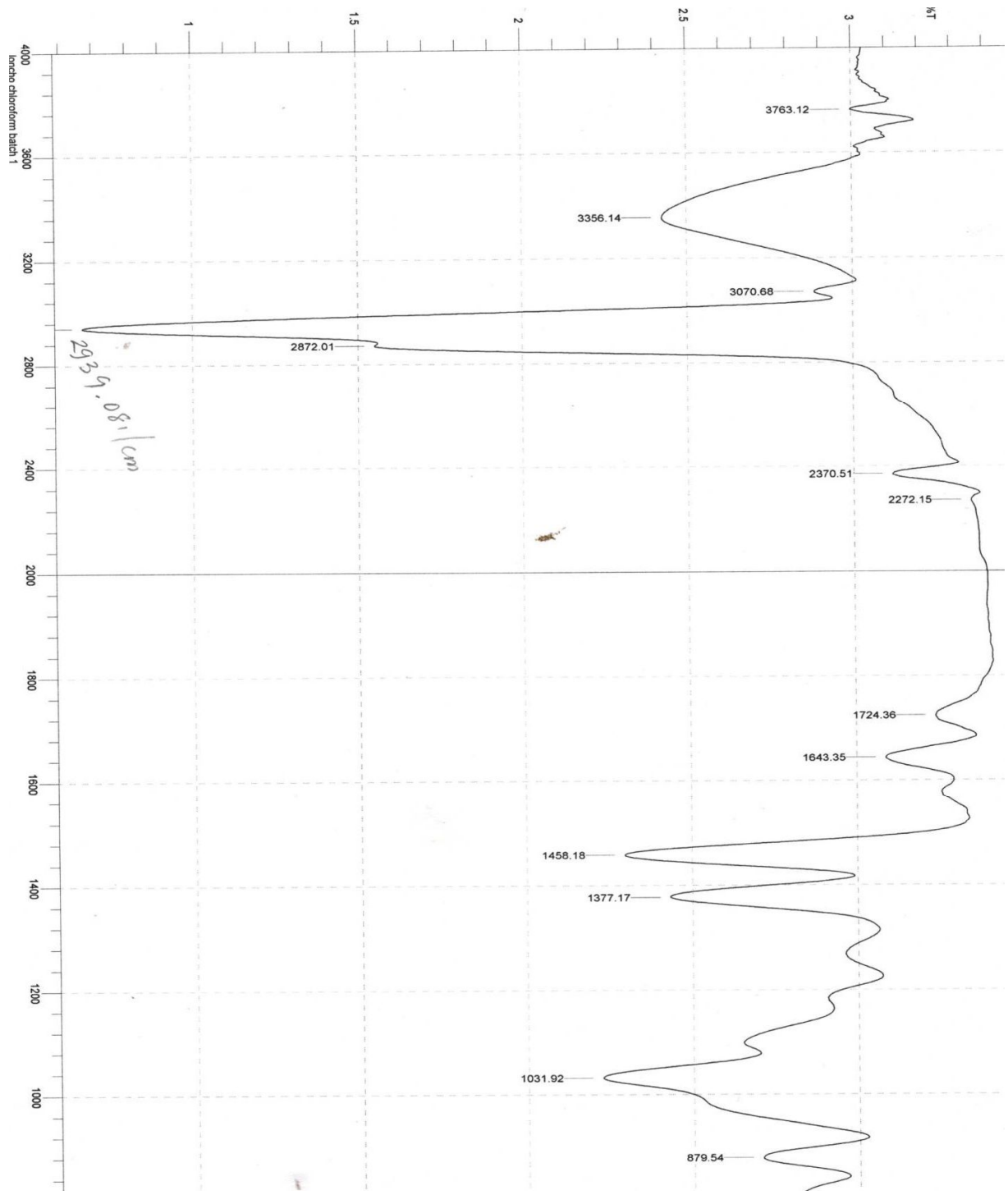

Appendix 3b-1: Mass spectrum of lupeol

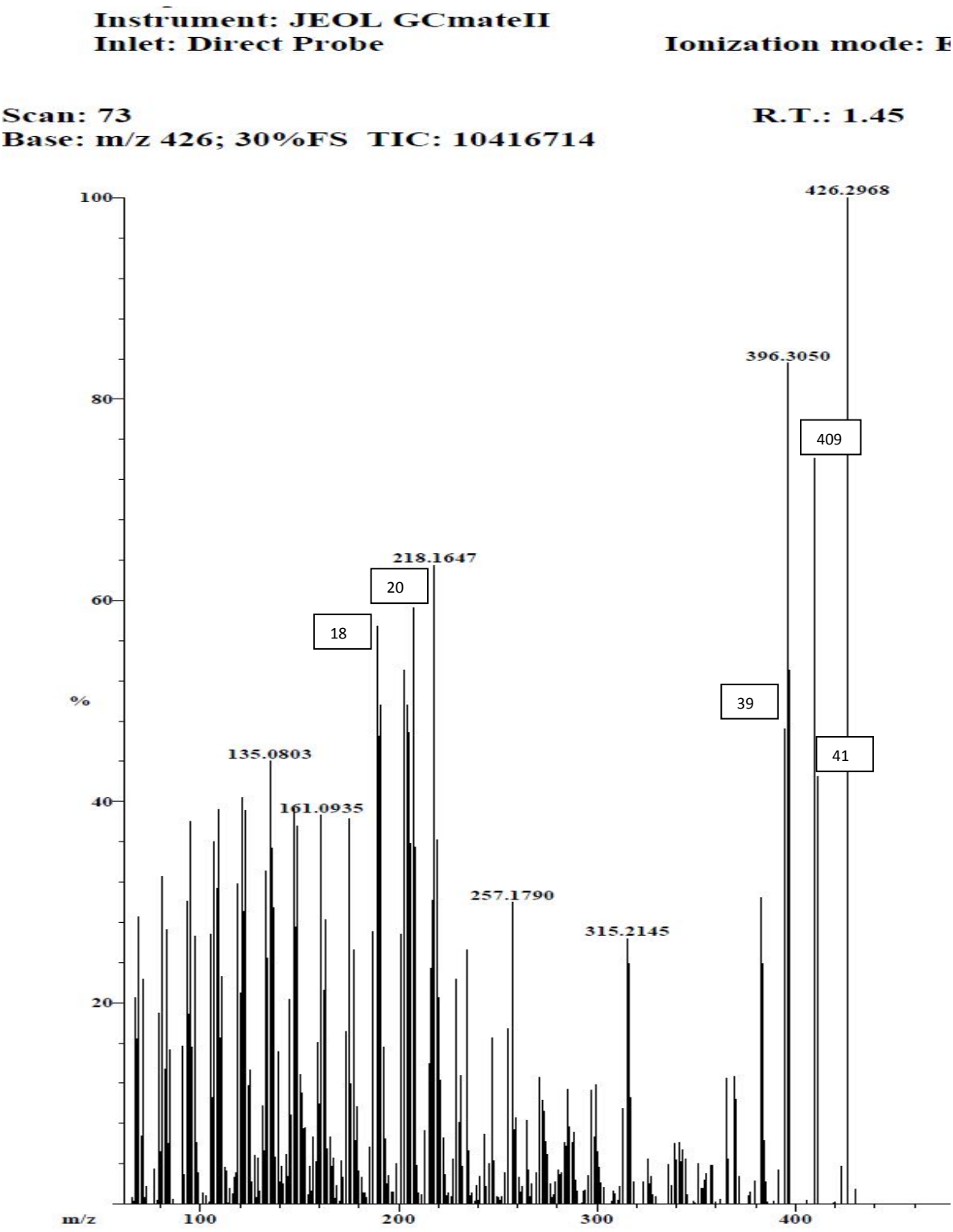

Appendix 3b-2: Mass spectral data 1 of lupeol

Instrument: JEOL GCmateII
Inlet: Direct Probe **Ionization mode: EI+**

Scan: 73 **R.T.: 1.45**
Base: m/z 426; 30%FS TIC: 10416714 **#Ions: 335**

Threshold: 1% of Base **Displayed TIC: 10416714**

Mass	%Base	Mass	%Base	Mass	%Base	Mass	%Base	Mass	%Base
67.2002	20.5	121.0762	40.4	162.1062	21.2	210.1380	1.1	271.1924	12.6
68.1321	16.4	122.0882	29.1	163.1154	28.3	213.1131	7.3	272.1954	10.3
69.0638	28.6	123.0898	39.1	164.1076	5.5	215.1531	14.0	273.1918	9.3
70.0693	6.8	124.0808	11.7	165.1028	6.7	216.1574	23.5	274.2113	6.3
71.0645	22.3	125.0874	13.4	166.1210	3.7	217.1792	30.2	275.2028	4.9
73.0331	1.8	126.1038	2.2	167.1288	4.6	218.1647	63.5	276.1787	2.0
77.0230	3.5	127.0829	4.9	169.0851	1.8	219.1599	36.2	279.2334	2.2
79.0320	19.0	129.0346	4.6	171.0753	4.3	220.1379	20.5	280.2033	3.4
80.0415	5.2	130.0785	1.3	172.1647	2.7	221.1372	12.3	281.1400	2.9
81.0503	32.6	131.0517	9.8	173.1029	17.2	222.1539	6.6	282.2126	3.1
82.0559	13.4	132.0615	5.3	175.1099	38.3	223.1806	2.9	283.1822	6.1
83.0652	27.3	133.0720	33.1	176.1347	11.9	225.1317	1.1	284.2576	5.8
84.0543	6.0	134.0773	24.5	177.1207	25.2	227.1495	4.5	285.2256	11.4
85.0782	15.3	135.0803	44.0	178.1337	6.3	229.1447	22.3	286.1861	7.6
91.0315	15.7	136.0900	35.3	179.1147	9.7	230.1515	8.1	287.2400	6.1
92.0466	2.9	137.0942	29.5	180.1332	3.3	231.1447	12.8	288.2079	7.2
93.0446	30.1	138.1052	4.7	181.1267	2.7	232.1796	3.8	289.2345	2.3
94.0555	18.9	139.0951	15.1	182.0773	1.1	234.1372	25.3	290.1705	1.2
95.0617	38.0	140.1010	2.2	183.1007	1.1	235.1231	5.3	293.2137	1.3
96.0630	15.6	141.0732	3.8	185.0961	5.7	237.1689	1.1	294.2142	1.4
97.0747	26.7	142.0581	2.0	187.0987	27.1	239.1513	1.8	295.2075	2.8
98.0709	6.1	143.0401	4.9	189.1228	57.5	241.1338	2.8	297.1945	11.4
99.0592	3.1	144.0631	2.8	190.1299	46.5	243.1487	6.9	298.2464	6.6
101.0427	1.1	145.0646	20.3	191.1217	49.6	244.1898	1.8	299.2107	11.9
105.0417	26.8	146.0790	8.8	192.1342	15.6	245.1601	4.0	300.1855	5.2
106.0588	10.6	147.0747	39.3	193.1167	6.5	247.1554	16.6	301.1797	3.7
107.0646	36.0	148.0897	27.6	194.1525	2.0	248.1438	4.3	302.2115	2.1
108.0696	31.4	149.0891	37.6	195.1365	2.8	253.1534	3.2	303.1957	1.7
109.0737	39.2	150.0982	12.8	196.1339	1.2	255.1565	17.5	308.2948	1.3
110.0769	16.6	151.0914	11.0	197.1265	1.2	257.1790	30.0	309.1436	1.0
111.0819	22.6	152.0912	7.5	199.0973	4.0	258.1891	7.4	311.2003	1.8
112.0747	3.7	153.0943	7.6	201.1111	26.8	259.1761	8.6	313.2089	9.5
113.0941	3.3	155.0941	3.7	203.1313	53.1	260.1942	2.6	315.2145	26.4
115.0592	1.6	156.1397	1.3	204.1414	49.6	261.2185	1.2	316.1967	23.9
116.0607	1.1	157.0581	6.7	205.1466	46.9	262.1987	1.7	317.2033	10.6
117.0522	2.7	158.0842	4.2	206.1543	35.8	264.2024	8.3	318.2068	2.2
118.0705	3.1	159.0808	16.0	207.1233	59.3	265.1460	3.4	323.1995	2.2
119.0646	31.8	160.1104	9.9	208.1246	35.4	267.1693	2.0	325.2200	4.5
120.0770	20.9	161.0935	38.6	209.1433	3.9	269.1622	3.2	326.2579	2.0

Appendix 3b-3: Mass spectral data 2 of lupeol continued

Instrument: JEOL GCmateII
Inlet: Direct Probe **Ionization mode: EI+**

Scan: 73 **R.T.: 1.45**
Base: m/z 426; 30%FS TIC: 10416714 **#Ions: 335**

(Continued)

Threshold: 1% of Base **Displayed TIC: 10416714**

Mass	%Base	Mass	%Base	Mass	%Base	Mass	%Base	Mass	%Base
327.2552	2.7	352.2790	1.6	371.2487	2.7	397.2758	53.0	676.5837	7.4
336.3090	3.9	353.2654	1.6	377.2873	1.2	409.2938	74.2	690.5657	5.3
337.2587	1.8	354.2968	2.4	379.2457	2.3	411.2688	42.5	704.6308	5.6
339.2475	6.0	355.2375	3.0	382.3106	30.5	423.3140	3.8	718.6777	2.5
340.2583	4.3	357.2382	3.9	383.2542	23.9	426.2968	100.0	732.6499	5.4
341.2612	6.1	358.2450	3.9	384.2694	6.3	430.1608	1.5	746.6460	2.0
342.2893	4.2	365.2493	12.5	385.3110	2.2	620.4791	5.8	760.6791	2.6
343.2188	5.4	366.2372	4.5	391.2755	3.4	634.5522	3.3		
344.2500	4.5	369.2791	12.6	394.2700	47.2	648.6115	10.8		
351.2601	4.0	370.2484	10.4	396.3050	83.6	664.5051	9.4		

Appendix 3c-1: ^{1}H- NMR spectrum 1 of lupeol

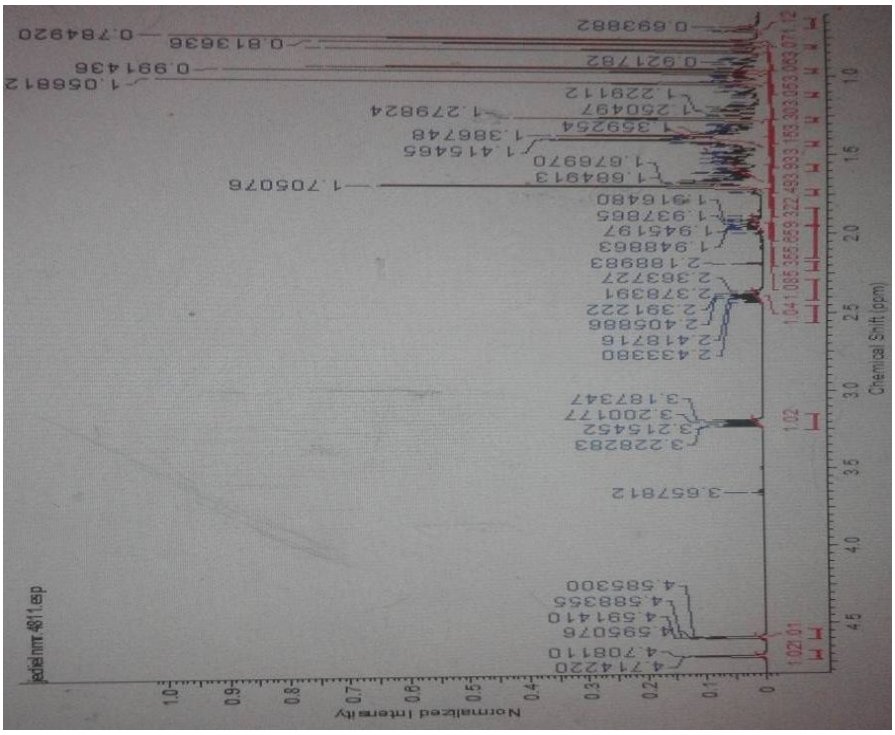

Appendix 3c-2: ^{1}H- NMR spectrum 2 of lupeol

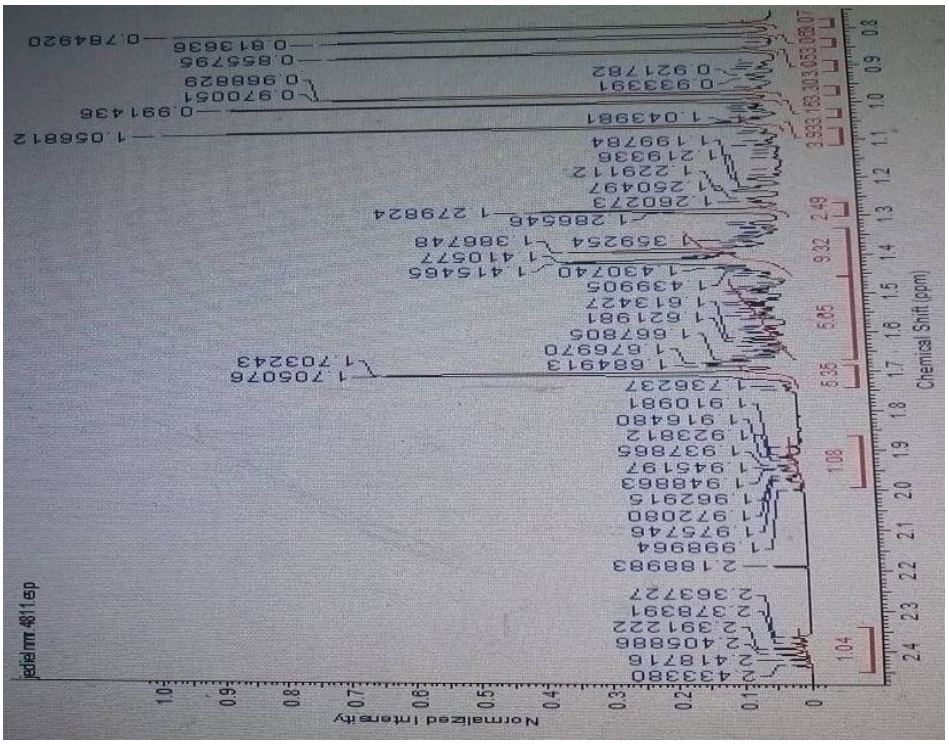

Appendix 3d-1: ^{13}C- NMR spectrum 1 of lupeol

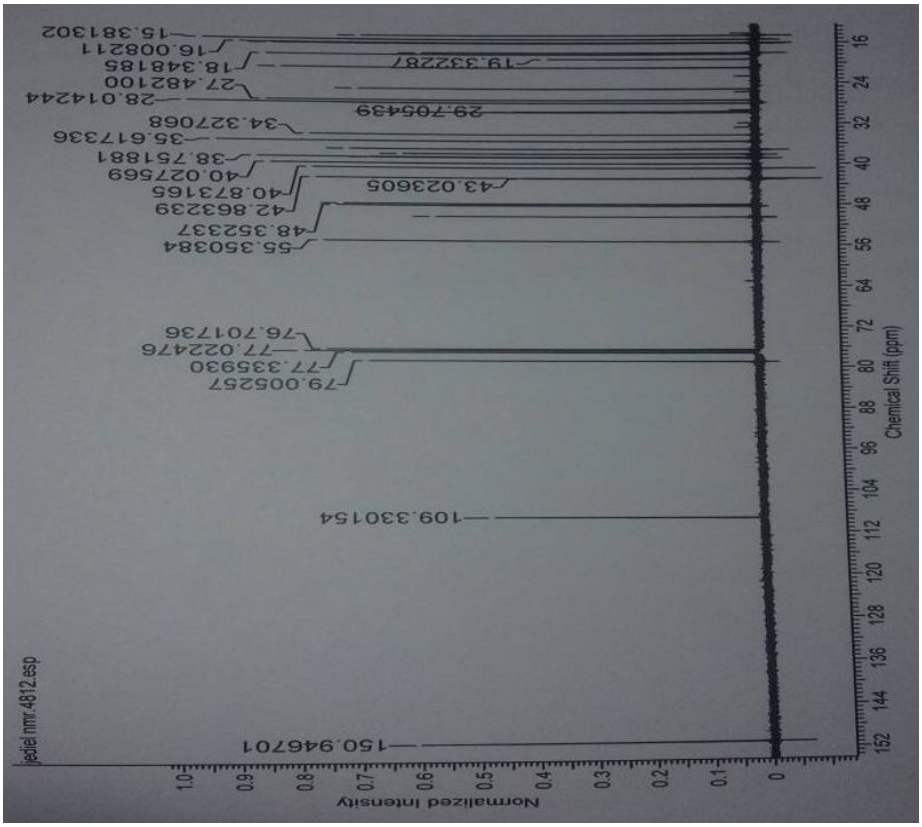

Appendix 3d-2: ^{13}C- NMR spectrum 2 of lupeol

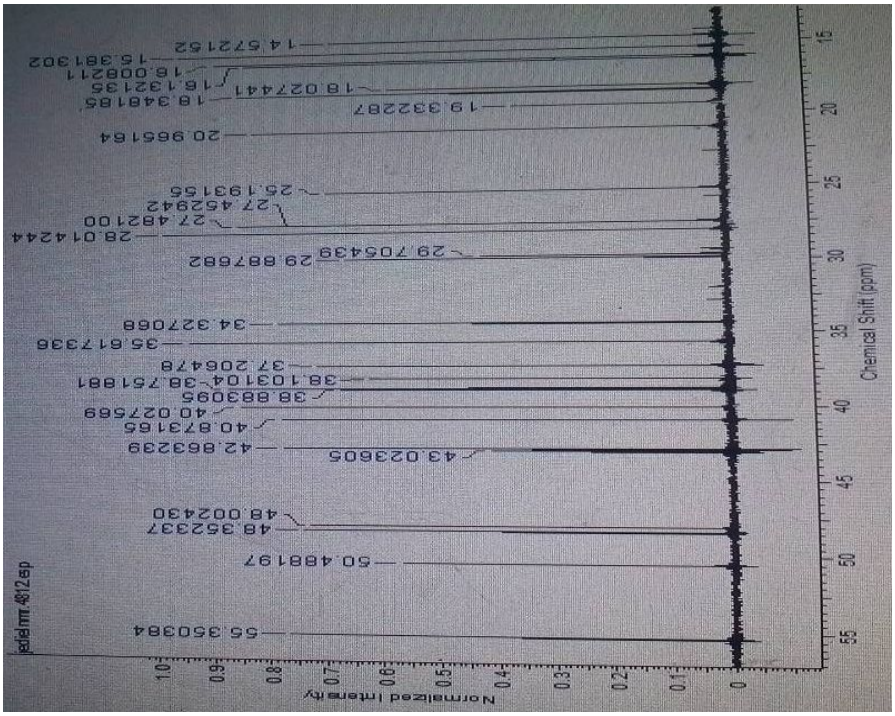

Appendix 3e-1: APT- NMR spectrum 1 of lupeol

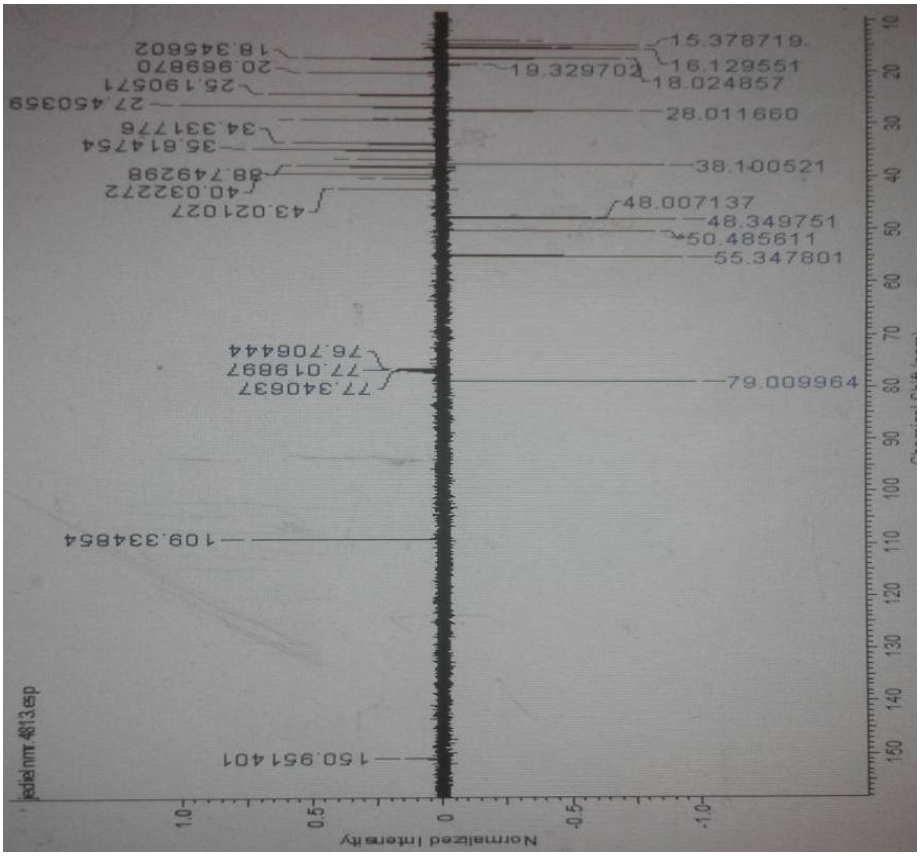

Appendix 3e-2: APT- NMR spectrum 2 of lupeol

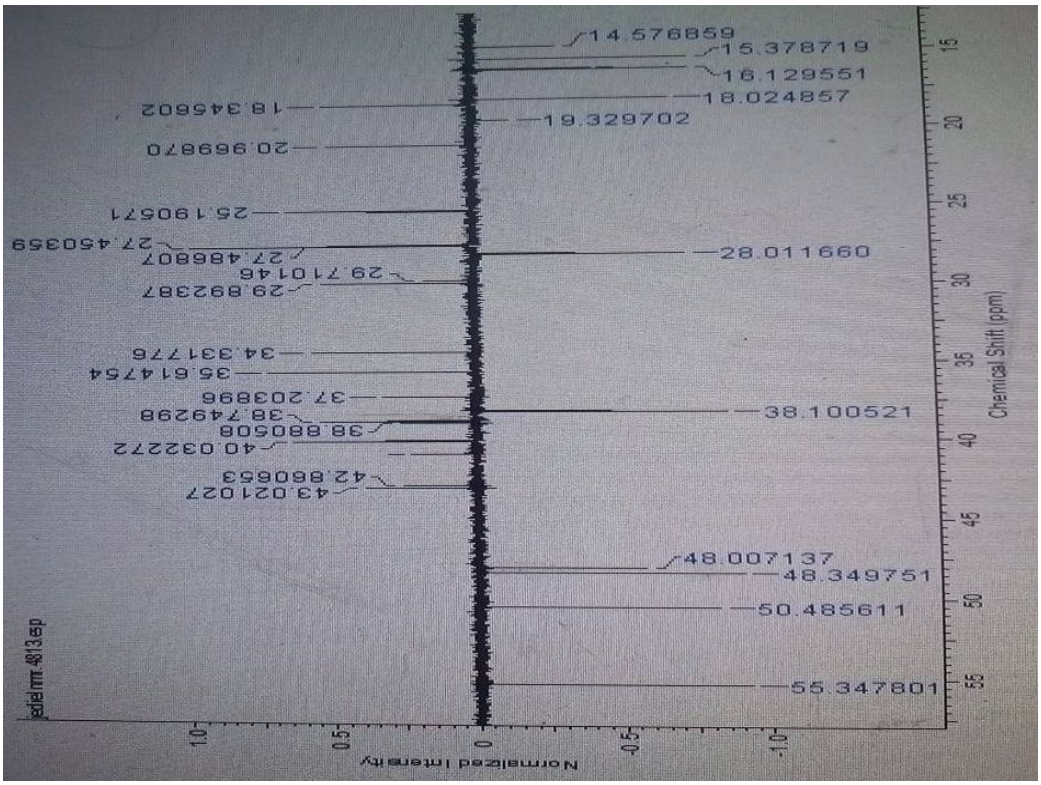

Appendix 4a: IR spectrum of β-sitosterol/stigmasterol in KBr

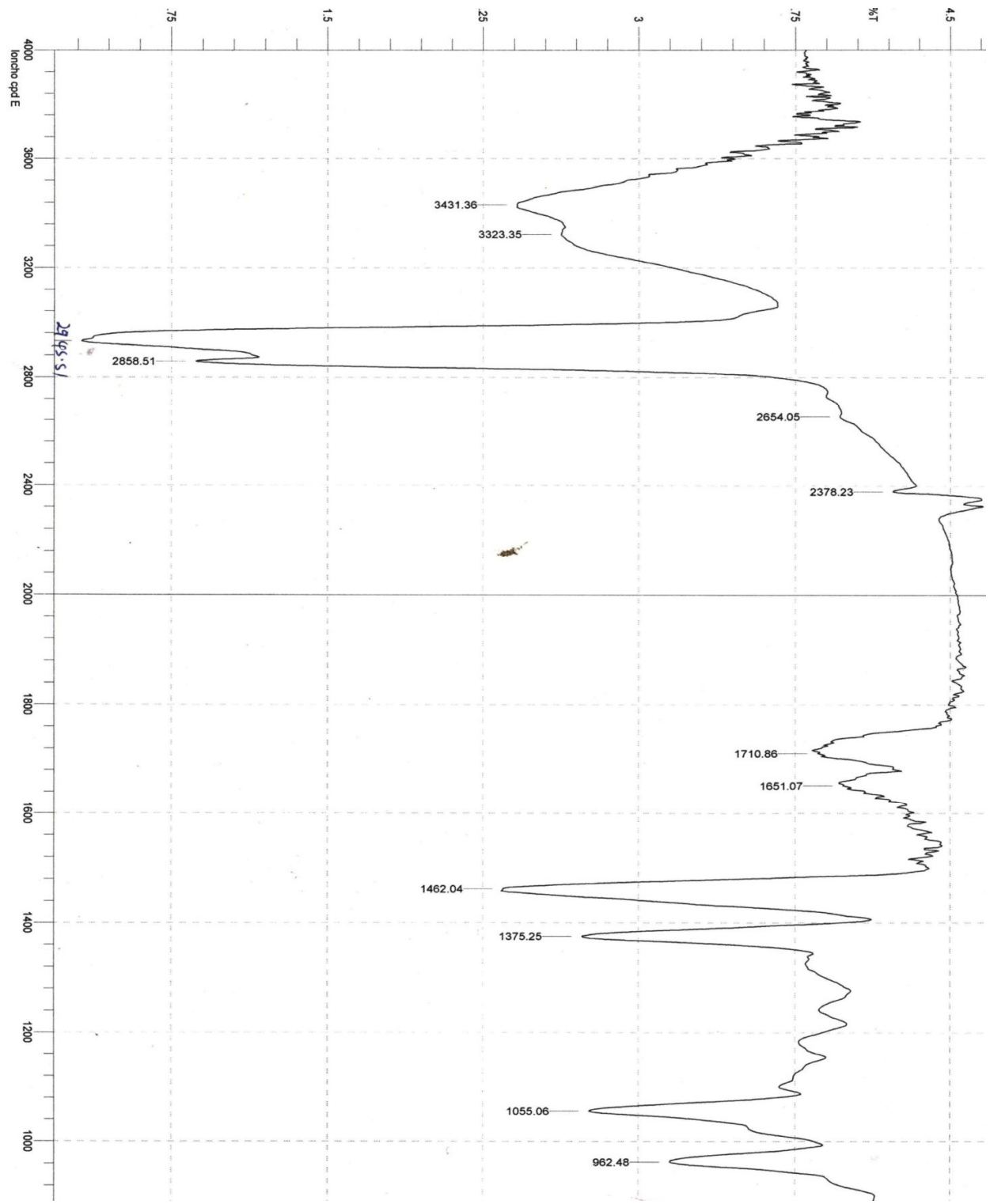

Appendix 4b-1: Mass spectrum of β-sitosterol/stigmasterol

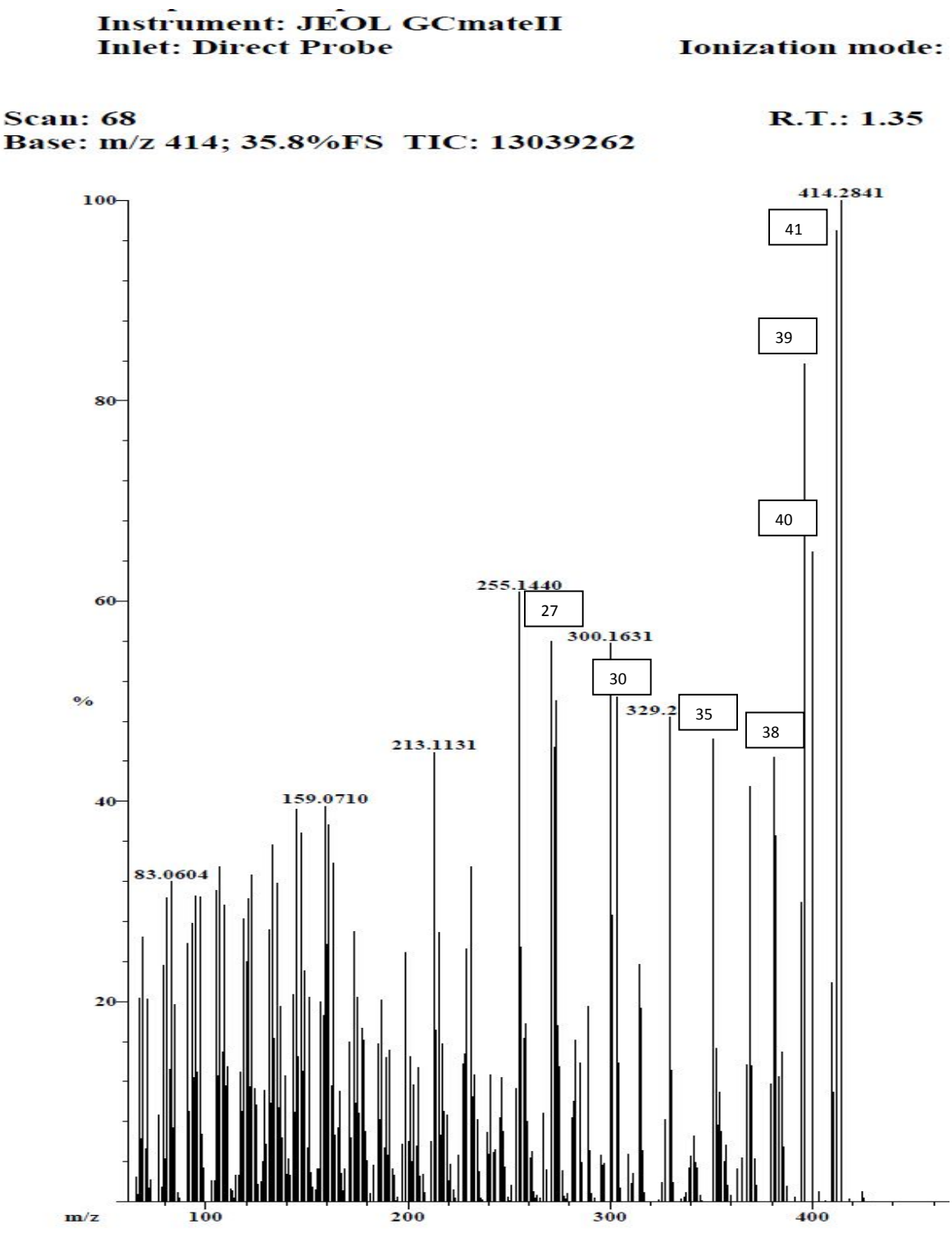

Appendix 4b-2: Mass spectral data of β-sitosterol/stigmasterol

Instrument: JEOL GCmateII
Inlet: Direct Probe **Ionization mode: EI+**

Scan: 68 **R.T.: 1.35**
Base: m/z 414; 35.8%FS TIC: 13039262 **#Ions: 301**

Threshold: 1% of Base **Displayed TIC: 13039262**

Mass	%Base	Mass	%Base	Mass	%Base	Mass	%Base	Mass	%Base
65.3321	2.4	117.0437	13.0	156.0941	3.3	203.1090	11.7	258.1350	17.8
67.2002	20.3	118.0563	9.0	157.0581	20.0	204.1414	5.5	259.1469	8.0
68.1201	6.3	119.0646	28.3	158.0777	18.6	205.1354	13.4	260.1942	4.4
69.0573	26.5	120.0712	24.0	159.0710	39.5	206.1132	2.6	261.1725	5.0
70.0649	5.3	121.0734	30.3	160.0872	25.7	207.1308	2.8	262.1610	1.0
71.0755	20.3	122.0796	11.5	161.0802	37.7	211.0821	6.0	267.1313	8.9
72.0732	1.4	123.0840	32.7	162.1129	11.6	213.1131	44.9	268.1563	3.2
73.0263	2.2	124.0808	11.3	163.0954	33.8	214.1396	17.1	271.1455	56.0
77.0230	8.6	125.0815	9.7	164.1110	6.6	215.1188	26.9	272.1655	45.4
78.0243	1.5	126.0950	1.7	165.1028	7.4	216.1651	6.6	273.1447	50.1
79.0367	23.6	127.0741	2.0	166.1345	11.1	217.1332	15.8	274.1685	17.6
80.0438	4.3	128.0363	4.0	167.0815	2.8	218.1456	9.1	275.1898	13.5
81.0455	30.3	129.0376	11.1	168.1360	1.1	219.1369	8.7	276.1873	3.1
82.0559	13.2	130.0457	5.8	169.0546	3.3	220.1495	2.1	281.1704	8.4
83.0604	32.0	131.0547	27.2	171.0855	16.0	221.1642	3.7	282.2083	10.0
84.0663	7.4	132.0735	9.9	172.1134	6.4	222.1308	1.2	283.1692	16.2
85.0758	19.7	133.0630	35.6	173.0926	27.0	225.1083	4.7	285.1514	13.9
91.0290	25.8	134.0743	16.3	174.1154	9.9	227.1417	13.8	286.1992	3.9
92.0390	9.0	135.0803	31.8	175.0996	20.5	228.1519	14.8	289.2213	19.5
93.0420	27.8	136.0900	9.4	176.1140	8.8	229.1211	25.2	290.2101	5.1
94.0505	12.4	137.0881	19.5	177.0999	17.4	231.1131	33.5	295.1631	4.7
95.0541	30.5	138.0867	6.4	178.0955	16.1	232.1282	10.5	296.1758	3.7
96.0604	13.0	139.0982	12.6	179.1007	7.0	233.1415	12.7	297.1768	3.8
97.0696	30.4	140.1102	2.7	180.1053	4.1	234.1571	8.2	300.1631	55.8
98.0735	6.8	141.0298	4.3	183.0021	3.7	235.1390	3.1	301.1752	28.6
99.0644	3.4	142.0768	2.7	185.0890	15.8	239.1151	7.0	303.2137	50.4
103.0272	2.1	143.0432	20.7	186.1032	8.2	240.1716	4.8	304.2174	13.9
104.0481	2.1	144.0631	9.0	187.0916	20.1	241.1257	12.7	305.1687	1.4
105.0417	31.1	145.0551	39.2	188.1076	5.4	242.1503	4.9	309.1710	4.7
106.0535	12.6	146.0695	14.5	189.1049	14.4	243.1487	5.2	310.2212	1.8
107.0592	33.4	147.0652	36.8	190.1371	4.6	245.1601	8.4	311.1730	2.8
108.0641	14.9	148.0929	13.1	191.1109	15.1	246.1364	12.5	314.1972	23.8
109.0710	29.6	149.0763	23.1	192.1017	3.3	247.1554	7.1	315.2054	19.3
110.0824	11.6	150.0949	5.4	193.1239	2.7	248.1723	3.5	316.2059	5.1
111.0791	13.5	151.0754	20.5	197.0571	5.8	251.1526	1.7	325.2480	2.0
112.0913	1.3	152.0719	2.9	199.0863	24.9	253.1410	11.3	327.2599	8.2
113.1024	1.2	153.0975	1.5	200.1195	6.0	255.1440	60.9	329.2349	48.4
115.0256	2.6	154.0682	1.2	201.1074	14.5	256.1584	25.4	330.2359	13.2
116.0522	2.6	155.0681	3.3	202.1347	4.0	257.1707	16.3	331.1819	1.9

Appendix 4b-3: Mass spectral data of β-sitosterol/stigmasterol continued

Instrument: JEOL GCmateII
Inlet: Direct Probe **Ionization mode: EI+**

Scan: 68 **R.T.: 1.35**
Base: m/z 414; 35.8%FS TIC: 13039262 **#Ions: 301**

(Continued)

Threshold: 1% of Base **Displayed TIC: 13039262**

Mass	%Base	Mass	%Base	Mass	%Base	Mass	%Base	Mass	%Base
339.2238	3.4	355.2375	7.1	371.2388	4.3	394.2649	29.9	664.4077	2.6
340.2583	4.5	356.3053	4.0	372.2156	1.7	396.2897	83.7	676.5313	1.6
341.2326	6.6	357.2625	5.7	379.2457	11.8	400.2573	64.9	690.5392	1.0
342.2655	4.0	358.2206	1.7	381.2828	44.4	403.1262	1.0	704.5107	1.6
343.1902	3.4	363.2288	3.3	382.2604	36.6	409.2679	21.9	732.6295	1.6
351.2119	46.2	365.2542	4.4	383.2341	12.5	410.3093	10.9		
352.2113	15.3	367.2512	13.7	385.2556	15.0	412.2709	97.0		
353.2751	7.7	369.2149	41.5	386.2180	5.5	414.2841	100.0		
354.2629	10.9	370.2137	13.6	387.2420	1.6	648.5217	1.5		

Appendix 4c-1: ^{1}H- NMR spectrum 1 of β-sitosterol/stigmasterol

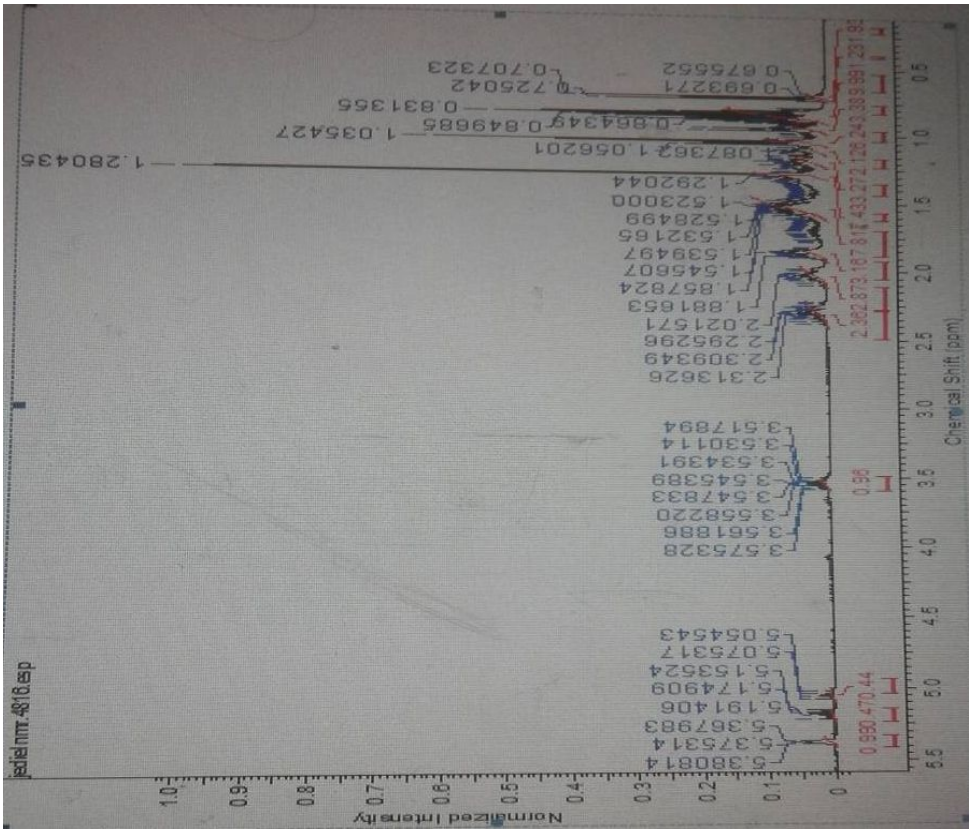

Appendix 4c-2: ^{1}H- NMR spectrum 2 of β-sitosterol/stigmasterol

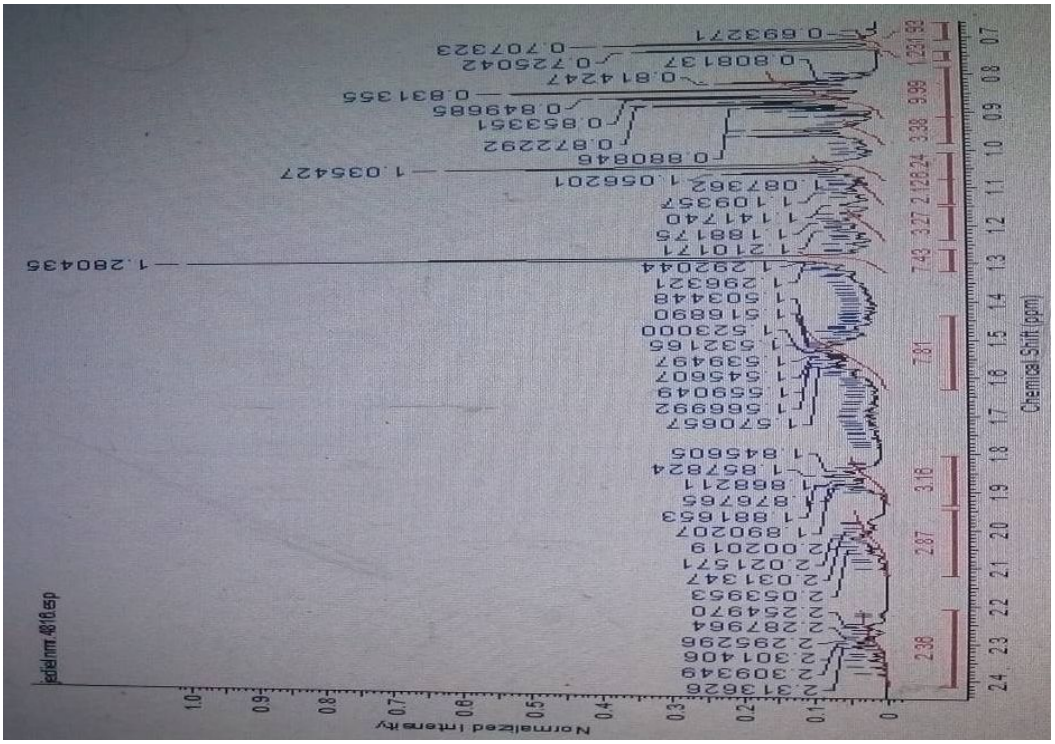

Appendix 4d-1: ^{13}C- NMR spectrum 1 of β-sitosterol/stigmasterol

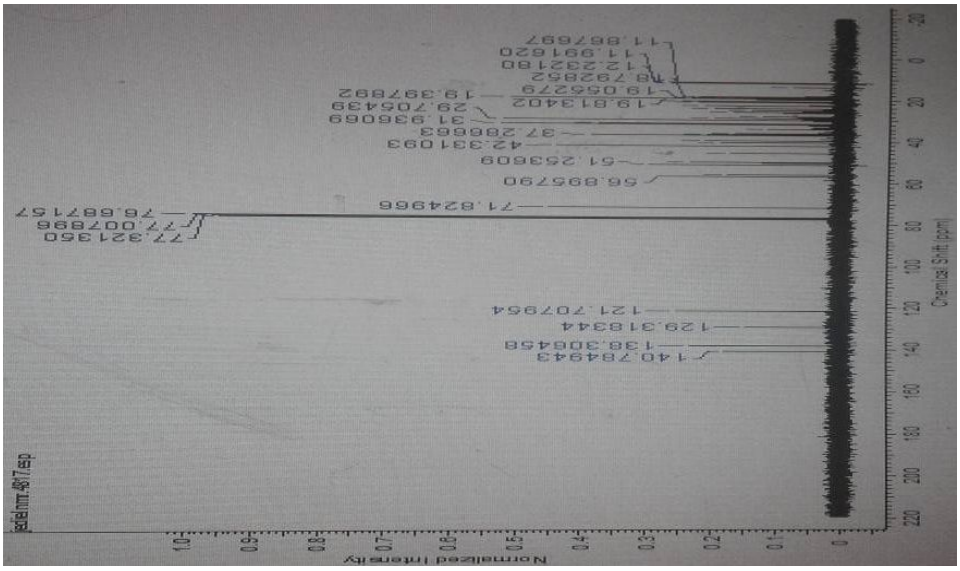

Appendix 4d-2: ^{13}C- NMR spectrum 2 of β-sitosterol/stigmasterol

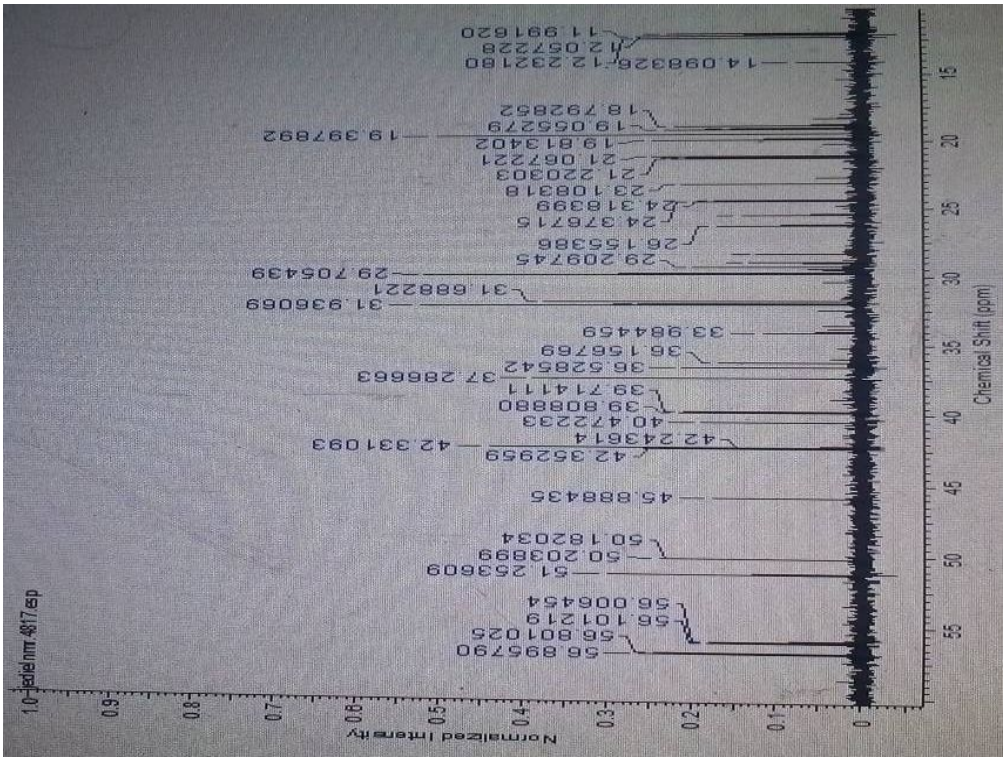

Appendix 4e-1: APT- NMR spectrum 1 of β-sitosterol/stigmasterol

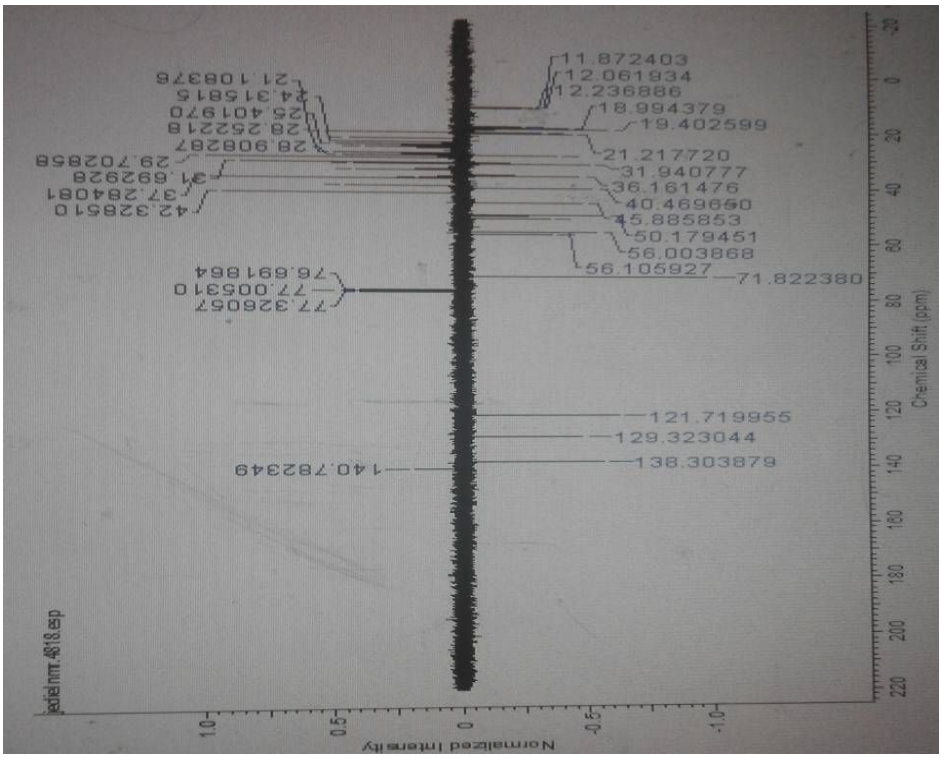

Appendix 4e-2: APT- NMR spectrum 2 of β- sitosterol/stigmasterol

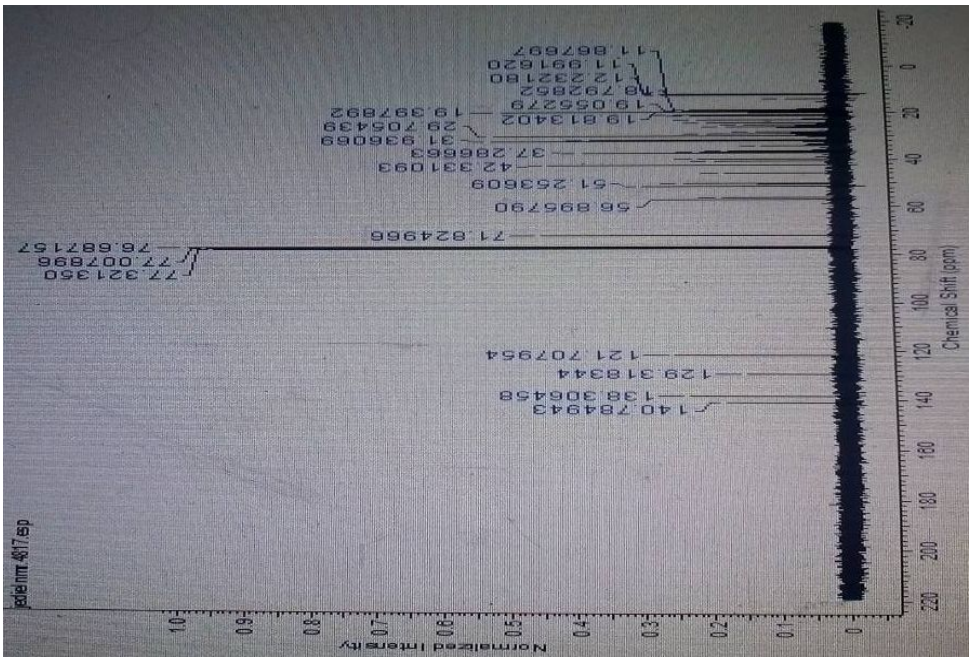

Appendix 5: Antimicrobial activity for crude extracts

Extract code	Extract name
1	Methanol extract
2	Chloroform extract
3	decoction
+ve	Positive control (gentamycin or nystatin for bacteria and fungi respectively)
-ve	Negative control (DMSO)

Escherichia coli ***Pseudomonas aeruginosa***

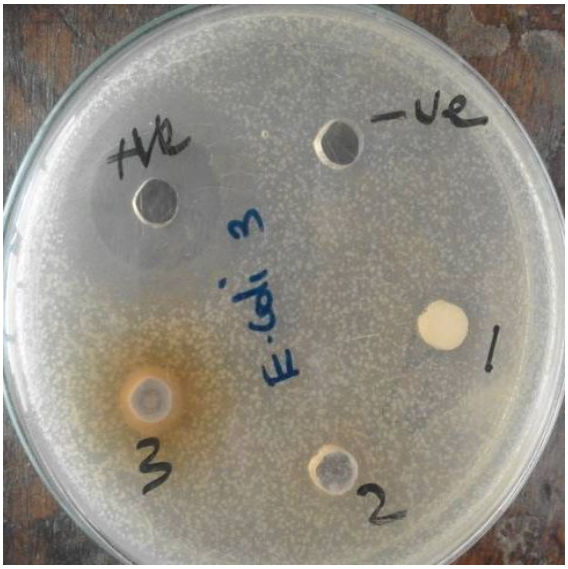

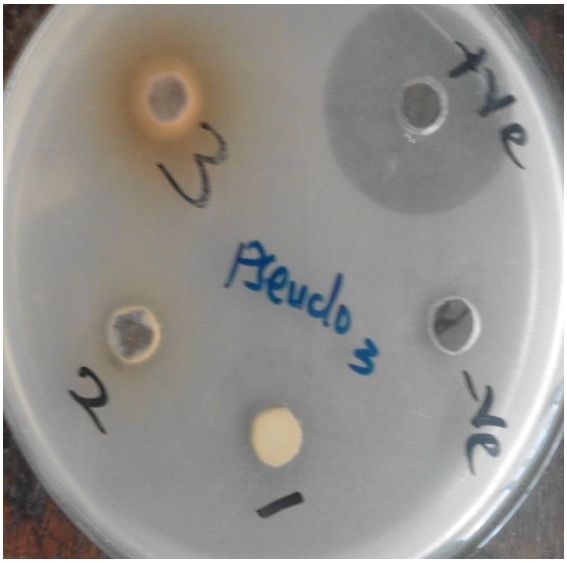

Saccharomyces cereviceae ***Staphylococcus aureus***

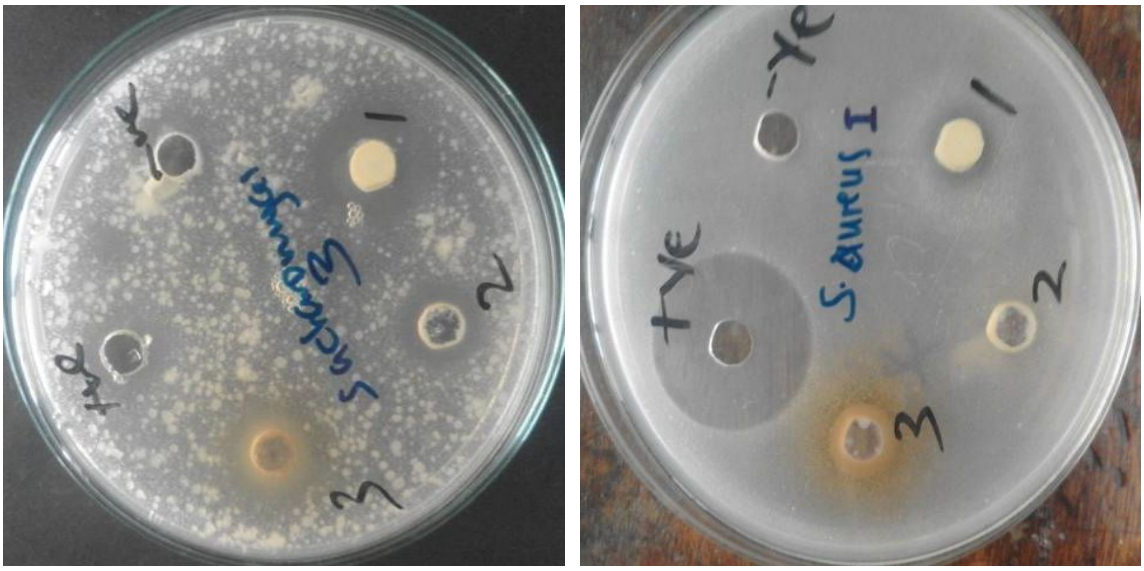

Appendix 6: Antibacterial and antifungal Inhibition zones for the isolated compounds

Table 7: codes for different isolates and standards

A	Non crystalline substance I
B	Lupenone (compound 1)
D	Lupeol (compound 2)
E	β-sitosterol/ stigmasterol (Compounds 3 and 4 mixture)
-VE	Negative control (Dimethyl sulfoxide/ distilled water)
+VE	Positive control (Gentamicin in bacterial cultures and nystatin in fungal cultures)

Saccharomyces cereviceae ***Pseudomonas aeruginosa***

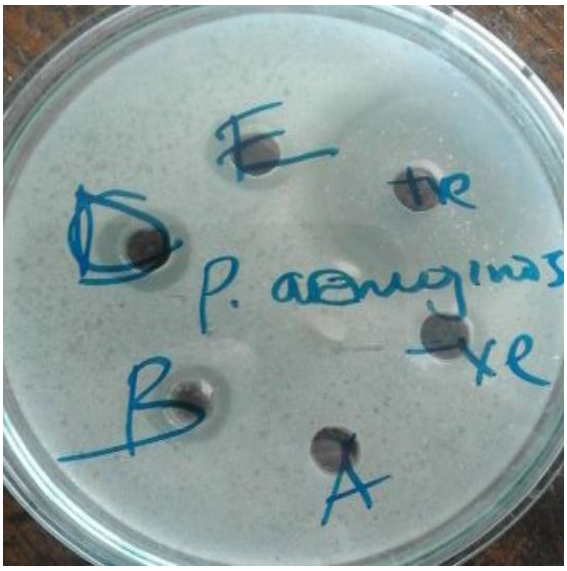

Escherichia coli ***Staphylococcus aureus***